

1985

Acidic and Chemical Properties of Molten Salt Hydrates

Stephen Keith Franzysen
College of William & Mary - Arts & Sciences

Follow this and additional works at: <https://scholarworks.wm.edu/etd>



Part of the [Physical Chemistry Commons](#)

Recommended Citation

Franzysen, Stephen Keith, "Acidic and Chemical Properties of Molten Salt Hydrates" (1985).
Dissertations, Theses, and Masters Projects. William & Mary. Paper 1539625305.
<https://dx.doi.org/doi:10.21220/s2-cvb1-hh82>

This Thesis is brought to you for free and open access by the Theses, Dissertations, & Master Projects at W&M ScholarWorks. It has been accepted for inclusion in Dissertations, Theses, and Masters Projects by an authorized administrator of W&M ScholarWorks. For more information, please contact scholarworks@wm.edu.

**ACIDIC AND CHEMICAL PROPERTIES
OF MOLTEN SALT HYDRATES**

A Thesis

Presented to

The Faculty of the Department of Chemistry
The College of William and Mary in Virginia

In Partial Fulfillment

of the Requirements for the Degree of
Master of Arts

by

Stephen Keith Franzysheh

1985

ProQuest Number: 10626543

All rights reserved

INFORMATION TO ALL USERS

The quality of this reproduction is dependent upon the quality of the copy submitted.

In the unlikely event that the author did not send a complete manuscript and there are missing pages, these will be noted. Also, if material had to be removed, a note will indicate the deletion.



ProQuest 10626543

Published by ProQuest LLC (2017). Copyright of the Dissertation is held by the Author.

All rights reserved.

This work is protected against unauthorized copying under Title 17, United States Code
Microform Edition © ProQuest LLC.

ProQuest LLC.
789 East Eisenhower Parkway
P.O. Box 1346
Ann Arbor, MI 48106 - 1346

APPROVAL SHEET

This thesis is submitted in partial fulfillment of
the requirements for the degree of
Master of Arts



Stephen Keith Franzysen

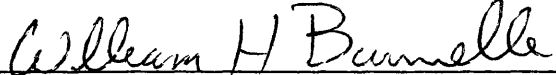
Approved, March 1985



Melvyn E. Schiavelli, Ph.D.



David W. Thompson, Ph.D.



William H. Bunnelle, Ph.D.

TABLE OF CONTENTS

	Page
ACKNOWLEDGEMENTS	IV
LIST OF TABLES	V
LIST OF FIGURES	VII
LIST OF SCHEMES	IX
ABSTRACT	X
INTRODUCTION	2
EXPERIMENTAL	54
RESULTS AND DISCUSSION	70
CONCLUSIONS	118
APPENDIX I	123
APPENDIX II	126
BIBLIOGRAPHY.	129

ACKNOWLEDGEMENTS

The author wishes to express his sincere appreciation to Professor Melvyn D. Schiavelli for his patient guidance and assistance throughout the course of this research. I would also like to thank Professor William H. Bunnelle and Professor David W. Thompson for their endless hours of help and advice both in the laboratory and in the classroom. Appreciation is also conveyed to Paul Drees and Louis Menges for their assistance with the graphs and drawings for this thesis.

I would also like to express my sincerest gratitude to my parents, Frank and Mary Ann Franzysen, to Cheryl Compton, and to my friends for their unceasing support, encouragement, and assistance throughout the past few years.

A special thanks is extended to my Mom for her endless patience and long hours put into typing this manuscript.

LIST OF TABLES

<u>Table</u>		<u>Page</u>
1	Experimental and Predicted pKa values of aquo metal ions.	12
2	Water chemical shifts for some molten salts showing the effect of the anion present.	23
3	Metal nitrate salts used to nitrate benzene.	53
4	Chemical shift for various molten salt hydrates.	71
5	Temperature effect on the chemical shift of $\text{Cd}(\text{NO}_3)_2 \cdot 4\text{H}_2\text{O}$.	74
6	Temperature effect on the chemical shift of $\text{Zn}(\text{NO}_3)_2 \cdot 6\text{H}_2\text{O}$.	74
7	Measured H_0 for $\text{Cd}(\text{NO}_3)_2 \cdot 4\text{H}_2\text{O}$.	78
8	Measured H_0 for $\text{Zn}(\text{NO}_3)_2 \cdot 6\text{H}_2\text{O}$.	78
9	Measured H_0 for $\text{AlCl}_3 \cdot 6\text{H}_2\text{O}$.	78
10	Measured H_0 for $\text{HNO}_3 \cdot 1.65 \text{H}_2\text{O}$.	78
11	Predicted H_0 for $\text{Cd}(\text{NO}_3)_2 \cdot 4\text{H}_2\text{O}$.	80
12	Predicted H_0 for $\text{Zn}(\text{NO}_3)_2 \cdot 6\text{H}_2\text{O}$.	80
13	Predicted H_0 for $\text{AlCl}_3 \cdot 6\text{H}_2\text{O}$.	81
14	Predicted H_0 for $\text{HNO}_3 \cdot 1.65\text{H}_2\text{O}$.	81
15	Wt & mole % aqueous HNO_3 with appropriate H_0 values.	83
16	Wt % and mole % for molten salt hydrate system of $\text{HNO}_3 \cdot 1.65\text{H}_2\text{O}/\text{Ca}(\text{NO}_3)_2 \cdot 4\text{H}_2\text{O}$ with appropriate H_0 values.	83
17	Measured and Predicted H_0 and chemical shift values for $\text{Cd}(\text{NO}_3)_2 \cdot 4\text{H}_2\text{O}$.	86
18	Measured and Predicted H_0 and chemical shift values for $\text{Zn}(\text{NO}_3)_2 \cdot 6\text{H}_2\text{O}$.	86

<u>Table</u>		<u>Page</u>
19	Measured and predicted H_0 and chemical shift values for $AlCl_3 \cdot 6H_2O$.	87
20	Measured and predicted H_0 and chemical shift values for $HNO_3 \cdot 1.65H_2O$.	88
21	n-Hexyl acetate in 10% HNO_3 melt.	93
22	n-Hexyl acetate in 7% HNO_3 melt.	93
23	n-Hexyl acetate in 5% HNO_3 melt.	93
24	n-Hexyl acetate in 2% HNO_3 melt.	94
25	n-Hexyl acetate in 1% HNO_3 melt.	94
26	n-Octyl acetate in 10% HNO_3 melt.	95
27	n-Octyl acetate in 7% HNO_3 melt.	95
28	n-Octyl acetate in 5% HNO_3 melt.	95
29	n-Octyl acetate in 2% HNO_3 melt.	96
30	n-Octyl acetate in 1% HNO_3 melt.	96
31	2-Octyl acetate in 10% HNO_3 melt.	97
32	2-Octyl acetate in 7% HNO_3 melt.	97
33	2-Octyl acetate in 5% HNO_3 melt.	97
34	2-Octyl acetate in 2% HNO_3 melt.	98
35	2-Octyl acetate in 1% HNO_3 melt.	98
36	Products of controlled reactions	103
37	Rates of ester hydrolysis in H_2SO_4	121
38	H_0 values for various wt. % of H_2SO_4	122

LIST OF FIGURES

<u>Figure</u>		<u>Page</u>
1	Relationship between the Hammett Acidity Function and the water activity for concentrated acid solutions.	8
2	Trends in H_0 with molarity for aqueous solutions of weak and strong acids and metal aquo complexes.	14
3	Trend in H_0 with H_2O /Acid ratio for strong and weak acids and metal aquo complexes.	15
4	Relationship between H_0 and log mole % of solute.	18
5	Concentration dependence of the proton chemical shift for aqueous solutions of strong acids.	19
6	Relationship between chemical shift and mole fraction of H_3O^+	21
7	Effect of temperature on the chemical shift of molten salt hydrates.	27
8	(A) 1H NMR shifts relative to experimental pKa (B) 1H NMR shifts relative to predicted pKa by optical basicity calculations.	30
9	Relationship between H_0 and chemical shift for strong acids	32
10	Relationship between H_0 and the hydrogen ion activity.	33
11	Ester hydrolysis mechanisms	39
12	Rate profiles for ester hydrolysis	43
13	Rate profiles for ester hydrolysis	44
14	Plot of chemical shift (ppm) vs mole % of solute for various molten salt hydrates.	72

<u>Figure</u>		<u>Page</u>
15	Plot of chemical shift vs mole % of $\text{Cd}(\text{NO}_3)_2 \cdot 4\text{H}_2\text{O}$ at various temperatures.	75
16	Plot of chemical shift vs mole % of $\text{Zn}(\text{NO}_3)_2 \cdot 6\text{H}_2\text{O}$ at various temperatures.	76
17	Plot of H_0 vs log mole % solute for various molten salt hydrates.	79
18	Plot of H_0 vs log chemical shift relative to the solvent for various molten salt hydrates.	89
19	Relationship between $-\log ([\text{B}]/[\text{BH}^+])$ and acid concentration.	125

LIST OF SCHEMES

<u>Scheme</u>		<u>Page</u>
1	Acid-catalyzed ester hydrolysis of n-octyl acetate.	108
2	Oxidation of 1-octanol to octanal/ oxidation of octanal to octanoic acid.	109
3	1,3-dipolar cycloaddition of NO_3^- to octanal.	110
4	Formation of 1-octyl nitrate ester.	111
5	Acid-catalyzed ester hydrolysis of 2-octyl acetate.	112
6	Oxidation of 2-octanol/oxidation of 2-octanone to give hexanoic acid via 1,3-dipolar cycloaddition.	113
7	Oxidation of 2-octanone to hexanoic acid/ 1,3-dipolar cycloaddition of NO_3^- to hexanal	114
8	Oxidation of 2-octanone to give heptanoic acid via 1,3-dipolar cycloaddition.	115
9	Formation of 2-octyl nitrate	116

A B S T R A C T

Experimental investigations have shown that molten salt hydrate systems are highly acidic in nature, compared to strong mineral acids. The accepted means of expressing this acidity is the Hammett Acidity Function (H_0) which can be measured spectrophotometrically.

Due to the experimental problems encountered in using this technique, we have proposed a rather novel approach to measuring the acidities of these systems by correlating the Hammett Acidity Function with the 1H NMR chemical shift of hydrate melts.

Once the relative acidities of these hydrate melts had been established our next goal was to examine the chemical properties and reactivities of these molten salt hydrates by employing them as a synthetic medium for certain acid catalyzed organic reactions.

The primary reaction we wanted to focus upon was the acid catalyzed ester hydrolysis reaction. Also a preliminary investigation was performed on nitration of aromatics in this medium.

The expected products were obtained along with a number of oxidation and nitration products which were confirmed by authentic samples that were independently synthesized. Also some controlled reactions were performed in which the individual products were introduced into the medium and its products analyzed in order to obtain a mechanistic route for the reaction.

The results of these reaction showed that molten salt hydrates are highly acidic with only a limited amount of free water available. They are also strong oxidizing agents and powerful nitrating agents.

ACIDIC AND CHEMICAL PROPERTIES

OF MOLTEN SALT HYDRATES

I N T R O D U C T I O N

In recent years there has been a growing interest in the physical and chemical properties of molten salt hydrates.¹ These quasi-fused salt systems are gaining technological importance due to their high thermal stability, low vapor pressure, high electrical conductance, and their strong acidic properties.² Much effort is being currently directed toward the use of molten salt hydrates in new electrometallurgical processes and development of the "molten salt reactor" in which the melt is used as a low internal resistance fuel element.¹

It is our purpose to explore further the acidic nature of these molten salt hydrates and attempt to correlate the Hammett Acidity Function with the proton magnetic resonance spectra of these melt systems. We have also examined the chemical properties and reactivity of these hydrate melts by employing them in selected acid-catalyzed organic reactions.

Theory of Acidity/Hammett Acidity Function

According to the classical ionization theory, the hydrogen ion concentration represented the quantitative measure of acidity, and a non-ionized medium did not have acidic properties.³ However a series of papers by Hantzsch⁴ concluded that non-ionized solutions may be as acidic, or even more acidic than highly ionized aqueous solutions. This was based on the evidence that non-ionized mediums often produce the same effect upon indicators as do more concentrated solutions of acid in water. Also, the rate of decomposition of diazoacetic ester, which is an acid catalyzed reaction, is greater in the non-ionized solution.⁴

The importance of the dielectric constant of the medium when measuring the acidity was suggested by Brönsted.⁵ He concluded that the measure of acidity should be the hydrogen-ion potential, which represents the work necessary to remove or add a hydrogen ion to a given system.

Closely related to this concept is the hydrogen-ion activity which is an exponential function of the hydrogen-ion potential.⁵ Loosely "bound" protons give a high activity, whereas firmly "bound" protons give a low activity. At infinite dilution the activity coefficients approach a value of one.³

The hydrogen-ion activity of a weakly ionized acid is independent of the dielectric constant of the medium, whereas the hydrogen-ion activity of a highly ionized acid will be greater in solvents with a low dielectric constant. This is demonstrated by the extremely low solubility of salts in the solvents of low dielectric constants, which is predicted by the interionic attraction theory of electrolytes.³

When the acidity of a solution is determined by means of a base indicator, what is being measured is the tendency of the acid present to transfer a hydrogen ion to a neutral organic indicator base, converting it to a positive ion.⁶ The base indicator is defined as a non-ionized substance, capable of adding one hydrogen ion per molecule without any complicating side reactions, and in such a way that the extent of the reaction can be determined by a color change.⁶ The ionization equilibria of the indicator base is defined as:



where K_{BH^+} is the conjugate acid dissociation constant. In a highly concentrated or non-aqueous acidic medium the activity coefficients of the ions in solution cannot be neglected when determining the acidity of the medium.⁷

$$K_{BH^+} = a_{H^+} a_B / a_{BH^+} = f_{H^+} [H^+] f_B [B] / f_{BH^+} [BH^+]$$

or

$$pK_{BH^+} = -\log(f_{H^+} [H^+] f_B [B] / f_{BH^+} [BH^+])$$

where a_X is the activity of X, f_X is the activity coefficient of X, and [X] is the molar concentration of X. The activity coefficients can be evaluated using the Debye-Hückel Equation.⁷

The Hammett Acidity Function is defined as $H_0 = -\log h_0$ where $h_0 = [H^+] f_{H^+} f_B / f_{BH^+}$ which rather conveniently arranges all the activity coefficients into one term. Each activity coefficient is taken by convention to approach unity at infinite dilution in water so that a_{H^+} becomes equal to $[H^+]$, then H_0 becomes equal to the pH in ideal dilute aqueous solutions.⁸

$$pK_{BH^+} = -\log ([B]/[BH^+]) - \log ([H^+]f_{H^+}f_B/f_{BH^+})$$

$$pK_{BH^+} = -\log ([B]/[BH^+]) + H_0$$

$$H_0 = pK_{BH^+} + \log ([B]/[BH^+]) \quad \text{or} \quad H_0 = pK_{BH^+} - \log ([BH^+]/[B])$$

Therefore, one can obtain a working definition for the Hammett Acidity Function, in which the pK_A and the concentrations can be determined very precisely, which is by far more convenient and accurate than approximating activity coefficients.

Since we define the Hammett Acidity Function as:

$$H_0 = -\log h_0 = -\log a_{H^+}(f_B/f_{BH^+})$$

then H_0 is independent of a particular indicator used to measure it. This follows from the fundamental assumption that the ratio f_B/f_{BH^+} is the same for different bases in a given solution.⁶ Also studies of several different strong acids gave almost identical pK_{BH^+} values for various indicators.⁸ This supports the fact that H_0 values are independent of the indicators used. (See Appendix I)

There has been an explicit study of the temperature effects on H_0 for aqueous solutions of some strong acids.⁹ The results indicate small but systematic changes in H_0 relative to the acid concentration with increasing temperatures. A systematic study on the influence of added salts on the acidity function was carried out by Harbottle.¹⁰ The results demonstrated that there was a large increase in $-H_0$ caused by the salt. Qualitatively an increase was expected since added salt should "salt out" the indicator causing the term f_B to increase thereby causing $-H_0$ to increase by definition:

$$-H_0 = \log [H^+] + \log (f_{H^+}/f_{BH^+}) + \log f_B$$

The term $\log (f_{H^+}/f_{BH^+})$ should also increase due to increased electrolytes.

In a similar study, Paul¹¹ showed that in water H_0 decreases linearly with increasing concentration of neutral salt. The magnitude of this effect was also explained on the basis of the tendency to salt out the indicator instead of a real decrease in the acidity of the solution. He attributed this salt effect for the marked increase of $-H_0$ over $\log [H^+]$ with increasing concentration of strong acid by itself, in the absence of added electrolyte.

A study by Moiseev and Flid¹² found that the effect of neutral salts on the acidity of aqueous solutions is independent of the nature of the salt.

Bascombe and Bell¹³ stated that f_B will increase with acid concentration, but the observed changes in the H_0 are too large to be accounted for as a salting out effect. Moreover the salting out effect will vary with the nature of the base and of the acid anion. Therefore they concluded that it seems highly probable that the increase in $-H_0$ with acid concentration is attributable to an increase in the ratio of f_{H^+}/f_{BH^+} , and that this is due to the hydration of the hydrogen ion. In other words the existence of H_3O^+ or the $H(H_2O)_X^+$ species is adequate to account for most of the increase in acidity, where the number of water molecules associated with a hydrogen ion is called the hydration number.

Wyatt¹⁴ also concluded that the hydration of ions is the most important factor in determining the large changes in the acidity function and water activity in concentrated acid solutions. Wyatt

also showed that completely ionized acids (H_2SO_4 , HClO_4 , HCl and HNO_3) all have the same water activity at specific H_0 values. From this the conclusion was drawn that the hydration equilibrium constants are practically the same for all strong acids. (See figure #1).

Dawber and Wyatt¹⁵ later suggested that the difference between the H_0 for a weak acid and for a fully dissociated acid at the same water activity was related to the extent of dissociation (α) of the weak acid by the equation:

$$(H_0)_{\text{WEAK}} - (H_0)_{\text{STRONG}} = \log [(1 + \alpha)/2\alpha]$$

Nitric acid is a particular interest since its extent of dissociation has been accurately determined over the whole range of concentrations by Raman spectroscopy.¹⁶ The agreement between the calculated and observed H_0 values supports the theory that the equilibrium constants for the hydration reaction of H_3O^+ are the same for all acid solutions.

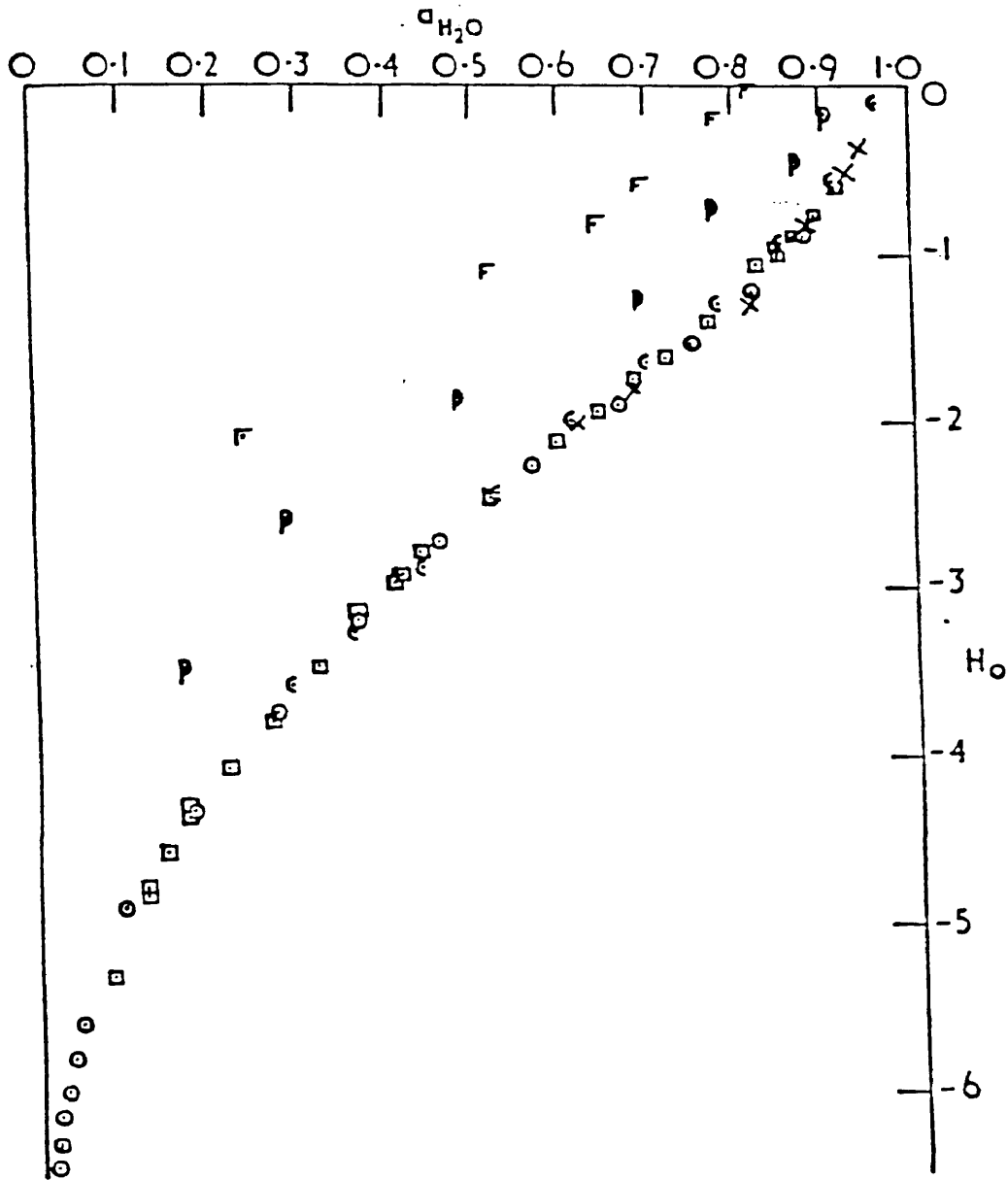
A study by Critchfield and Johnson¹⁷ found that at a fixed concentration of hydrogen ion and neutral salt, the H_0 of a solution is a linear function of the heat of solution of the dissolved salt, where each solution contains the same ionic concentration of salt = I ($I = M(n/2)$; M = molarity, n = number of ions in the salt molecule)

$$H_0 = -\log[\text{H}^+] - I(0.20 + 5 \times 10^{-3} \Delta H_S)$$

ΔH_S = heat of solution of the salt in kcal/g mole

Therefore H_0 is a function of the hydrogen ion concentration, ionic concentration of the salt, and heat of solution of the salt, but it is independent of the nature of the salt.

FIGURE # 1



○ H_2SO_4

□ HClO_4

⊖ HCl

× HNO_3

⊕ H_3PO_4

⌈ HF

(adapted from reference # 14)

The decrease in H_0 upon addition of neutral salts to the acid solutions represents an increase in the acidity of the solution which is associated with an increase in hydrogen ion concentration.¹⁷ It is very probable that the hydrogen ion is made more "active" by losing waters of hydration. Salts with the highest positive heats of solution have a great affinity for water and thereby tend to compete with the hydrogen ion for waters of hydration.¹⁷

Acidic Nature of Metal Aquo Complexes and Molten Salt Hydrates

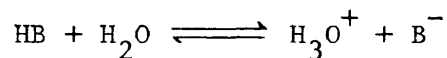
Metal ions in aqueous solutions interact strongly with the water molecules to form aquo complexes.¹⁸ The metal ion - water interaction involves appreciable polarization of the water molecule and this results in the electron charge clouds of the aquo ligands being attracted toward the central metal ion. This in turn causes a decrease in the electron density on the hydrogen atom allowing the metal aquo ion to behave as a Brönsted-Lowry Acid.¹⁸

Restricted studies on the $ZnCl_2/H_2O$ systems using Hammett indicators showed that some of these melts are highly acidic.¹⁹ Other studies have shown that mixtures of $Al(NO_3)_3 \cdot 10H_2O$ and $AlCl_3 \cdot 10H_2O$ dissolve noble metals more rapidly than boiling aqua regia.²⁰

However, the measured pK_A values of metal aquo complexes are usually greater than that of mineral acids by several orders of magnitude.¹⁹ This is surprising since one would expect a positively charged species such as Al^{3+} would be more liable to release protons than would a neutral oxy acid such as HNO_3 , but the

measured pK_A values are 4.97 and -1.27, respectively.¹⁹

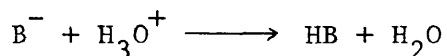
An alternative way to express the acidity of the metal aquo complex is the Optical Basicity Scale.¹⁸ This method assumes that the acidity of the medium depends upon the state of the anion after dissociation of one or more protons.²¹



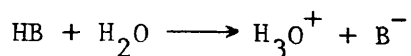
If the affinity of the anion, B^- , for protons is greater than that of H_2O , then HB will be a weak acid, whereas if it is less, then HB will be a strong acid. Therefore an important factor influencing acid strength is anion basicity.²²

The dissociation equilibrium of the acid HB involves competition between the resulting anion and water molecules for the proton. Therefore the difference between the optical basicity of the anion, λ_{B^-} , and that of water, λ_{H_2O} , is related to the acid strength.²¹

Therefore, the attraction that the anion has for regaining its proton depends upon its basicity or electron donating ability, and this can be expressed in numerical terms as optical basicity.¹⁸ This may be regarded as a means of quantifying Lewis basicity. Thus, anions with a high optical basicity are weak acids.²¹



Whereas a strong acid readily dissociates to give a weak base with a low affinity for protons.



Examination of the experimental optical basicity values for a wide range of oxidic materials has revealed that it is possible to assign basicity moderating parameters γ to certain elements.²³

This parameter expresses the influence that the central atom has upon the electron donating power of oxygen. It expresses the ability of the central atom to contract the electron cloud of the oxygen atom.²² The general equation for optical basicity is expressed as:

$$\lambda_B = 1 - \left[\frac{n}{2z} \left(1 - \frac{1}{\gamma_H} \right) + \frac{m}{2z} \left(1 - \frac{1}{\gamma_M} \right) \right]$$

Where λ_B is calculated for the conjugate base of the metal aquo complex: $[M(H_2O)_3(OH)]^{(X-1)+}$ or $[M(M_2O)_5(OH)]^{(X-1)+}$

n = number of protons in the conjugate base of the metal aquo complex

z = number of oxygen molecules in the conjugate base of the metal aquo complex

γ_H = basicity - moderating parameter for hydrogen = 2.50

γ_M = basicity - moderating parameter for the aquometal ion

M = aquometal ion with an oxidation number m

The basicity - moderating parameters are closely related to Pauling electronegativity, x, by the equation: $\gamma = 1.36 (X-0.26)$.

Finally the pK_A values for the metal aquo complex can be predicted using the following equation: $pK_A + 1.74 = 5.83 (\lambda_B - 0.40)$.

Optical Basicity calculation applied to the metal aquo complexes predicted pK_A values that are very much more negative than those determined experimentally.¹⁸ These results showed that Al^{3+} melts have acidities comparable to strong mineral acids such as HNO_3 . (See Table #1)

The reason for the large difference between experimental pK_A values and those predicted by optical basicity calculations, which

TABLE # 1

Experimental and Predicted pK_a Values of Aquometal Ions

metal ion	γ_M	exptl pK_a^a	four- coordination		six- coordination	
			λ^b	pK_a^c	λ^b	pK_a^c
Ca ²⁺	1.00	12.85	0.475	2.6	0.45	1.2
Mg ²⁺	1.28	11.44	0.42	-0.6	0.41	-1.2
Zn ²⁺	1.82	8.96	0.36	-4.1	0.375	-3.2
Al ³⁺	1.65	4.97	0.33	-5.8	0.35	-4.7
Li ⁺	1.00		0.475	2.6	0.45	1.2
Na ⁺	0.87		0.49	3.7	0.46	1.9
HNO ₃		-1.27 ^d				

^a Experimental value from data obtained for dilute aqueous solutions (C. F. Baes and R. E. Mesmer, "Hydrolysis of Cations", Wiley-Interscience, New York, N.Y., 1976). ^b λ is calculated for the conjugate base $[M(H_2O)_3(OH)]^{(n-1)+}$ or $[M(H_2O)_5(OH)]^{(n-1)+}$ from eq 3. ^c Predicted pK_a values are obtained from eq 2. ^d λ for NO_3^- is 0.39 and hence the predicted pK_a is -2.3.

(adapted from reference # 18)

amounts to 10-12 pK units, probably arises from outer-sphere hydration or hydrogen bonding which the metal aquo complex experiences in aqueous solution.¹⁸ Thus it would be expected that concentrated solutions of metal salts having a sufficiently low water to metal ratio to minimize outer-sphere hydration would show an increase in acidity.¹⁹

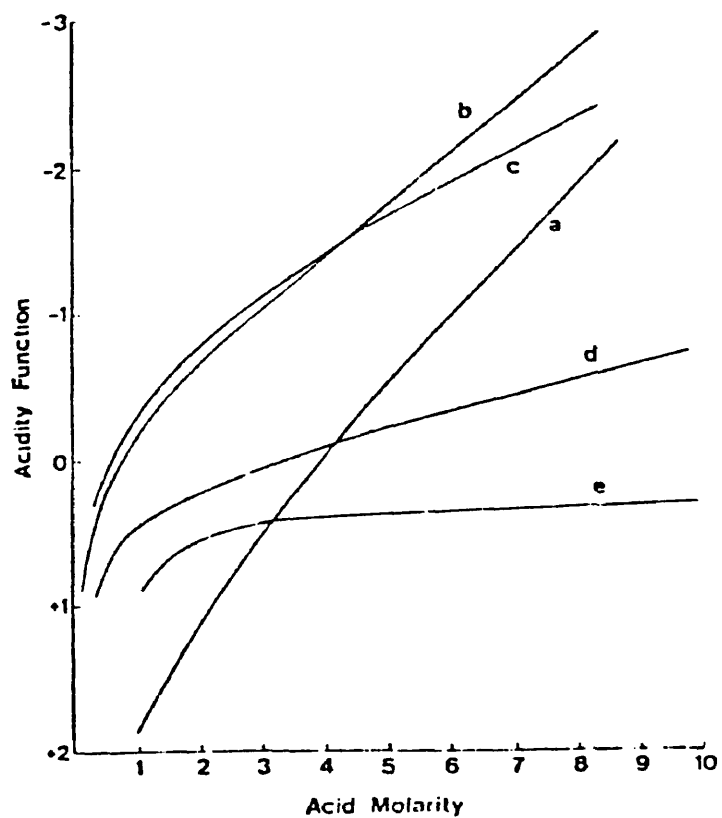
Experimental evidence shows that typical strong acids such as HCl or H₂SO₄ exhibit a large increase in their protonating power as their aqueous solutions become more concentrated. This is in contrast with weak acids such as Acetic Acid where there is very little increase.¹⁸

The Hammett acidity function showed that in dilute solution the ZnCl₂/H₂O system behaves as a weak acid.¹⁸ This low acidity of the metal aquo ion in dilute solution can be attributed to the attenuating effects of water molecules outside the hydration sphere.¹⁹ As the water content decreases, minimizing outer-sphere hydration, the protonating power of the metal salts increased rapidly. This indicates that when the metal aquo complex is rid of outer sphere water molecules, it becomes a very strong acid.¹⁸ (See fig #2 and #3.)

Due to these facts there has been much interest in concentrated electrolyte solutions in which the water content is insufficient to satisfy more than the first coordination sphere of the ions.²⁴ Such systems have been termed as "hydrate melts."²⁵ Particular interest has arisen from the studies of molten salt hydrates containing multivalent cations such as Mg²⁺, Zn²⁺, and Ca²⁺ which bind water strongly.²⁵⁻³¹ These melts are considered fused salts of large

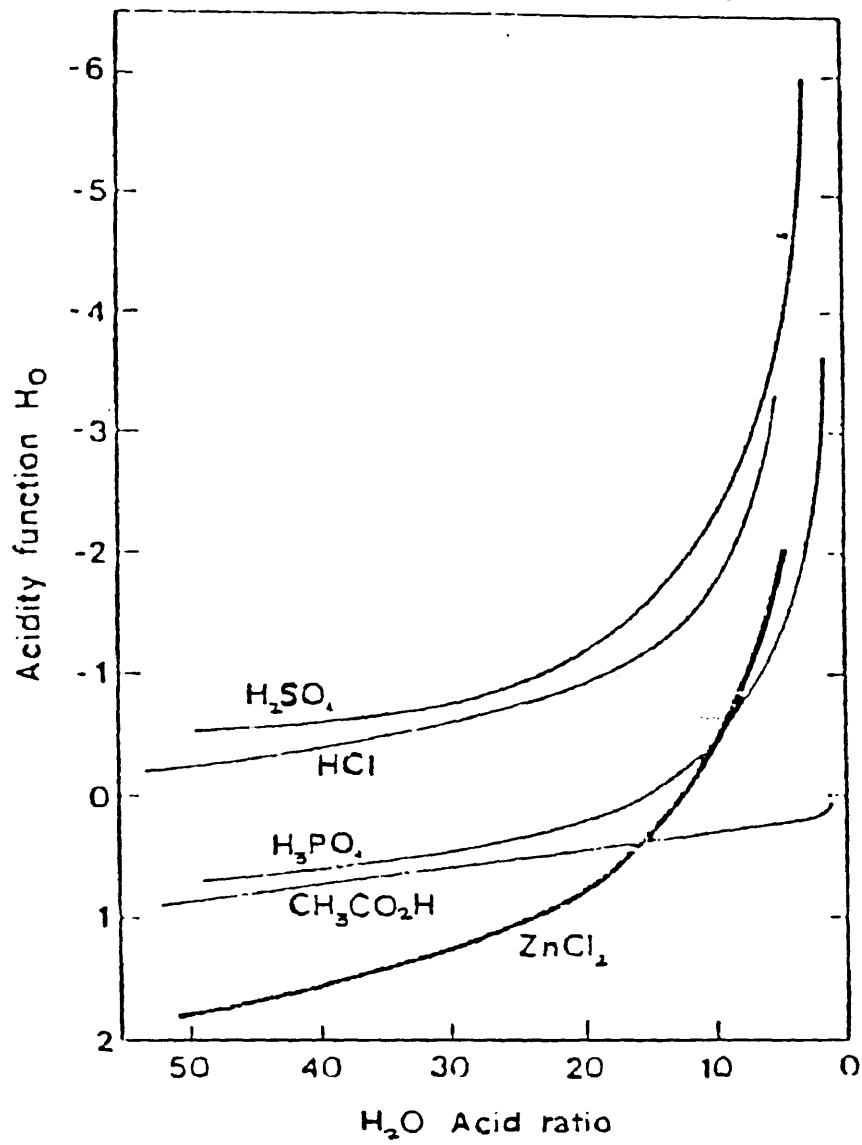
FIGURE # 2

Trend in the Hammett Acidity Function, H_0 , with molarity for aqueous solutions of : (a) $ZnCl_2$ (b) HCl (c) HNO_3 (d) H_3PO_4 (e) CH_3CO_2H



(adapted from reference # 19)

FIGURE # 3



(adapted from reference # 22)

hydrated multivalent cations such as $\text{Ca}(\text{H}_2\text{O})_4^{2+}$ or $\text{Mg}(\text{H}_2\text{O})_6^{2+}$.²⁵⁻²⁷

Many of these molten salt hydrates are liquids at low temperatures which is very unusual for solutions of their ionic strength.² In effect they are highly concentrated ionic liquids with a low H_2O to metal ratio.¹⁹

Molten salt hydrates readily dissolve weak organic bases and their protonating power is so great the acidity is measurable only on the Hammett acidity scale¹⁸, where the Hammett acidity function is defined as: $\text{H}_0 = \text{p}K_{\text{BH}^+} + \log ([\text{B}]/[\text{BH}^+])$

Since there is a linear relationship between concentration and absorbance, the ratio of base to conjugate acid in the molten salt hydrate is taken as $A_{\text{B}}/A_{\text{BH}^+}$, where A_{B} is the experimental absorbance of the base and A_{BH^+} is the difference between the experimental absorbance of the diluted solution and A_{B} .¹⁸

However, extensive use of organic indicators is limited due to decomposition reactions, especially oxidation, of the indicator. These decomposition reactions can be eliminated to an extent by mixing the acidic metal hydrates with $\text{Ca}(\text{NO}_3)_2 \cdot 4\text{H}_2\text{O}$ to form supercooled melts which remain liquids at room temperature for extended periods of time.³²

Molten $\text{Ca}(\text{NO}_3)_2 \cdot 4\text{H}_2\text{O}$ does not protonate any of the base indicators to a measurable extent. However, additions of even small amounts of HNO_3 causes a large increase in acidity. For example, a mixture of 0.047 mole % HNO_3 in $\text{Ca}(\text{NO}_3)_2 \cdot 4\text{H}_2\text{O}$ (which is 0.0035M) has $\text{H}_0 = -0.62$. This is comparable in acidity to 2M HNO_3 in aqueous solution.³²

Experimental results of Schiavelli and Ingram³² show that the addition of various mole % of HNO_3 , $\text{Al}(\text{NO}_3)_3 \cdot 9\text{H}_2\text{O}$, and $\text{Cd}(\text{NO}_3)_2 \cdot 4\text{H}_2\text{O}$ to the "solvent" $\text{Ca}(\text{NO}_3)_2 \cdot 4\text{H}_2\text{O}$ gives a linear relationship between H_0 and the log of the mole % of solute (See figure #4)

Extrapolation of this data gives a $H_0 = -2.1$ for pure $\text{Al}(\text{NO}_3)_3 \cdot 9\text{H}_2\text{O}$ which correlates very well with a value of $H_0 = -2.3$ predicted by ^1H NMR results of the pure melt.³³ This confirms the expectations that ^1H NMR shift and protonation of organic indicators respond very similarly to changes in proton acidity.^{18,19,22}

^1H NMR Studies of Concentrated Electrolyte

Solutions and Molten Salt Hydrates

A variety of experimental and theoretical studies have shown the dependence of nuclear magnetic resonance absorbance frequencies upon the electronic environment of the nucleus.³³⁻³⁶

In aqueous acid and electrolyte solutions the position of the proton magnetic resonance shift was found to be dependent upon the concentration of the solution and the extent of dissociation of the electrolytes in solution. Since fast chemical exchange averages the chemical shift of the proton over the different chemical species, the proton resonance was a singlet in these solutions.³⁷

Experimental evidence shows that in concentrated solutions of HNO_3 , HClO_4 , and H_2SO_4 there is incomplete dissociation resulting in a variety of interactions between acid anions and protons which is evidenced by increasing deviations from linearity of the plot of

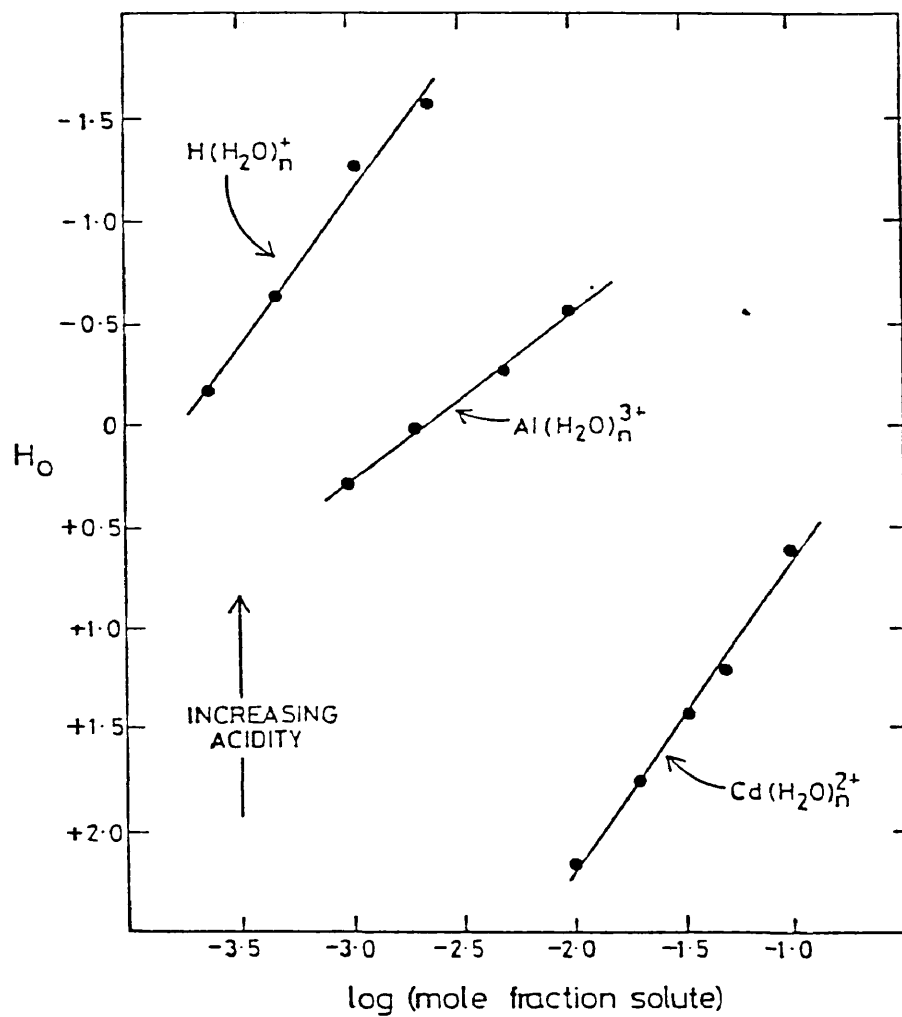
δ vs mole fraction of protons present as H_3O^+ .³⁷ (See figure #5.)

FIGURE # 4

Hammett Acidity trends of Molten Salt Hydrates in

$\text{Ca}(\text{NO}_3)_2 \cdot 4\text{H}_2\text{O}$ at 25°C

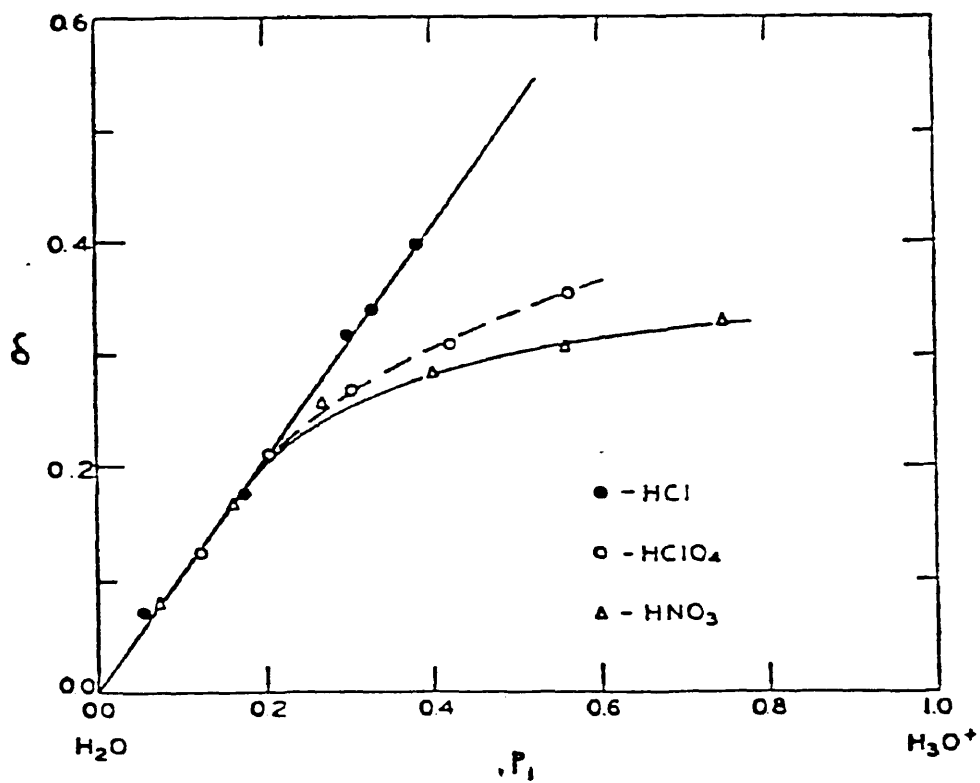
semilogarithmic plots of H_0 vs. $\log(\text{mole fraction of solute})$



(adapted from reference # 32)

FIGURE # 5

The concentration dependence of the proton chemical shift in aqueous solutions of strong monobasic acids, where p_1 is the fraction of protons present in H_3O^+



(adapted from reference # 37)

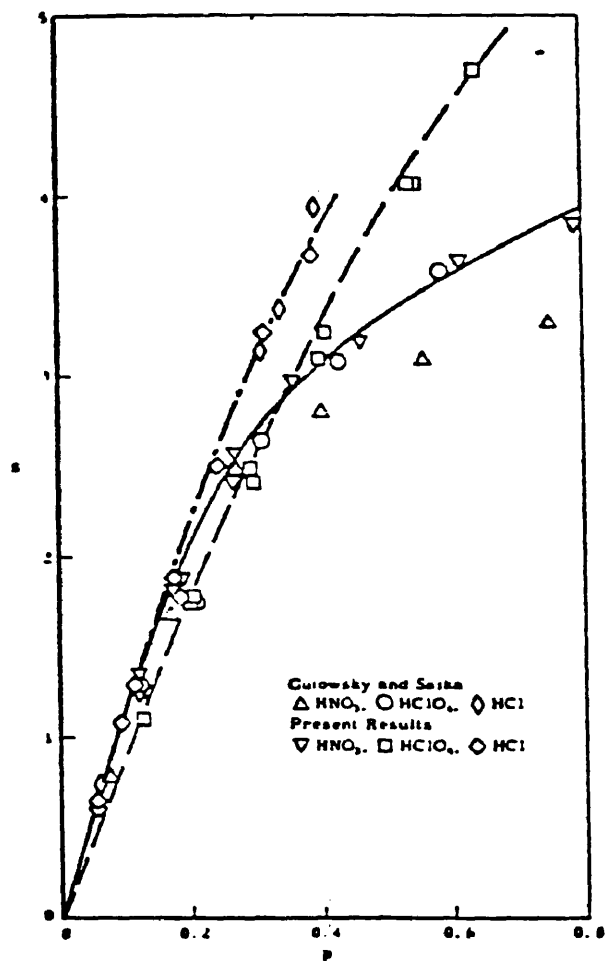
Quantitative studies³⁸ regarding the incomplete dissociation of Nitric Acid, concluded the deviations are due to the presence of nitrate and hydrogen ions at the lower range and nitrate and nitronium ions at the upper range.

The observed resonance shift (S or δ) is shown as a function of the quantity p where $p = 3x/(2-x)$ and x is the stoichiometric mole fraction of acid. Therefore, the quantity p is the stoichiometric or apparent mole fraction of the hydrogen in H_3O^+ , on a total hydrogen basis.^{37,38} (See figure #6.)

Several pmr studies³⁹⁻⁴⁴ have shown that the addition of electrolytes to water induce a displacement of the water proton magnetic resonance signal and that the magnitude and direction of displacement depends on the concentration and nature of the electrolyte ion. Hindman³⁹ has postulated that upfield shifts are caused by disruption of the bulk water hydration bonds in forming primary and secondary hydration spheres, and the downfield shifts are due to polarization and proton deshielding of water in the primary ionic hydration spheres and to non-electrostatic interactions between molecules and polarizable non-inert gas configuration cations.

In the hydrate melts there are no bulk water structures or any non-inert gas configuration cations. Therefore, the changes in the position of the water proton magnetic resonance signal with changes in the melts cationic composition can be ascribed to changes in the extent of proton deshielding due to cationic polarization of the water molecule.²⁴

Hindman³⁹ also suggested that the efficiency of the cation in



(adapted from reference # 38)

inducing polarization and ^1H deshielding in a water molecule bound in the primary hydration layer, increases with increasing charge to radius-squared ratio (z/r^2) of the cation, if the bound water molecule exhibits a constant orientation with respect to the cation.

Consequently the transfer of water molecules from one cation to another of larger z/r^2 , in a hydrate melt, is expected to cause a downfield shift in the water proton resonance.²⁴ For example, the addition of a comparatively small concentration of $\text{Mg}(\text{NO}_3)_2 \cdot 6\text{H}_2\text{O}$ to $\text{Ca}(\text{NO}_3)_2 \cdot 4\text{H}_2\text{O}$ produces a relatively large downfield shift of the water proton resonance signal since the much larger z/r^2 ratio of Mg^{2+} favors both its selective hydration and proton deshielding when Mg^{2+} is permitted to compete with Ca^{2+} for available water.²⁴

Later studies by Hester and Ellis⁴⁵ have shown that the chemical shift was not simply a function of the ionic potentials of the cations. The three metal ions studied, Mg^{2+} , Zn^{2+} , and Ca^{2+} have ionic radii of 0.65, 0.74, and 0.99 Å respectively. The molten nitrate melt containing 4 H_2O per mole, gave shifts in the order of $\text{Zn}^{2+} > \text{Mg}^{2+} > \text{Ca}^{2+}$ (increasing downfield shifts relative to TMA ion).

In addition the observed chemical shift was found to depend strongly on the nature of the anion present. Results show Mg^{2+} with 4 H_2O has shifts in order of $\text{OAc}^- > \text{NO}_3^- > \text{ClO}_3^-$ (See table #2.) Although the anion binds water less strongly than a cation, the effect of the anion binding on the magnetic screening of the water molecule can have a pronounced effect on the pmr spectra.⁴⁵

Anion binding of water must occur directly through the protons,

TABLE # 2

Water chemical shifts, δ (downfield from tetramethylammonium ion), from aqueous molten salts at 95°

System	$\delta(\pm 0.02)$ (p.p.m.)	$\delta(\pm 1)$ (c./sec.)
Zn(NO ₃) ₂ ·6.3H ₂ O	2.16	130
Zn(NO ₃) ₂ ·6.0H ₂ O	2.22	133
Zn(NO ₃) ₂ ·3.5H ₂ O	2.40	144
Mg(NO ₃) ₂ ·Zn(NO ₃) ₂ ·7.7H ₂ O	2.05	123
Mg(NO ₃) ₂ ·6.2H ₂ O	1.93	116
Mg(NO ₃) ₂ ·3.1H ₂ O	1.95	117
Mg(ClO ₃) ₂ ·6.0H ₂ O	1.63	98
Mg(ClO ₃) ₂ ·5.5H ₂ O	1.62	97
Mg(ClO ₃) ₂ ·4.5H ₂ O	1.60	96
Mg(OAc) ₂ ·4.0H ₂ O	2.16	130
Ca(NO ₃) ₂ ·4H ₂ O	1.28	77 ¹⁰

(adapted from reference # 45)

while cation binding is associated primarily with the oxygen atom. Therefore the transmission of the polarizing field effect of the cation must pass through the O-H chemical bond to affect the protons. Therefore it seems reasonable to describe aqueous molten salts in terms of extensively disordered lattice structures, whereby water molecules are polarized between anions and cations, feeling the effects of both simultaneously.⁴⁵

Increasing temperatures causes a linear upfield shift of the water proton resonance in $\text{Ca}(\text{NO}_3)_2 \cdot 4\text{H}_2\text{O}$ of magnitude of $4.0 \times 10^{-3} \pm 0.5 \times 10^{-3}$ ppm/deg C.²⁴ This may be compared with the temperature coefficient of δ reported for pure water which is $9.5 - 10.2 \times 10^{-3}$ ppm/deg C.^{41,44,46} The upfield shift of the proton resonance with increasing temperature in pure H_2O has generally been attributed to a decrease in hydrogen bonding.⁴⁷

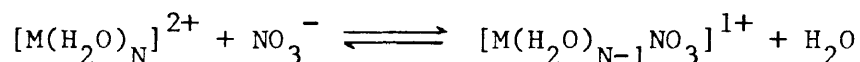
One explanation for the water molecule in the primary hydration sphere of the cation contributing to the temperature dependence of the water proton chemical shift, is that the water molecule - metal ion orientation of minimum potential energy in a hydrated species is also the orientation which effects maximum proton deshielding.³⁹ This is probably the orientation in which the axis of the oxygen-cation bond bisects the H-O-H angle in the water molecule. As the temperature is increased the thermal energy of the water molecule permits increasing deviations of the average H_2O -ion orientation from that of minimum potential energy and hence observed upfield shifts of the water resonance.³⁹

It has been proposed by Angell²⁵ that molten salt hydrates such

as alkaline earth nitrates are somewhat similar to very concentrated electrolyte solutions, and in these melts all the water molecules are bound in the inner-sphere coordination sites around the multivalent metal ion.

Vibrational spectroscopic studies⁴⁸, on the other hand, have proposed that the nitrate ion competes effectively with water molecules for inner-sphere coordination sites around the metal ion in concentrated aqueous solutions⁴⁸ and in molten salt hydrates.⁴⁹

Hester and Ellis⁴⁵ applied this information as a possible explanation for the temperature dependence of the water protons NMR chemical shift in the molten salt hydrate system. The displacement reaction which is temperature dependent,

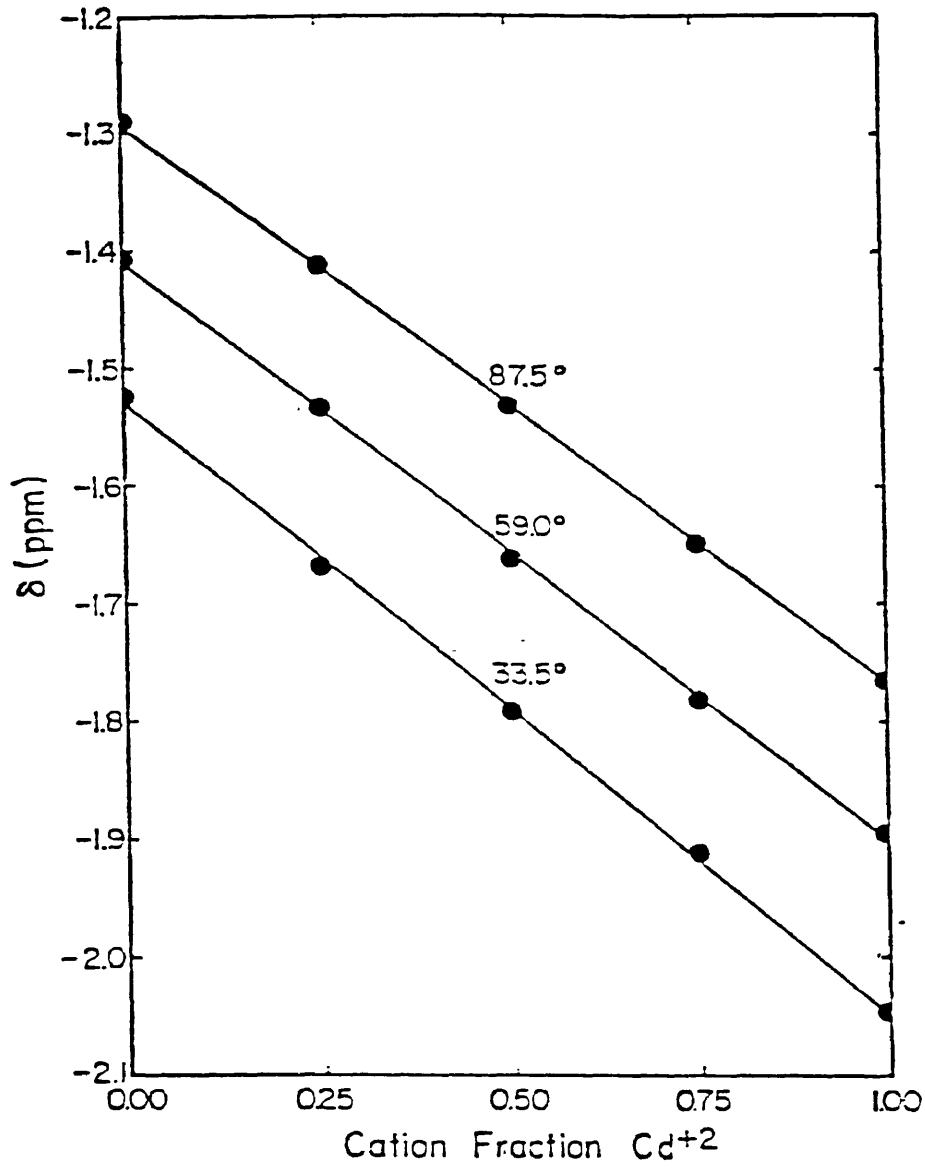


liberates the water molecule as the temperature rises. The water protons become more shielded as they move outside the primary hydration sphere of the positively charged metal ion center. These results were consistent with vapor pressure measurements made by Trip and Braunstein.⁵⁰

An alternative explanation has been suggested by studying systems in which the acidic metal hydrate is mixed with $Ca(NO_3)_2 \cdot 4H_2O$ to form a supercooled melt.² There is much interest in $Ca(NO_3)_2 \cdot 4H_2O$ systems which stem from the fact that they may be considered an ideal quasi-fused salt. PMR, conductance, and density studies indicate that virtually all the waters of hydration are retained in the coordination sphere of the polarizing Ca^{2+} ion.

The results of pmr measurements of $Ca(NO_3)_2 \cdot 4H_2O / Cd(NO_3)_2 \cdot 4H_2O$ melts with respect to the internal standard TMA ion, gives one

FIGURE # 7



(adapted from reference # 2)

proton peak due to the rapid water molecule and/or proton exchange in the hydration spheres of Ca^{2+} and Cd^{2+} . Since the water/total cation ratio is constant in these melts, the plot of the chemical shift vs composition is linear which indicates that the two ions are equally hydrated.² (See figure #7.)

If free water exists in the nitrate ion environment, as suggested by Hester and Ellis⁴⁵, then one would expect to have a proton chemical shift similar to that found in KNO_3 or $(\text{CH}_3)_4\text{NNO}_3$ solutions. However, earlier results²⁴ showed that in concentrated KNO_3 or $(\text{CH}_3)_4\text{NNO}_3$ solutions, the water proton resonance occurs well upfield from that of $\text{Ca}(\text{NO}_3)_2 \cdot 4\text{H}_2\text{O}$.

Hence the production of "free" water in these melts would have resulted in a concentration induced change in δ opposite to those found or at least cause a departure from linearity of the plot of δ vs cation fraction.²

In summary a number of possible sources of the upfield shift with increases in temperature for such hydrate melts have been suggested:^{24,45,51}

(1) Weakening or breaking of hydrogen bonds between anions and the water molecules in the cation hydration sheath.⁴⁵

(2) Changes in the relative configuration of the waters of the hydrated cationic entity itself.²⁴

(3) Changes in the magnetic anisotropic effects due to the on-set of rotation of asymmetric anions.^{51,52}

(4) A temperature dependent equilibrium involving anion-water exchange in the primary hydration sheaths of the cation.⁴⁵

Detailed considerations of each of these effects by Malinowski and Knapp⁵³ lead to the conclusion that only effect #1 is sufficiently general to account for this observed behavior. In this case a correlation should exist between the magnitude of the temperature dependence of δ and the hydrogen bond-strength indicating a pKa value for the anion.⁵³

One of the more interesting findings in these pmr studies was the magnitude of the downfield shift for $\text{Al}(\text{NO}_3)_3 \cdot 10\text{H}_2\text{O}$ solutions.²⁰ Unlike their behavior in dilute solution, aluminum salts in ultra-concentrated solutions do not hydrolyze to yield insoluble basic products. This may be because there is no bulk solvent present from which basic products could precipitate.²⁰

Under high concentration conditions, the $\text{Al}-\text{H}_2\text{O}$ interactions responsible for hydrolysis in dilute solution, produce solutions in which the protons on the water molecules are very loosely bound. This is reflected in the value of δ which is greater than HNO_3 with the same number of moles of water/moles of salt.²⁰

This is partly because the Al^{3+} ion is in direct contact with six of ten H_2O molecules present, whereas HNO_3 transfers its proton primarily to a single H_2O molecule leaving nine relatively unaffected which averages the signal to a more upfield value. Nevertheless highly concentrated solutions of $\text{Al}(\text{NO}_3)_3$ and related salts must be regarded as a class of strong protonic acids.²⁰

Values of the proton chemical shifts in dilute aqueous solutions have been studied and the results analyzed in terms of proton deshielding due to polarization of the oxygen by adjacent cations, and the attraction for water protons exercised by anions of

differing basicity.²⁰ Ellis and Hester⁴⁵ demonstrated that anion effects act to deshield the protons due to a particular orientation of the water molecule in the strong cation field.

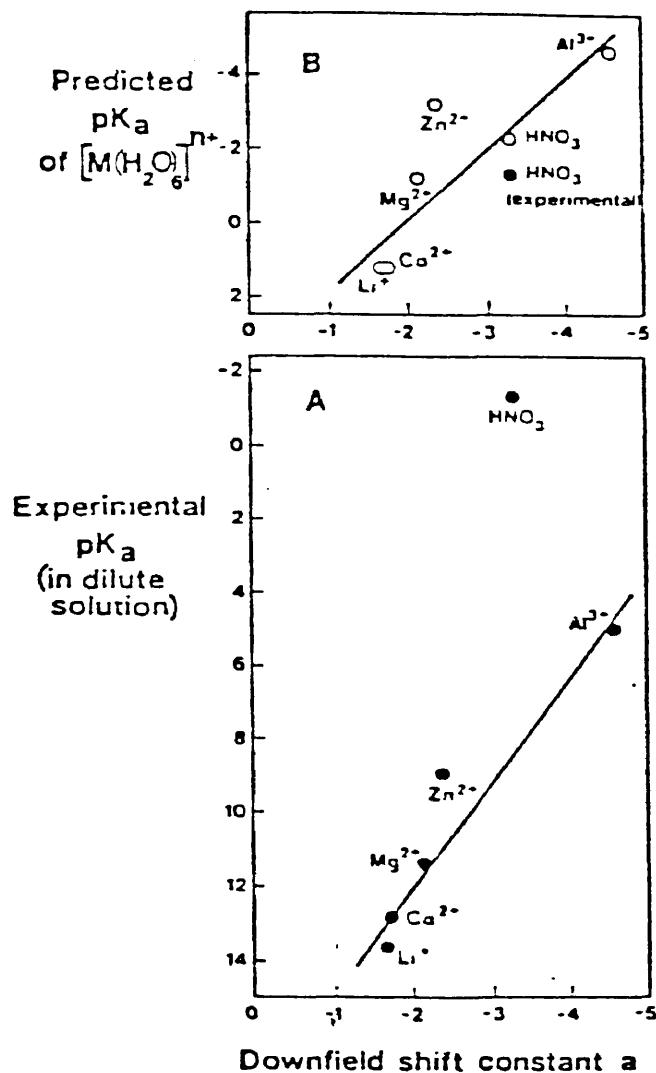
A correlation of the anion deshielding effect with known physical constants may be attempted by recognizing the relation between the proton transfer process and that which determines the strength of a weak acid. Studies by Gurney⁵⁴ have shown that the pKa value attributed to a given acid is related to the electrical work of proton transfer from the anion in question to a particular reference energy state. Since the displacement away from the H₂O oxygen implies a deshielding of the proton, hence a downfield shift in δ , δ for solutions of a given cation should move downfield with increasing anion pKa.⁵⁴

The plot of the downfield shift vs experimental pKa values of the metal aquo ions makes it apparent that the deshielding effects caused by cations such as Mg²⁺ or Zn²⁺ is fairly similar to that of Nitric Acid (see figure #8). However the extent to which the point for Nitric Acid lies off the line indicates the inadequacy of pKa values measured for metal ions in dilute solutions.²⁰ These pKa values for metal aquo ions are far too positive to do justice to the acidic properties. The predicted pKa values obtained from optical basicity calculations seem to be a better indication of the true acidity of the salt hydrates, in that the pKa values of the metal aquo ions correspond with that of HNO₃ which was predicted by ¹H NMR data.¹⁸

A study done by Zarakhani and Vinnik⁵⁵ demonstrated that the chemical shifts of proton magnetic resonance in acids depends

FIGURE # 8

^1H NMR shifts in ppm relative to TMA ion for salt hydrates $\text{M}(\text{NO}_3)_n \cdot 10\text{H}_2\text{O}$ and Nitric Acid vs. (A) experimental pK_a values and (B) predicted pK_a values from optical basicity calculations.



(adapted from reference # 18)

directly on the concentration of the acid. The chemical shift δ_H values were compared directly with the Hammett Acidity Function H_0 data for some strong acids and the relationship was found to be linear (see figure #9).

Since HCl, H_2SO_4 , $HClO_4$, and HNO_3 are almost completely dissociated in dilute solutions, this study further investigated a possible relationship between the chemical shift and the hydrogen ion activity. The acidity of the medium can be described by the equation:

$$h_0 = a_{H^+} (f_B/f_{BH^+}) = (a_{H_3O^+}/a_{H_2O}) (f_B/f_{BH^+})$$

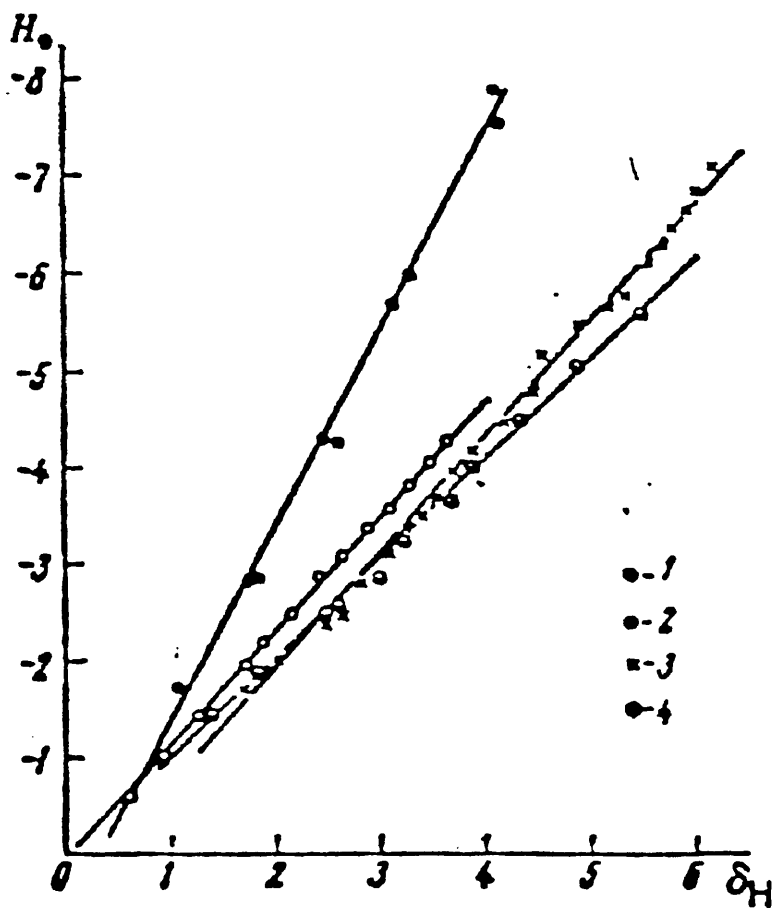
It was postulated that with changes in the acidity of the medium f_B/f_{BH^+} changes much less than $a_{H_3O^+}$. It was shown that the dependence of δ_H on $\log a_{H_3O^+} (f_B/f_{BH^+})$ is a linear relationship (see figure #10). The variance in the slopes for different acids was attributed to the influence of the anions.

Therefore it was concluded that the observed chemical shifts of the proton magnetic resonance in aqueous acid solutions characterizes the hydrogen ion activity of the solvated protons.⁵⁵

FIGURE # 9

Dependence of H_o on $\delta_H \times 10^6$

1) $HClO_4$ 2) HCl
 3) H_2SO_4 4) HNO_3

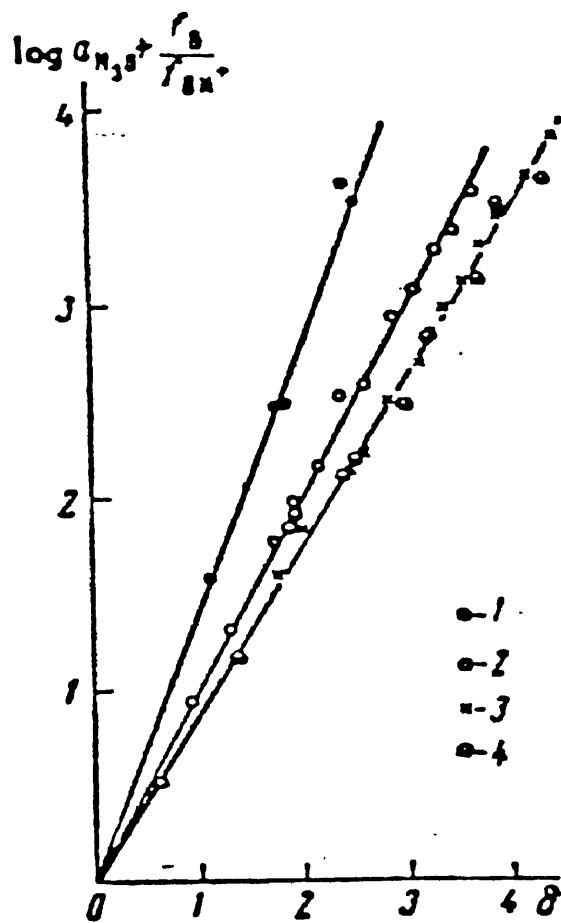


(adapted from reference# 55)

FIGURE # 10

Dependence of $a_{\text{H}_3\text{O}^+}(f_{\text{B}}/f_{\text{BH}^+})$ on $\delta \times 10^6$

1) HClO_4 2) HCl 3) H_2SO_4 4) HNO_3



(adapted from reference # 55)

In the next phase of this research project we wanted to focus on the chemical properties and reactivity of these molten salt hydrates by employing them in selected acid catalyzed reactions in order to evaluate their usefulness as a synthetic medium for performing organic chemistry.

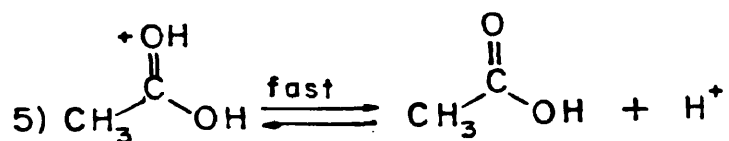
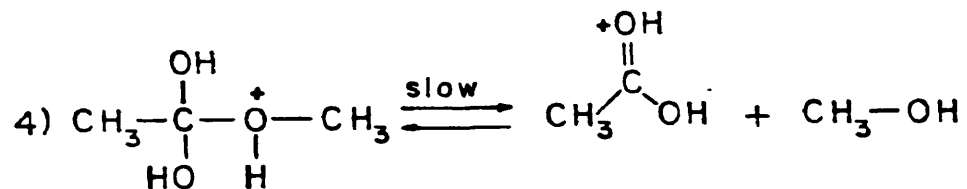
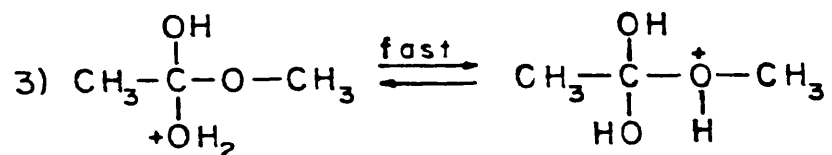
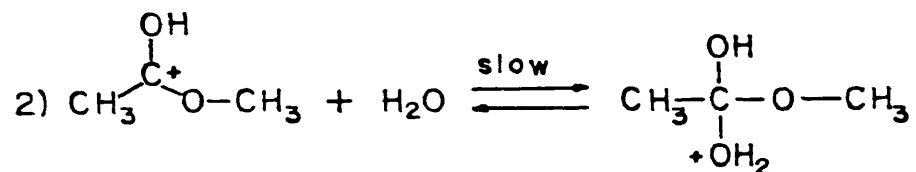
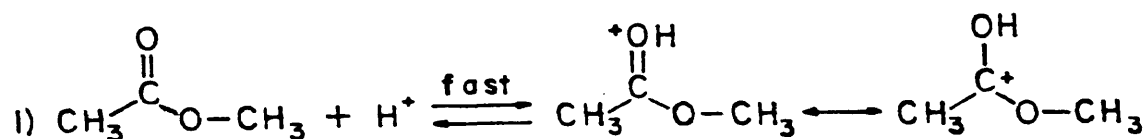
The primary reaction we wanted to concentrate on was the acid catalyzed ester hydrolysis reaction. By studying the kinetics of this reaction we felt we could obtain some valuable information and insight into the chemical nature of these hydrate melts.

We also wanted to examine the potential that this medium may possess for nitrating aromatic compounds.

Ester Hydrolysis Reaction

Esters react with water to yield the corresponding carboxylic acid and alcohol. The reaction is generally slow but is strongly catalyzed by either acid or base.⁵⁶

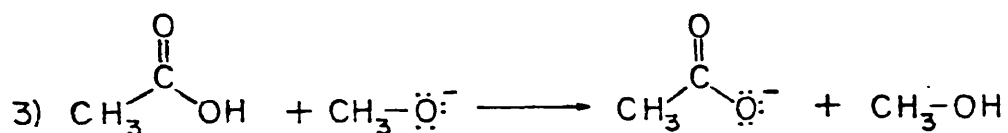
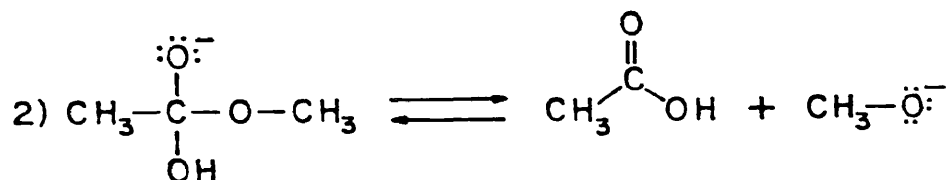
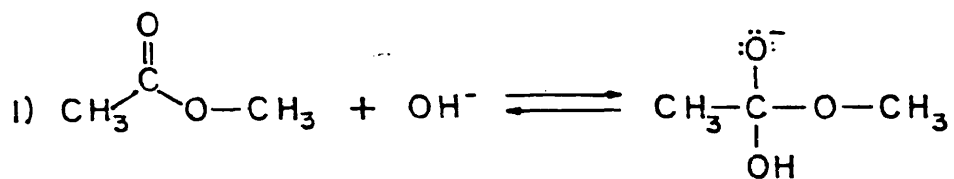
The acid-catalyzed esterification reaction is an equilibrium process but practically can be driven to completion using a large excess of water. The probable mechanism under acid-catalyzed conditions involves the following steps:



Even though the carbonyl double bond is polarized, water is not a sufficiently strong nucleophile to add to it at a reasonable rate. Furthermore, addition of water to methyl acetate would produce an intermediate bearing both a positive and negative charge. Since charge separation requires electronic energy, this type of addition is exceptionally slow.⁵⁶

In the presence of mineral acids, the ester may be protonated, which makes the species much more electrophilic and reacts much faster with the weak nucleophile, water, than does the unprotonated ester, also the addition involves no charge separation.⁵⁶

A Saponification reaction or base-catalyzed ester hydrolysis has the following probable mechanism:



In aqueous base, two nucleophiles are present, H_2O and OH^- . Since OH^- is a much stronger nucleophile than H_2O , it adds much more rapidly to the carbonyl carbon. After the addition has taken place, elimination of either the nucleophile, reversing the initial addition, or the methoxide ion, giving acetic acid, may occur.⁵⁶

Since acetic acid is a weak acid and the methoxide ion is a strong base, a rapid acid-base reaction then occurs, yielding acetate ion and methanol. Because of the great difference in acidity between acetic acid ($pK_a \sim 5$) and methanol ($pK_a \sim 16$), this last step is essentially irreversible.⁵⁶

In ester hydrolysis one extra complication is introduced because the cleavage of either of two bonds leads to the same product.⁵⁷

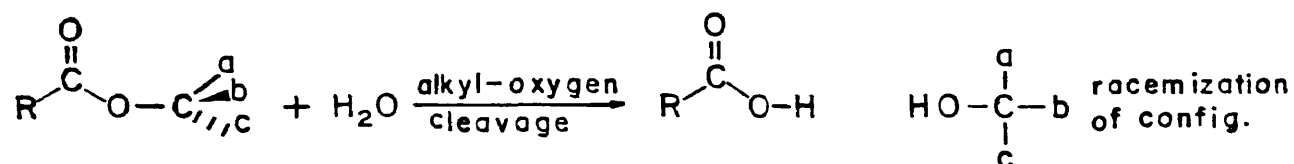
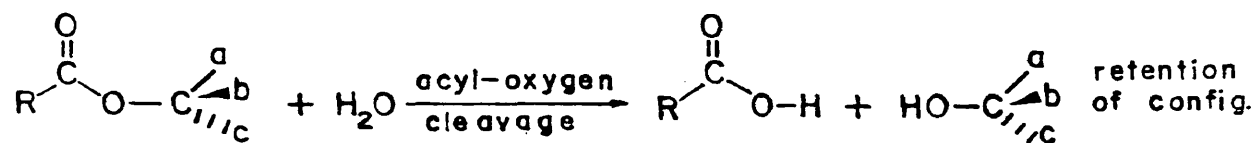
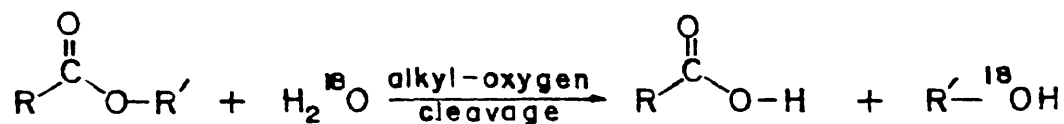
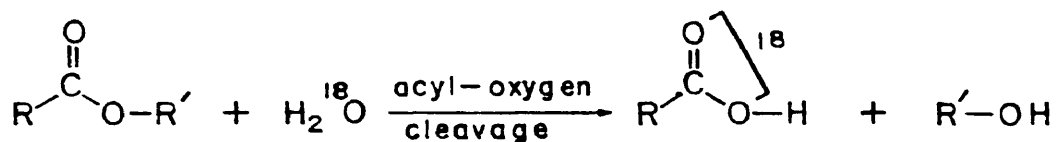
Acyl-Oxygen Cleavage:



Alkyl-Oxygen Cleavage:



The occurrence of acyl-oxygen or alkyl-oxygen cleavage may be determined by isotopic labeling⁵⁸ and by stereochemical methods.⁵⁹



Ingold⁶⁰ has classified the acid -and base- catalyzed hydrolysis of esters into eight possible mechanisms, depending on the following conditions:

- (1) Acid or base catalyzed.
- (2) Unimolecular or bimolecular.
- (3) Acyl or alkyl cleavage.

All eight of these are S_N1 , S_N2 , or tetrahedral mechanisms. Of the eight only six have actually been observed in the hydrolysis of carboxylic esters.

The two most common ester hydrolysis mechanisms are $A_{AC}2$ (acid-catalyzed, acyl-oxygen cleavage, bimolecular) and $B_{AC}2$ (base-catalyzed, acyl-oxygen cleavage, bimolecular).⁶¹ (See figure #11.)

$A_{AC}1$ mechanism involving the acyl-oxygen cleavage are rare, being found only when R is very bulky, so bimolecular attack is sterically hindered, and then only in ionizing solvents. The $B_{AC}1$ mechanism has yet to be observed.⁵¹

The mechanisms involving alkyl-oxygen cleavage are ordinarily S_N1 and S_N2 mechanisms in which OCOR (acyloxy group) or its conjugate acid is the leaving group. Two of these mechanisms $B_{AL}1$ and $A_{AL}1$ occur readily when R' comes off as a stable carbonium ion, such as when R' is a tertiary alkyl, allyl, benzyl, etc. The $B_{AL}2$ mechanism is very rare and $A_{AL}2$ has yet to be observed.⁶¹

Bunnett⁶² proposed a criterion for distinguishing A-1 and A-2 hydrolysis mechanisms, which is applicable to the ester hydrolysis reaction. The Bunnett equation states:

$$\log K_{OBS} + H_O = w \log a_{H2O} + C$$

		Basic catalysis		Acid catalysis	
		Alkyl cleavage	Acyl cleavage	Alkyl cleavage	Acyl cleavage
Name	Type				
AAC1	SN1	$ \begin{array}{c} \text{R}-\text{C}-\text{OR}' \xrightleftharpoons{\text{H}^+} \text{R}-\text{C}^{\oplus}-\text{OR}' \rightleftharpoons \text{R}-\text{C}-\text{OR}'^{\oplus} \xrightarrow{\text{H}_2\text{O}} \text{R}-\text{C}^{\oplus}-\text{OH} \xrightarrow{\text{ROH}} \text{R}-\text{C}-\text{OR}'^{\oplus} \xrightarrow{\text{H}_2\text{O}} \text{R}-\text{C}-\text{OH}_2^{\oplus} \xrightarrow{\text{ROH}} \text{R}-\text{C}-\text{OH} \xrightarrow{\text{H}^+} \text{R}-\text{C}-\text{OH} \\ \text{A} \qquad \qquad \qquad \text{B} \qquad \qquad \qquad \text{C} \qquad \qquad \qquad \text{D} \end{array} $			
		$ \text{R}-\text{C}-\text{OR}' \xrightleftharpoons{\text{H}^+} \text{R}-\text{C}^{\oplus}-\text{OR}' \xrightarrow{\text{H}_2\text{O}} \text{R}-\text{C}-\text{OH}_2^{\oplus} \xrightarrow{\text{ROH}} \text{R}-\text{C}-\text{OH} \xrightarrow{\text{H}^+} \text{R}-\text{C}-\text{OH} $			
AAC2	Tetra- hedral	$ \text{R}-\text{C}-\text{OR}' \xrightleftharpoons{\text{H}^+} \text{R}-\text{C}^{\oplus}-\text{OR}' \xrightarrow{\text{H}_2\text{O}} \text{R}-\text{C}-\text{OH}_2^{\oplus} \xrightarrow{\text{ROH}} \text{R}-\text{C}-\text{OH} \xrightarrow{\text{H}^+} \text{R}-\text{C}-\text{OH} $			
AAL1	SN1	$ \text{R}-\text{C}-\text{OR}' \xrightleftharpoons{\text{H}^+} \text{R}-\text{C}^{\oplus}-\text{OR}' \xrightarrow{\text{H}_2\text{O}} \text{R}-\text{C}-\text{OH}_2^{\oplus} \xrightarrow{\text{ROH}} \text{R}-\text{C}-\text{OH} \xrightarrow{\text{H}^+} \text{R}-\text{C}-\text{OH} $			
AAL2	SN2	$ \text{R}-\text{C}-\text{OR}' \xrightleftharpoons{\text{H}^+} \text{R}-\text{C}^{\oplus}-\text{OR}' \xrightarrow{\text{H}_2\text{O}} \text{R}-\text{C}-\text{OH}_2^{\oplus} \xrightarrow{\text{ROH}} \text{R}-\text{C}-\text{OH} \xrightarrow{\text{H}^+} \text{R}-\text{C}-\text{OH} $			
BAC1	SN1	$ \text{R}-\text{C}-\text{OR}' \xrightarrow{\text{slow}} \text{R}-\text{C}^{\oplus} + \text{OR}'^- \xrightarrow{\text{OH}^-} \text{R}-\text{C}-\text{OH} + \text{OR}'^- \longrightarrow \text{R}-\text{C}-\text{O}^- + \text{ROH} $			
BAC2	Tetra- hedral	$ \text{R}-\text{C}-\text{OR}' \xrightarrow{\text{slow}} \text{R}-\text{C}-\text{OR}' \xrightarrow{\text{OH}^-} \text{R}-\text{C}-\text{OH} + \text{OR}'^- \longrightarrow \text{R}-\text{C}-\text{O}^- + \text{ROH} $			
BAL1	SN1	$ \text{R}-\text{C}-\text{OR}' \xrightarrow{\text{slow}} \text{R}-\text{C}-\text{O}^- + \text{R}'^+ \xrightarrow{\text{H}_2\text{O}} \text{R}'\text{OH}_2^{\oplus} \xrightarrow{\text{OH}^-} \text{R}'\text{OH} $			
BAL2	SN2	$ \text{R}-\text{C}-\text{OR}' \xrightarrow{\text{OH}^-} \text{R}-\text{C}-\text{O}^- + \text{R}'\text{OH} $			

(adapted from reference # 61)

It was shown that for a large number of organic reactions the plot of $\log K + H_0$ is linear with respect to the $\log a_{H_2O}$ of the reaction medium. The slopes of these plots (W) vary over a wide range, and on the basis of comparison with reactions of known mechanisms, it is possible to group ester hydrolysis reactions into four types according to the magnitude of the W parameter and the role of water in the rate determining step.⁶²

The theoretical interpretation of W is that it is a measure of the transition-state hydration requirements on a scale relative to the difference in hydration changes between protonating a substrate molecule and a Hammett indicator base.⁶³

The Bunnett treatment has been modified by Yates and his co-workers⁶⁴ in an attempt to minimize the extent of the necessary approximations and to simplify the interpretation of observed water activity dependence.

$$\log K + M H_0 = r \log a_{H_2O} + C$$

Where M is a constant (0.62) to correct the H_0 scale. The water activity dependence r corresponds closely to the number of water molecules required to convert a protonated substrate to the transition state, or the approximate "order" of the reaction in water. Therefore, the values of r obtained in different acid regions can reasonably be interpreted in terms of hydrolysis mechanisms.⁶³

Regions where $r=2$ corresponds to hydrolysis by the A_{AC}^2 mechanism. Areas where r becomes negative but is fairly close to zero ($r=-0.2$) corresponds to the A_{AC}^1 mechanism. Water is essentially not involved in the rate determining step, hence the

water activity dependence is effectively zero.⁶⁵ Regions where r is negative but significantly less than zero ($r=-0.5$) corresponds to a unimolecular fission of the protonated ester by the A_{AL}^1 mechanism. The strongly negative water activity dependence indicates water is actually being released in the rate determining step, which is reasonable for a strongly hydrated ester conjugate acid being converted to a weakly hydrated carbonium ion.⁶⁵

As proposed by Bunnett and reaffirmed by Yates, there are four different types of ester hydrolyses as predicted by rate-acidity profiles.⁶³

Type I is characterized by an initial steady increase in rate with acid concentration, passing through a local maximum at 50-60% H_2SO_4 followed by a rate decrease almost to zero, then a final modest increase in highly concentrated (> 90%) acid. This behavior is typical of primary alkyl acetates.⁶³

Type II is similar except that the rate maximum occurs at a significantly lower value of k , whereas the final rate increase occurs much earlier, is much sharper, and is strongly structure dependent. The behavior has been found to be typical of secondary alkyl, benzyl, and allyl acetates.⁶³

Type III shows no observable rate maximum, although the rate increases in moderately concentrated acid regions in a fashion similar to Type I and II. However the rates continue to increase until they are too fast to follow by conventional methods by about 70% H_2SO_4 . This behavior has been found for vinyl and substituted phenyl acetates.⁶³

Type IV resembles the previous cases in that there is only a monotonic rate increase with acidity, but it is much sharper, and extremely rapid even in dilute acids. This behavior is found only for *t*-butyl and *p*-methoxy benzyl acetate.⁶³ (See figure #12 and 13.)

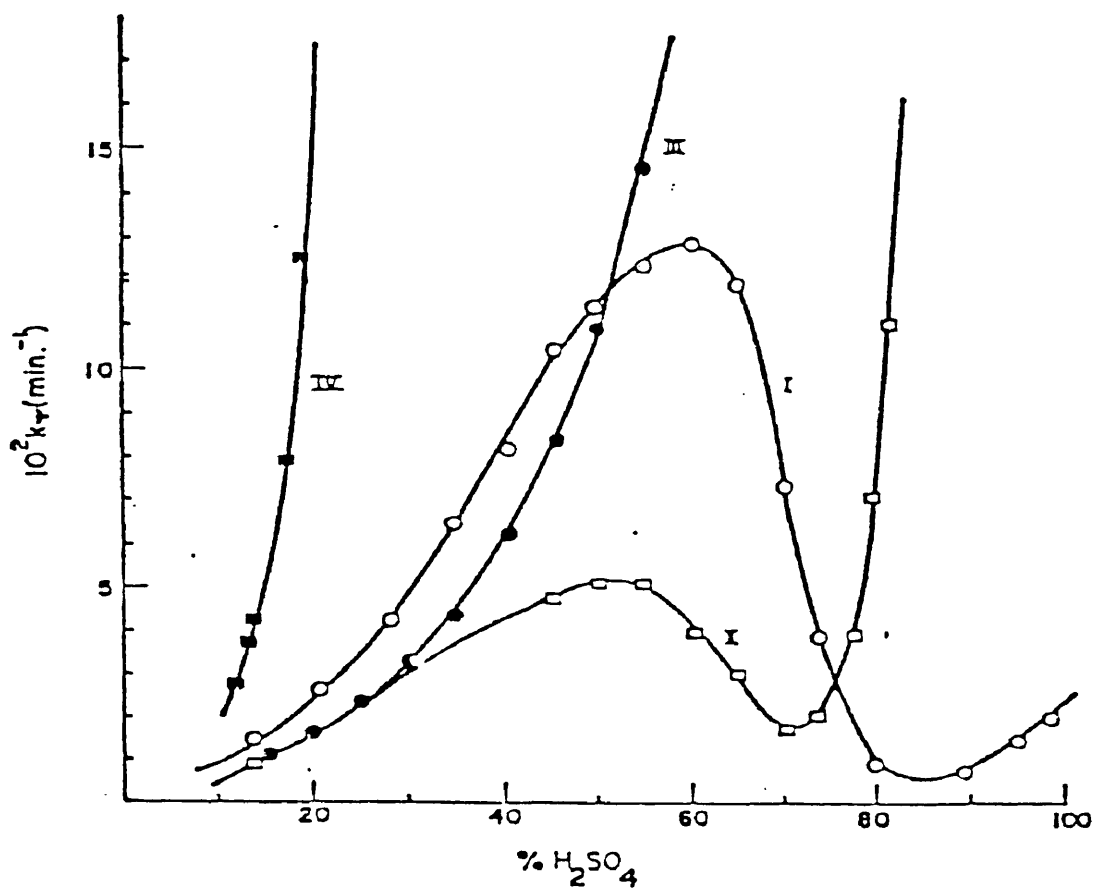
The early rate maxima for type I and II esters are easily understood in terms of the normal $A_{AC}2$ mechanism.⁶³ At about 60% H_2SO_4 further increases in concentration of the reactive ester conjugate acid, brought about by increasing acidity, are more than offset by the rapidly decreasing availability of water required for the bimolecular hydrolysis step. The final rate increase in still more concentrated acids where a_{H_2O} is extremely small, suggests a gradual transition to an A_1 process.⁶³ Confirmation of this was obtained from exchange studies on ^{18}O -labeled esters of type I and II at various acidities.⁶⁶

Hydrolysis of primary esters change from a predominant $A_{AC}2$ mechanism below 90% H_2SO_4 to the $A_{AC}1$ mechanism in more concentrated acids where the acylium ion is generated. The secondary, benzyl, and allyl esters change from the $A_{AC}2$ to the $A_{AL}1$ mechanism. This is consistent with the fact that their rate profiles are more structure dependent. The acidity at which the final sharp rate increase occurs/corresponds roughly to the order of the stability of the carbonium ion being generated in the $A_{AL}1$ process.⁶³

It seems reasonable that type III esters undergo changes in mechanism at higher acidities. Assuming that vinyl and phenyl acetates are also initially hydrolyzed by the $A_{AC}2$ process, the fact that their rates continue to increase even more sharply even when

FIGURE # 12

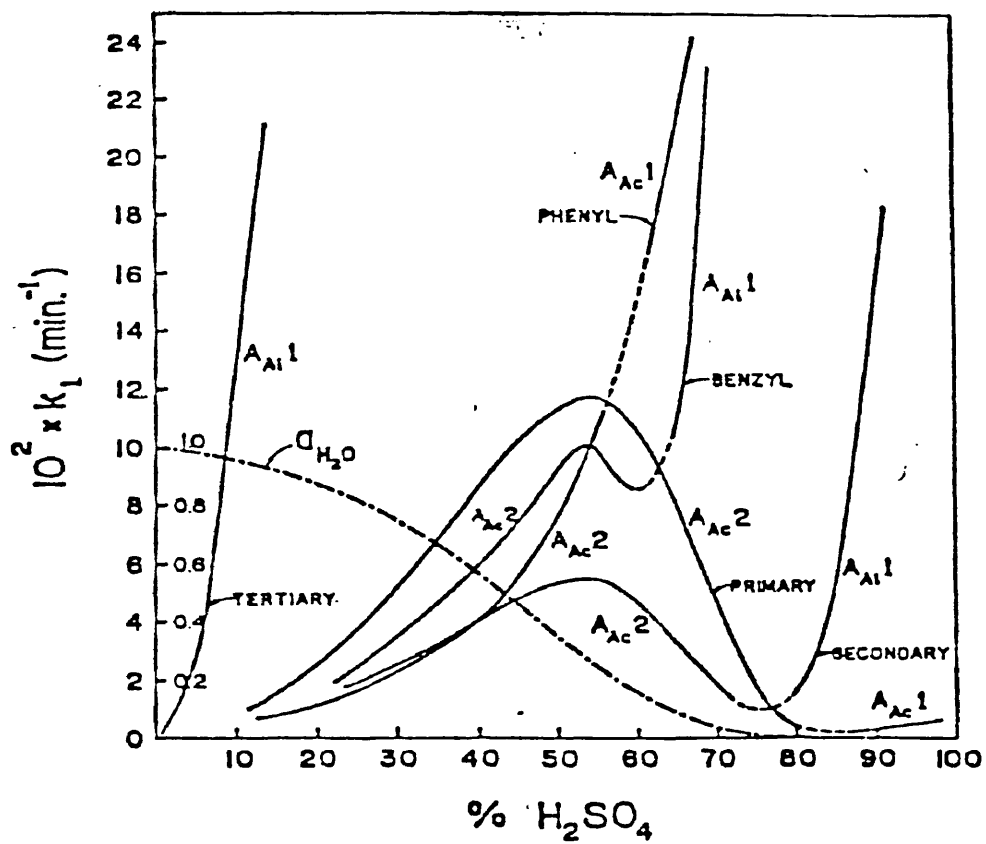
Typical rate profiles for acetate hydrolysis: type I, primary alkyl acetates; II, secondary alkyl, benzyl, and allyl acetates; III, vinyl, phenyl, and substituted phenyl acetates; IV, t-butyl, and p-methoxybenzyl acetate.



(adapted from reference # 63)

FIGURE # 13

Typical rate - acidity dependence for primary, secondary, tertiary, benzyl, and phenyl acetate hydrolysis.



(adapted from reference #65)

$a_{\text{H}_2\text{O}}$ becomes extremely small cannot be explained by the A_{AC}^2 process over the whole acid range. Of the two possible alternative mechanisms, A_{AL}^1 can be ruled out since phenyl carbonium ions are very unlikely. Therefore the mechanism apparently changes to the A_{AC}^1 process. This is consistent with the fact that the observed order of reactivity of substituted phenyl acetates in the 0-5% acid region is exactly reversed in more concentrated acids.⁶³

Of the remaining esters, tert-butyl acetate probably reacts by the A_{AL}^1 mechanism over the whole acidity range. Bunton and Wood⁶⁷ have demonstrated by ^{18}O -exchange studies that t-butyl acetate undergoes the Alkyl-oxygen fission in the dilute and moderately concentrated acid regions.

Unlike the other benzyl acetates, p-methoxybenzyl acetate resembles t-butyl acetate closely in its rate profile, suggesting that the stability of the p-methoxy benzyl cation is sufficient to give rise to the A_{AL}^1 hydrolysis mechanism. However in dilute acids ^{18}O -tracer studies show that initially the hydrolysis has a large A_{AC}^2 component, much like other benzyl esters.⁶³

Of the various kinetic treatments used for proposing mechanisms of acid-catalyzed ester hydrolysis reactions such as the Bunnett hydration parameter treatment⁶² and the Yates modification or r-parameter treatment⁶⁵, these all require assumptions leading to the cancellation of important activity coefficient terms. Also they depend heavily upon the Hammett acidity function and linear logarithmic relationships.⁶⁸

A simpler treatment has been proposed which is based on the transition-state theory, which uses the hydronium ion activities

directly. This approach does not involve any assumptions concerning acidity functions, water activity, or hydration parameters. There is no cancellation of activity coefficient ratios and it is not dependent on linear logarithmic relationships.⁶⁹

The activity coefficient f^*s^{\wedge} can be determined by the equation:

$$\log f^*s^{\wedge} - \log k_0 = \log a_H^* - \log k + \log f_S - \log K_{SH^+}$$

Where k_0 is the rate constant for the slow step, K_{SH^+} is the dissociation constant for the protonated substrate, f_S is the substrate activity coefficient, k is the observed pseudo-first order rate constant, and a_H^* is the proton activity.⁶⁸ The parameters a_H^* , k , and f_S can be experimentally determined. Since the $\log f^*s^{\wedge}$ must approach zero in dilute acid solutions, a plot of $\log (f^*s^{\wedge}/k_0)$ vs acid concentration gives a value of $-\log k_0$ as the intercept. Therefore it is possible to estimate medium variations of the transition state activity coefficient for any acid-catalyzed reaction.⁶⁸

The behavior of $\log f^*s^{\wedge}$ as a function of some parameter of the reaction medium such as acid concentration or water activity, should then reflect the solvation requirements or characteristics of the transition state. This behavior can be interpreted in terms of possible transition-state structures, and thus provide important mechanistic information.⁶⁹

According to the A2 mechanism, nucleophilic attack by water results in the rate-determining formation of the tetrahedral intermediate. In the alternative A1 mechanism the unimolecular cleavage of either the acyl-oxygen ($A_{AC}1$) or the alky-oxygen ($A_{AL}1$)

bond occurs, and the intermediate acylium or carbonium ion is formed in the rate determining step.⁶⁸

In the case of the bimolecular mechanism A2, the intermediate and/or transition state has the character of an oxonium ion, with a carbon bound to three oxygen atoms, which is a structure with a high demand for hydration (hydrogen bonding) stabilization. On the other hand, both A1 pathways produce intermediates of carbonium ion character, systems of low hydration requirements. Consequently, activity coefficients of the A2 and A1-type transition states, considered as a measure of the free energy of transfer of a species from pure water to a given aqueous acid, would be expected to exhibit significant differences in their response to the change in composition of the reaction medium.⁶⁸

For the oxonium ion-like A2 transition state, a decrease in the availability of water results in destabilization of the system, a "salting-out" effect which causes a rapid increase in the $\log f^*s^{\wedge}$ value. The activated complex characterizing the A1 hydrolysis pathway, lacking sites for specific hydrogen-bonding interactions, shows much lower sensitivity to the changes in the medium composition, and therefore a weaker "salting-out" effect.⁶⁸

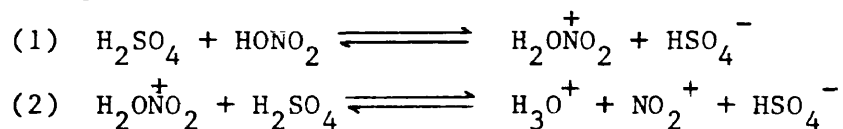
For most acetates a common pattern of behavior is observed in dilute acid regions, that is a pronounced salting-out effect on f^*s^{\wedge} , characteristic of the A_{AC}^2 mechanism, due to the rapid increase of the relative free energy of the oxonium ion-like state as a consequence of the removal of water from the reaction medium. At some acidity, dependent upon the ester structure, a smaller salting out effect on f^*s^{\wedge} is observed. This is interpreted as

mechanistic change to the A1 pathway. The A_{AC}^1 mechanism is characterized by the rate determining unimolecular formation of an acylium ion. This pathway is often seen for more sterically hindered substrates, where the A2 mechanism with the tetrahedral intermediate causes steric strain at the reaction center. The other A1 mechanism, A_{AL}^1 , is characterized by the formation of the carbonium ion formed in the rate-determining step.⁶⁸

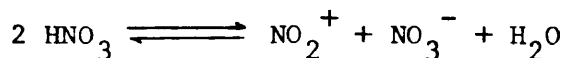
Aromatic Nitration Reactions

Most aromatic compounds, whether of high or low reactivity, can be nitrated, because of the wide variety of nitrating agents that are available. For benzene, simple alkylbenzenes, and other less reactive compounds, the most common nitrating agent is a mixture of concentrated nitric and sulfuric acid.⁶¹

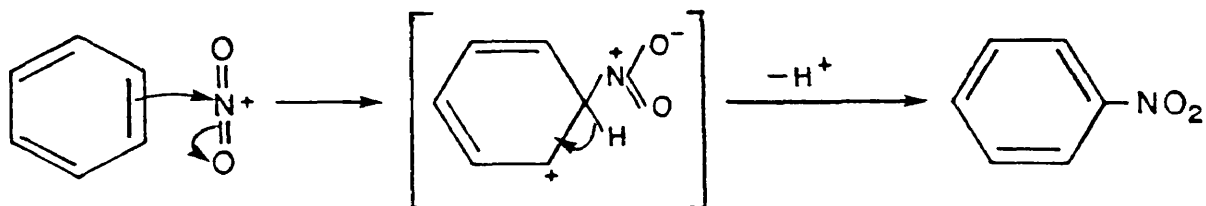
In this mixture an equilibrium is established in which many species are present, one of which is the nitronium ion, NO_2^+ . Raman spectra of HNO_3 in aqueous H_2SO_4 solutions shows that above 92% H_2SO_4 over 90% of HNO_3 is ionized to the nitronium ion.⁷⁰ In the mixture, an acid-base reaction takes place in which H_2SO_4 acts as an acid and HNO_3 acts as a base.⁵⁶



In concentrated HNO_3 alone, a similar acid - base reaction can occur in which one molecule of HNO_3 acts as an acid and the other acts as a base.



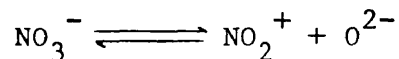
The structure of the nitronium ion is known from spectroscopic measurements. The molecule is linear, and is a powerful electrophilic reagent. It reacts directly with benzene to give a pentadienyl cation intermediate.⁵⁶



Since the nitro group is deactivating, subsequent nitration reactions are slower once one group has entered the ring. The nitro group is an important functional group in aromatic chemistry because it can be converted easily to other functional groups. The nitration reaction thus provides a route to many substituted aromatic compounds.⁵⁶

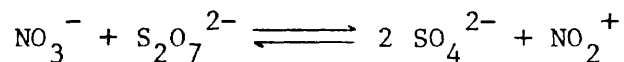
There has been some limited use of molten salts as a reaction media for the nitration of organic compounds. A study by Temple, Fay, and Williamson⁷¹ using Na, Li, and K nitrate melts containing $S_2O_7^{2-}$, found that they were able to successfully nitrate benzene and some analogs at temperatures between $250^{\circ} - 300^{\circ}C$.

It has been shown that the nitrate ion has a tendency to dissociate into nitronium and oxide ions,



but under normal conditions the equilibrium concentration of NO_2^+ is very small.⁷² Since the nitronium ion is known to be the agent responsible for the nitration of organic compounds when nitric acid is used⁶⁰, it was of interest to increase the NO_2^+ concentration by pushing the equilibrium to the right. This was accomplished by

adding certain ions which combine with O^{2-} , such as $S_2O_7^{2-}$, causing the equilibrium constant for the overall reaction to increase substantially.⁷²



The actual experimental procedure was performed by introducing the organic material as a vapor into nitrogen carrier gas, and the combined vapors were passed through the melt, which was heated to 250-300°C. The vapor from the reaction vessel was cooled by a series of cold traps, collected, dried, and analyzed by gas chromatography.⁷¹

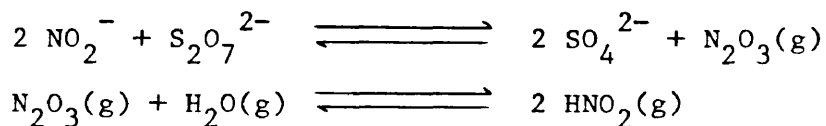
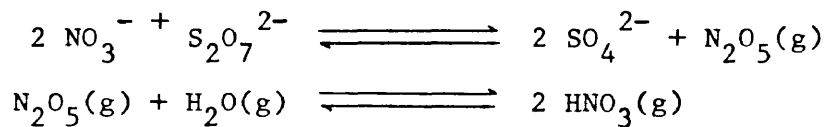
It was also shown that without the addition of potassium pyrosulfate no nitration products were obtained, and the yield of nitrated products decreased as the melt temperature increased. This was believed to be due to the gradual removal of water from the melt at higher temperatures. When water vapor was deliberately added to the reaction mixture at a specific temperature, the yield increased by ~5%.⁷³

Re-examination of the nitration of benzene by a pyrosulfate solution in a molten nitrate salt medium, found that the reaction could occur in the vapor phase above the melt and therefore was not a true melt reaction.⁷³

Therefore the nitrating agent must be produced in the melt and persist long enough to bring about the gaseous reaction. Since NO_2^+ was not identified polarographically in the molten nitrate⁷⁴, and since NO_2 vapor will not nitrate benzene vapor, and also the fact that water is essential for the reaction, lead to the conclusion that the agents responsible for nitration and nitrosation are

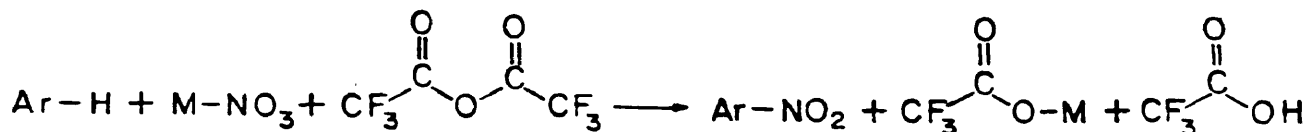
probably gaseous molecules of HNO_3 and HNO_2 , respectively.⁷³

Although these molecules are unstable, they may persist long enough to bring about the reactions observed. They may be produced in the following reactions:



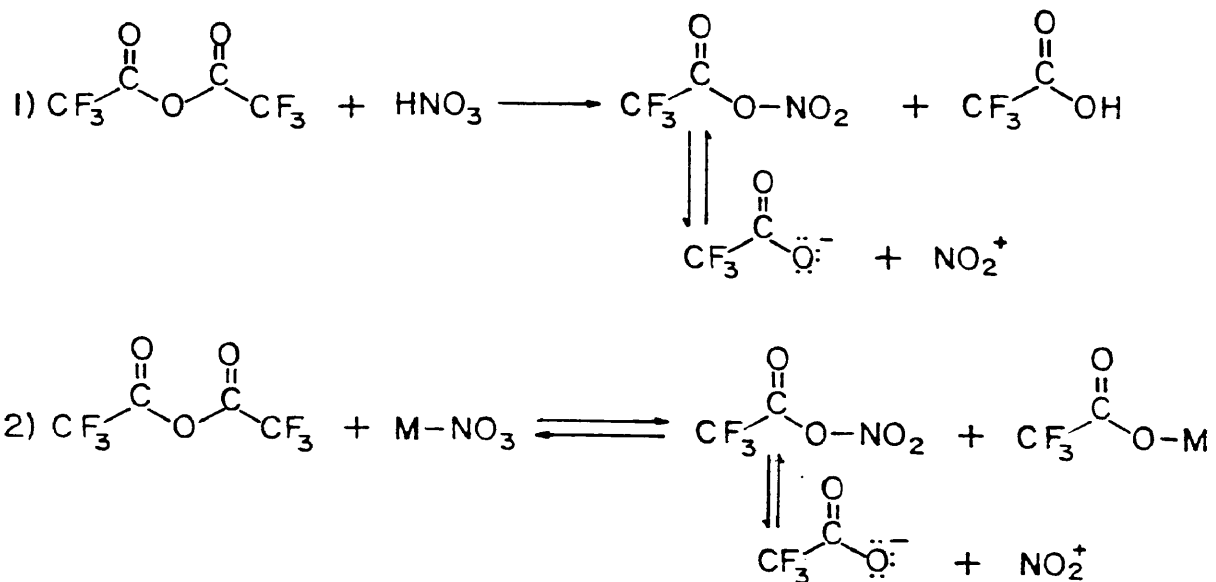
Since the reaction appears to take place in the vapor phase, nitration experiments can no longer be offered in support of the existence of NO_2^+ and NO^+ in these melt systems.⁷³

Inorganic nitrate salts in the presence of a strong mineral acid such as HNO_3 in the Trifluoroacetic Anhydride (TFAA) have shown to be a very effective nitrating agent.⁷⁵ The general reaction is written as:



The rate of the reaction was found to be dependent upon the solubility of the inorganic salt in the organic solvent used as a reaction medium. Chloroform was the solvent most often employed in these reactions.

In this reaction there are two possible sources of the nitronium ion:



Since the generation of the nitronium ion is dependent only on a source of nitrate and is independent of the metal cation, it is possible to use any metal nitrate salts in these reactions. Accordingly a variety of metal nitrate salts were employed for the nitration of benzene, and the results are recorded in Table #3.

In general, these reactions proceeded satisfactorily, giving good yields of products. Both sodium and lead nitrates give poorer yields of nitrobenzene because of their insolubility in the reaction medium. Even after 15 hours, these salts had not completely dissolved.⁷⁵

With certain substrates, oxidation rather than nitration is observed as a major reaction. For example, mixtures of TFAA and NH_4NO_3 oxidize cycloheptatriene to the tropylium salt and triphenyl phosphine to triphenyl phosphene oxide. Similarly when phenol is treated with inorganic salts in TFAA it is readily oxidized to 1,2- and 1,4- benzoquinone.⁷⁵

TABLE # 3

Nitration of Benzene with Various
Salts at 25 °C^a

salt	reaction time, h	yield, ^b %
NH ₄ NO ₃	2	99
NaNO ₃	15	67
KNO ₃	24	98
Cu(NO ₃) ₂ ·3H ₂ O	5	98
AgNO ₃	15	86
Pb(NO ₃) ₂	15	46
Cd(NO ₃) ₂ ·4H ₂ O	24	93
Cr(NO ₃) ₃ ·9H ₂ O	24	92

^a 5 mL of benzene, 0.01 mol of nitrate, 0.35 mol of TFAA, and 10 mL of CHCl₃. ^b Yield based on nitrate salt.

(adapted from reference # 75)

EXPERIMENTAL

¹H NMR Measurements on Molten Salt Hydrates:

Various mole percentages of hydrate melt were prepared by weighing out specific amounts of the solute $\text{Cd}(\text{NO}_3)_2 \cdot 4\text{H}_2\text{O}$, $\text{Zn}(\text{NO}_3)_2 \cdot 6\text{H}_2\text{O}$, $\text{AlCl}_3 \cdot 6\text{H}_2\text{O}$, or $\text{HNO}_3 \cdot 1.65 \text{H}_2\text{O}$ and exact amounts of the solvent $\text{Ca}(\text{NO}_3)_2 \cdot 4\text{H}_2\text{O}$ directly into 5mm NMR tubes.

Analytical Reagent Grade Mallinckrodt $\text{Ca}(\text{NO}_3)_2 \cdot 4\text{H}_2\text{O}$ was employed as the solvent in all of these molten salt hydrate systems. The translucent crystals were used without further purification after a melting point determination was performed. Analytical Reagent Grade Mallinckrodt $\text{Cd}(\text{NO}_3)_2 \cdot 4\text{H}_2\text{O}$ and $\text{Zn}(\text{NO}_3)_2 \cdot 6\text{H}_2\text{O}$ along with Fisher Reagent Grade $\text{AlCl}_3 \cdot 6\text{H}_2\text{O}$ were all white crystalline solids, which gave sharp melting points. They were all used as solutes without further purification. Also used as a solute was ultrapure Nitric Acid from J. T. Baker Chemical Company.

Once the mixtures were carefully weighed out on a Mettler Analytical Balance, the 5mm NMR tubes were sealed with pressure caps and gently heated in a water bath between 70° and 90°C in order to melt the salts and give a liquidus medium. During this melting process, the NMR tubes were repeatedly inverted to insure homogeneity of the melt. The samples were then allowed to cool to room temperature, whereby the solution became a clear, viscous, super-cooled hydrate melt. The NMR tubes were then reweighed to assure that there was no loss of H_2O in the sample during the melting process.

The ^1H NMR spectra was then run on a Varian FT-80A Spectrometer. A sealed coaxial inner cell of 25% TMS in Acetone- d_6 , purchased from Wilmad, was used as an external reference so as not to effect the chemical nature of the molten salt hydrate medium. Since it has been frequently stated that use of an internal standard renders somewhat unreliable the comparison of values between solutions of different salts and different concentrations of the same salt.⁴⁵ Spinning the sample at 20-24 rev/sec the NMR spectra showed large spinning side bands symmetrically disposed on both sides of the absorption peak due to the inhomogeneities of the viscous medium. This problem was eliminated by spinning the sample at 50-55 rev/sec which caused the absorption peak to become much sharper and with a much higher intensity, whereas the spinning side bands decreased in intensity and shifted out further from the main absorption peak.

The proton magnetic resonance spectra of all the hydrates melts studied were found to consist of two unsplit peaks corresponding to the water protons and the TMS protons.

Finally we measured the temperature effects on the proton resonance signal of the molten salt hydrates using a Varian FT-20/FT80-A Variable Temperature Accessory. Since TMS is so volatile we changed our external reference to 5% 3-(Trimethylsilyl) propionic acid, sodium salt in D_2O . But because of the weak resonance frequency of D_2O in the very small coaxial inner cell of the 5mm NMR tubes we were not able to lock up the magnetic field. Therefore we

were forced to switch to 10mm NMR tubes where a much larger coaxial inner cell is used.

The temperature of the probe was measured before and after each sample was run to ensure a constant temperature. Also each sample was allowed to equilibrate 30-45 minutes in the temperature probe before running the spectra.

Acid Catalyzed Ester Hydrolysis in Molten Salt Hydrate Mediums

The following mole percentages of hydrate melt were prepared by accurately weighing out the solvent $\text{Ca}(\text{NO}_3)_2 \cdot 4\text{H}_2\text{O}$, which was pre-melted to a viscous liquid, and the solute $\text{HNO}_3 \cdot 1.65\text{H}_2\text{O}$, into a 50 mL erlenmeyer flask, so as to obtain accurate mole percentages and insure proper mixing of the melt.

Mole % of $\text{HNO}_3 \cdot 1.65 \text{H}_2\text{O}$	Wt $\text{Ca}(\text{NO}_3)_2 \cdot 4\text{H}_2\text{O}$ Melt (g)	Wt $\text{HNO}_3 \cdot 1.65$ (g)
10%	50.0	2.181
7%	50.0	1.477
5%	50.0	1.033
2%	50.0	0.4006
1%	50.0	0.1983

Approximately 5mL of $\text{HNO}_3 \cdot 1.65 \text{H}_2\text{O} / \text{Ca}(\text{NO}_3)_2 \cdot 4 \text{H}_2\text{O}$ melt
 ($= 3.7 \times 10^{-2}$ moles) was added to each 10mL glass ampule via
 a graduated cylinder. Then two drops of either n-Hexyl Acetate,
 n-Octyl Acetate, or 2-Octyl Acetate was added via a Pasteur pipet.
 A small amount of ester was used so as not to effect the nature of
 the molten salt medium.

Ester	M.W. of Ester (g/mole)	Wt of 2 drops (g)*	No. Moles Present
n-Hexyl Acetate	144.21	0.023	1.6×10^{-4}
n-Octyl Acetate	172.27	0.025	1.5×10^{-4}
2-Octyl Acetate	172.27	0.025	1.5×10^{-4}

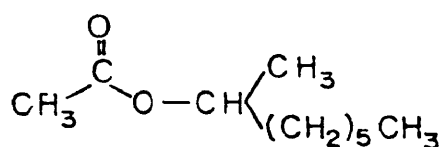
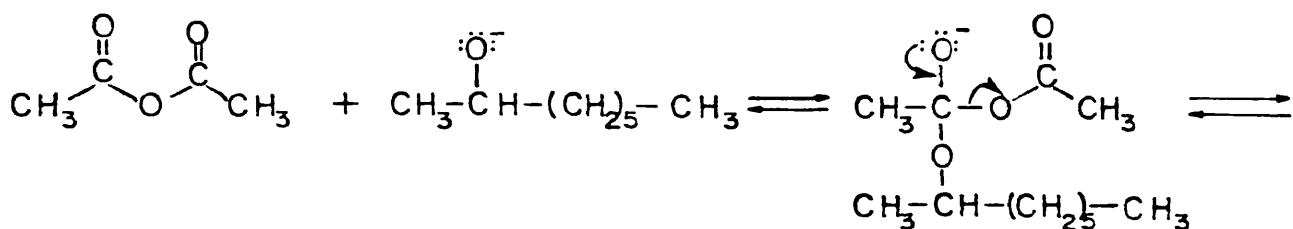
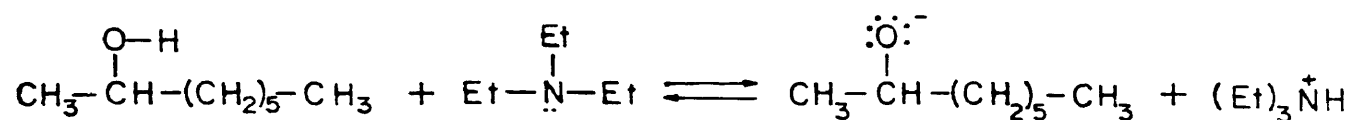
*These values were derived by weighing 10 drops of the particular
 ester 10 different times, each time using a different Pasteur
 pipet. Therefore, we obtained avg wt/drop of ester.

In addition a small glass bead was added to each ampule in order to thoroughly mix the heterogenous system. The ampules were then sealed, placed on a shaker apparatus, and immersed in a 76⁰C oil bath and vigorously shaken. The reaction of each ester in each different mole percentage of $\text{HNO}_3 \cdot 1.65 \text{H}_2\text{O} / \text{Ca}(\text{NO}_3)_2 \cdot 4\text{H}_2\text{O}$ melt were followed over time. The heterogeneous reaction mixtures were allowed to react for 2, 4, 6, 8, 12, 16, 24 hours and sometimes longer depending on the extent of the reaction.

After the pre-determined reaction time, the ampules were opened and the reaction mixture was washed with 2mL of DI water to dilute the acetic acid present. The organic products were then extracted with 2mL of hexane.

The products were analyzed on a Hewlet Packard 5790A series Gas Chromatograph using a 25 meter Crosslinked Methyl Silicone Capillary Column and a Flame Ionization Detector. The flow rate was ≈ 1 mL/min with a split ratio of $\approx 100/1$. This analysis was done isothermally at an oven temperature of 120⁰C. The average injection size was 1-2 mL.

The esters n-hexyl and n-octyl acetate were commercially available from Aldrich, and were used without further purification after G.C analysis. 2-octyl acetate was synthesized using 2-octanol and a 10% mole excess of triethylamine and acetic anhydride.



2-Octyl Acetate

The reagents were carefully weighed into a 250 mL erlenmeyer flask, fitted with a tuttle flask cover, placed on a steam bath, and swirled periodically. With time the solution began to turn yellow. After eight hours the solution was removed from the steam bath and diluted with 50 mL of Hexane. The solution was then poured into a 500 mL separatory funnel and washed with 1 M H_2SO_4 to remove any residual triethylamine. The bottom aqueous layer was drained off and the organic layer was washed with 1 M Na_2CO_3 to remove the by-product acetic acid. Once again the bottom aqueous layer was drained off and the organic layer was dried with anhydrous MgSO_4 and then filtered. In order to purify the ester a vacuum distillation was performed. The initial forerun was collected at 95°C at 45 torr. The product was collected at $102\text{--}103^\circ\text{C}$ at 33 torr which was a colorless liquid. G.C. analysis showed the product to be 98% pure and its IR spectra, taken on a Perkin-Elmer Model 1320 Infrared

Spectrophotometer, matched the Sadtler file of 2-Octyl Acetate.

The products of the ester hydrolysis reaction were analyzed by capillary gas chromatography. The identities of the products were confirmed by comparing retention times and by spiking the reaction mixture with authentic samples. These were either commercially available or synthesized according to the following procedures.

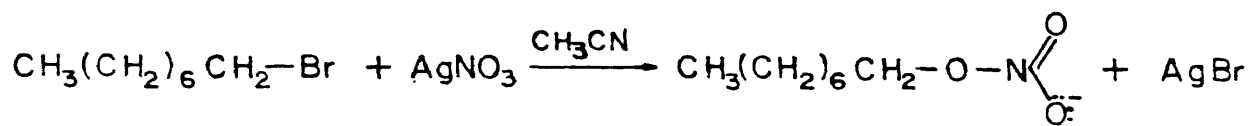
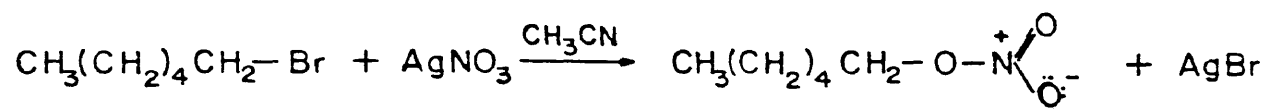
Hexanoic acid, 2-hexanone, and 2-octanone were all synthesized by an oxidation reaction using a standard Jones Reagent which was 2.67 M in Cr (VI).

Initially the exact amount of aldehyde or alcohol was weighed into a 50 mL erlenmeyer flask to give 10 mmoles of starting material. Next 10 mL of acetone was added and the solution placed in an ice bath. Then 2.5 mL (6.67 mmoles) of the standard Jones Reagent was added slowly via a 5cc syringe, while vigorously swirling the flask. At this point the solution was dark green with solid Cr salt precipitates. The solution was then diluted with 15 mL of DI water and poured into a 125 mL separatory funnel. The organic product was then extracted twice with 10 mL portions of methylene chloride, dried with anhydrous MgSO_4 and filtered. The solution was then placed on the roto-vap to strip off the solvent. All the products were colorless liquids. By G.C. analysis the products were 97-99% pure, and their IR spectra corresponded with those in the Sadtler files.

An oxidation reaction was also performed in the synthesis of Octanal except this was done under much milder non-aqueous conditions using pyridinium chlorochromate.⁷⁶ Initially 8.084g

(37.5 mmoles) of pyridinm chlorochromate was weighed into a 250 mL, 3-necked round bottom flask which was fitted with a condenser. Then 50 mL of methylene chloride was added. Next 3.257g (25.01 mmoles) of 1-Octanol was slowly added and the solution was stirred for two hours. 25 mL of ethyl ether was then added to the mixture, and the liquid was decanted from the insoluble black, gummy residue. The insoluble residue was washed three times with 10 mL portions of ethyl ether to extract any residual product. The extracted aliquots were combined and passed through a Silica Gel column to remove any residual Cr salts and to purify the product. The ether was then stripped off using a roto-vap giving a clear liquid with a faint yellowish tinge. G.C. analysis was performed showing 99% purity. The IR spectra matched that of the Sadtler Files.

The synthesis of n-Hexyl and n-Octyl nitrate ester was a nucleophilic displacement type reaction using an alkyl halide and silver nitrate.⁷⁷



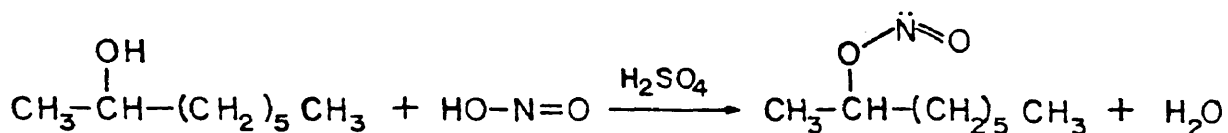
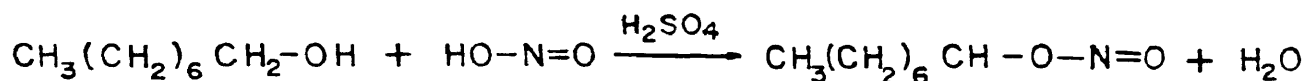
Initially 11.6g (6.83×10^{-2} moles) of AgNO_3 was weighed into a 50 mL erlenmeyer flask and 11.0 mL of Acetonitrile was added. While stirring the solution 8.45g (5.12×10^{-2} moles) of 1-bromohexane or 9.89g (5.12×10^{-2} moles) of 1-bromooctane was slowly added over a five minute time period. After the mixture was stirred at room temperature for 16 hours, the crystals of Silver

Bromide were removed by suction filtration. The filtrate was then placed in a 50 mL single neck round bottom flask, fitted with a condenser, and refluxed for 1-1/2 hours.

Upon cooling, the solution was filtered once again. The filtrate was then diluted with 25 mL of DI H₂O and transferred to a 125 mL separatory funnel. The nitrate ester was then extracted with 10mL of ethyl ether and dried with anhydrous sodium sulfate. The solution was then placed on the rotary evaporator to strip off the solvent. Both products were clear liquid with a faint yellowish tinge.

G.C. analysis of the product showed 99% purity and the vibrational-stretching frequencies in the IR spectra were easily rationalized to the product.

The final class of compounds that had to be synthesized was the Nitrite Ester.⁷⁸ For identification purposes both n-Octyl and 2-Octyl nitrite were made, under identical reaction conditions.



Initially a 500 mL 3-necked round bottom flask was charged with 38.16g (0.55 moles) of sodium nitrite (NaNO₂) and 150 mL of H₂O. The flask was cooled in an ice-salt mixture, and the solution stirred until the temperature fell to = 0⁰C.. Then a solution of

10 mL of DI H₂O, 25.0g (0.25 moles) of H₂SO₄, and 65.0g (0.50 moles) of either 1-octanol or 2-octanol was made up in a large erlenmeyer and placed in the ice-salt bath in order to cool it down to $\approx 0^{\circ}\text{C}$. The concentrated sulphuric acid helps keep the alcohol in solution but it does not dissolve the nitrite ester. Once the alcohol solution had cooled down it was very slowly introduced beneath the surface of the nitrite solution via a 50cc syringe. The alcohol solution was added slowly enough so that practically no gas evolved, and so that the temperature was maintained at $\pm 1^{\circ}\text{C}$. This required approximately 1.5 hours, during which time the reaction was stirred vigorously in order to keep the solid sodium sulfate in motion. After the final addition, the mixture was allowed to stand in the ice-salt bath for approximately one hour. At this time the reaction mixture was a yellow foam with large amounts of solid precipitate. The liquid was decanted into a 500 mL separatory funnel where two layers immediately separated. The lower aqueous layer was drained off, and the organic layer was washed twice with 5 mL portions of a solution which consisted of 100 mL H₂O, 25.0g of NaCl, and 2.0g of NaHCO₃. The organic layer was then dried with anhydrous sodium sulfate and filtered to give a bright yellow liquid for both products.

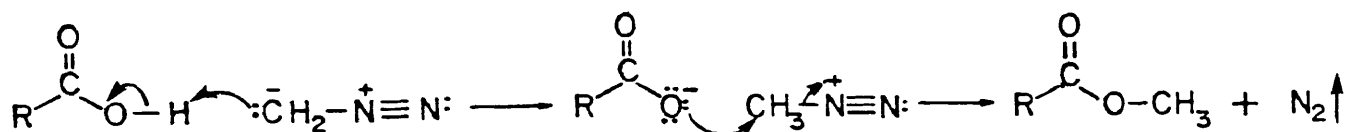
According to G.C. analysis n-octyl nitrite was 98% pure and 2-Octyl nitrite was 90% pure. Both IR spectra gave reasonable stretching and vibrational bands.

In analyzing the products of the ester hydrolysis reaction the presence of a series of carboxylic acids was suspected. By washing the products with a weak base such as 0.1M Na₂CO₃ the supposed

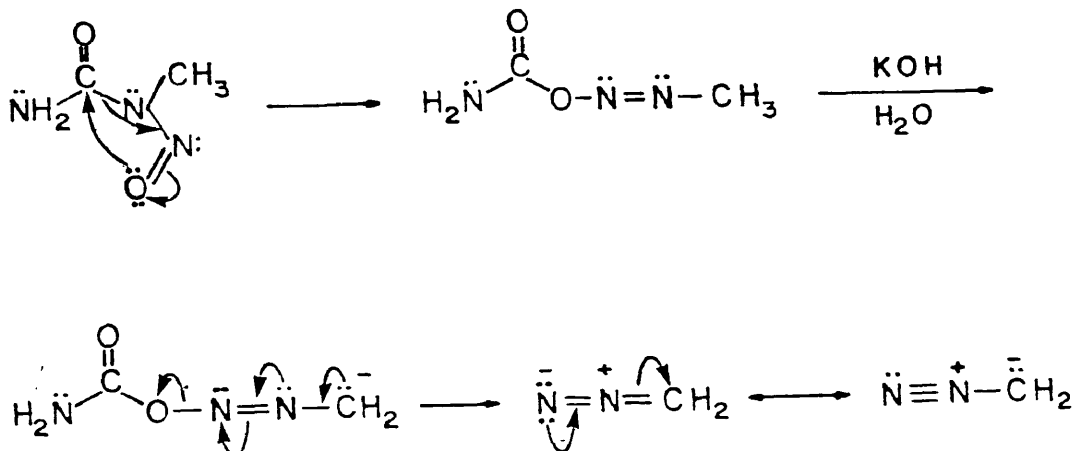
carboxylic acid peaks on the G.C. disappeared.

The retention times of a series of standard carboxylic acids were compared to the products. Spiking some of the products allowed the identification of each carboxylic acid present.

Using diazomethane the carboxylic acids were converted to their methyl esters and monitored the conversion by capillary G.C.



Initially a diazomethane solution was prepared in ether from the precursor N-methyl-N-nitroso urea.



A series of carboxylic acid standards were prepared and their retention times checked by capillary G.C. The diazomethane solution was carefully added drop-wise to the standard. The solution began to fizz as N_2 gas was given off. The addition of CH_2N_2 was continued until the solutions turned yellow and evolution of N_2 gas was no longer observed. A few drops of acetic acid were then added to quench any excess diazomethane. Next the solutions were analyzed by capillary gas chromatography to obtain the retention times of the methyl esters of these carboxylic acids.

Finally diazomethane was added to specific products of the ester hydrolysis reaction, where a series of carboxylic acids were believed to be present. As expected, G.C. analysis demonstrated that the carboxylic acids present were converted to their corresponding methyl esters.

Next some controlled experiments were performed in which the identified products of the ester hydrolysis reaction, which were either commercially available or synthesized as previously described, were introduced into the molten salt hydrate reaction medium of several compositions and allowed to react over a full range of time. The products of these reactions were then analyzed and identified by G.C. analysis. These controlled experiments lead to a great deal of mechanistic information about the overall reaction.

Originally some of these ester hydrolysis reactions were attempted on a slightly larger scale. Approximately 20 mL of the melt and five drops of ester was added to a 100 mL, 3-neck round bottom flask, fitted with a condenser. The reaction medium was

stirred vigorously and heated to 75⁰C using an oil bath. Nitrogen was purged through the system to maintain an inert atmosphere.

5 mL aliquots were taken from the reaction vessel at specific time intervals, washed with 2 mL of DI water and extracted with 2 mL of hexane. Upon performing capillary G.C. analysis, only trace amounts of starting materials and products were found. Due to the heterogeneous nature of the reaction medium we concluded that taking aliquots was not an efficient means of extracting the products. Upon working up the entire pot mixture the starting material and products were detected, but under these conditions the reactions performed in sealed ampules yielded a wider variety of products. Due to this fact and the inconvenience of having to work up the entire pot mixture, sealed ampules were used.

A series of shorter chain esters were also studied. Among these were n-butyl acetate, sec-butyl acetate, and tert-butyl acetate. In performing the G.C. analysis, the corresponding alcohols of these esters were very difficult to separate from typical solvents such as methylene chloride and ethyl ether even using variable temperature programs. Therefore, longer chain esters were utilized so that the corresponding alcohols could be separated easily from the solvent on the G.C.

An introductory study and product analysis was performed on the acid catalyzed ester hydrolysis of benzyl acetate using the molten salt hydrate medium.

Various mole percentages of the reaction medium were allowed to react over a range of times. Upon cooling to room temperature, all of the reaction mediums showed a large quantity of a white

crystalline precipitate.

The reaction mixture was washed with DI water and the solid was taken up in methylene chloride. The product was analyzed by capillary gas chromatography. The identity of the crystalline product was confirmed to be benzoic acid by the comparison of retention times of standards and by converting the benzoic acid in the reaction medium to its methyl ester using diazomethane and comparing the conversion on the G.C. relative to standards.

Nitration of Aromatics in the Molten Salt Hydrate Medium

A brief preliminary investigation was performed in order to assess the potential usefulness of molten salt hydrates as a medium for nitrating aromatics.

Various mole percentages of $\text{HNO}_3 \cdot 1.65 \text{ H}_2\text{O} / \text{Ca}(\text{NO}_3)_2 \cdot 4\text{H}_2\text{O}$ melt were prepared. Approximately 5 mL of the melt and two drops of benzene were added to each ampule along with a glass bead to insure proper mixing. The ampules were then sealed, placed on a shaker apparatus, immersed in a 76°C oil bath, and shaken vigorously.

After a pre-determined amount of time, the reaction vessels were opened, diluted with 2 mL of DI water, and the products extracted with 2 mL of methylene chloride.

The products were analyzed on the Hewlett Packard 5790A series Gas Chromatograph using a 25 meter Cross-linked Methyl Silicone Capillary Column with a Flame Ionization detector. This analysis was performed using a variable temperature programmed run in order to separate the unreacted benzene from the solvent.

Preliminary results showed that this molten salt hydrate medium

is capable of rapidly nitrating benzene to form nitrobenzene.

R E S U L T S A N D D I S C U S S I O N

¹H NMR and Hammett Acidity Function Measurements:

The proton magnetic resonance spectra of all the molten salt hydrate systems consisted of one unsplit peak corresponding to a weighted average signal for the water molecules in the hydrate melt. The singlet occurs due to rapid proton exchange of the water molecules in the hydration spheres of the metal cations.

The chemical shift values, which were very reproducible, were measured relative to an external standard of Tetramethylsilane at 28⁰C (See Table #4).

Changes in the position of the water proton resonance signal and the magnitude of the downfield shift with changes in the melt composition can be attributed to changes in the extent of proton deshielding due to polarization of the water molecule by both the metal cation and the anion.

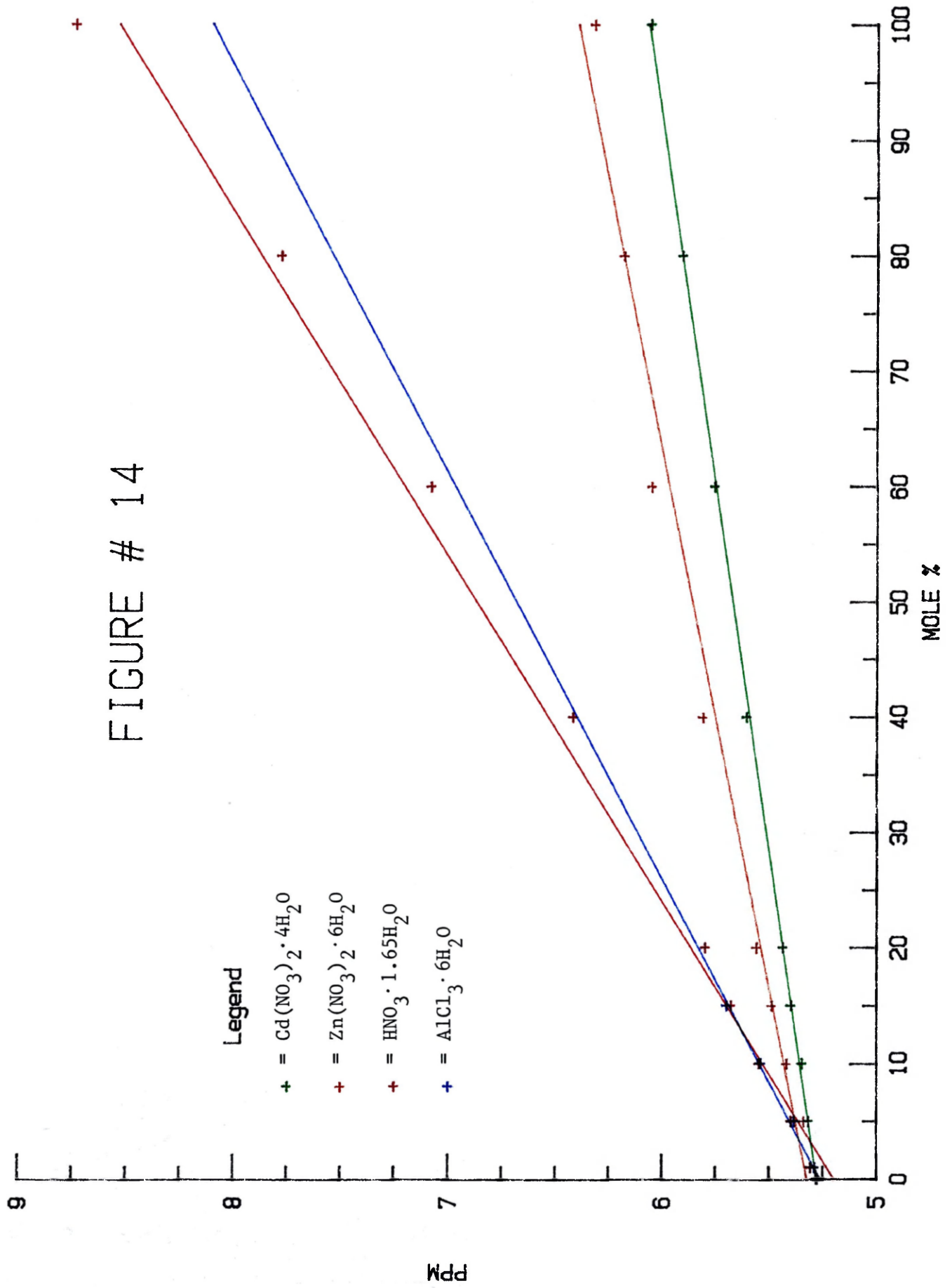
Graphical analysis of these data shows a direct linear correlation between the chemical shift and the mole % of the solute (See Figure #14).

Therefore, a conclusion can be drawn that the position of the proton magnetic resonance signal of any of these hydrate melt systems is dependent on the concentration of the solute.

TABLE #4

Salt	Mole % Salt	Chemical Shift (ppm)	Linear Regression Data
$\text{Cd}(\text{NO}_3)_2 \cdot 4\text{H}_2\text{O}$	0	5.28	Slope = 0.00786 Intcp = 5.2817 Corr. = 0.9997
	5	5.32	
	10	5.35	
	15	5.40	
	20	5.44	
	40	5.61	
	60	5.76	
	80	5.91	
	100	6.06	
$\text{Zn}(\text{NO}_3)_2 \cdot 6\text{H}_2\text{O}$	0	5.28	Slope = 0.01071 Intcp = 5.3241 Corr. = 0.9917
	5	5.34	
	10	5.42	
	15	5.49	
	20	5.56	
	40	5.81	
	60	6.05	
	80	6.18	
	100	6.32	
$\text{HNO}_3 \cdot 1.65\text{H}_2\text{O}$	0	5.28	Slope = 0.03338 Intcp = 5.1991 Corr. = 0.9962
	1	5.31	
	5	5.40	
	10	5.55	
	15	5.68	
	20	5.80	
	40	6.42	
	60	7.08	
	80	7.78	
	100	8.74	
$\text{AlCl}_3 \cdot 6\text{H}_2\text{O}$	0	5.28	Slope = 0.02838 Intcp = 5.2630 Corr. = 0.9947
	1	5.29	
	5	5.38	
	10	5.54	
	15	5.70	

FIGURE # 14



The temperature effects on the proton magnetic resonance shifts of the $\text{Cd}(\text{NO}_3)_2 \cdot 4\text{H}_2\text{O}/\text{Ca}(\text{NO}_3)_2 \cdot 4\text{H}_2\text{O}$ and $\text{Zn}(\text{NO}_3)_2 \cdot 6\text{H}_2\text{O}/\text{Ca}(\text{NO}_3)_2 \cdot 4\text{H}_2\text{O}$ hydrate melt systems were measured relative to an external standard of 5% 3-(Trimethyl Silyl) propionic acid, sodium salt. (See Tables #5 and #6.)

Increasing temperatures causes an upfield shift of the water proton resonance signal in these hydrate melt systems of $\sim 5 \times 10^{-3}$ ppm/ $^{\circ}\text{C}$.

Graphical analysis shows that the chemical shift is linear function of the temperature. (See Figure #15 and #16.)

The temperature dependence of the chemical shift of these hydrate melts is generally attributed to a weakening or breaking of the hydrogen bonds between anions and the water molecules in the cationic hydration sheath, thereby causing increased shielding of the protons.^{2,24,45,53}

TABLE #5

Mole % of $\text{Cd}(\text{NO}_3)_2 \cdot 4\text{H}_2\text{O}$	Chemical Shift (ppm) at 28°C	Chemical Shift (ppm) at 35°C	Chemical Shift (ppm) at 45°C
0	5.28	4.64	4.59
5	5.32	4.66	4.63
10	5.35	4.72	4.67
15	5.40	4.76	4.71
20	5.44	4.80	4.74
40	5.61	4.94	4.87
60	5.76	5.10	5.04
80	5.91	5.26	5.22
100	6.06	5.42	5.40

TABLE #6

Mole % of $\text{Zn}(\text{NO}_3)_2 \cdot 6\text{H}_2\text{O}$	Chemical Shift (ppm) at 28°C	Chemical Shift (ppm) at 35°C	Chemical Shift (ppm) at 45°C
0	5.28	4.64	4.59
5	5.34	4.71	4.66
10	5.42	4.79	4.74
15	5.49	4.86	4.81
20	5.56	4.93	4.87
40	5.81	5.17	5.11
60	6.05	5.36	5.32
80	6.18	5.53	5.49
100	6.32	5.69	5.65

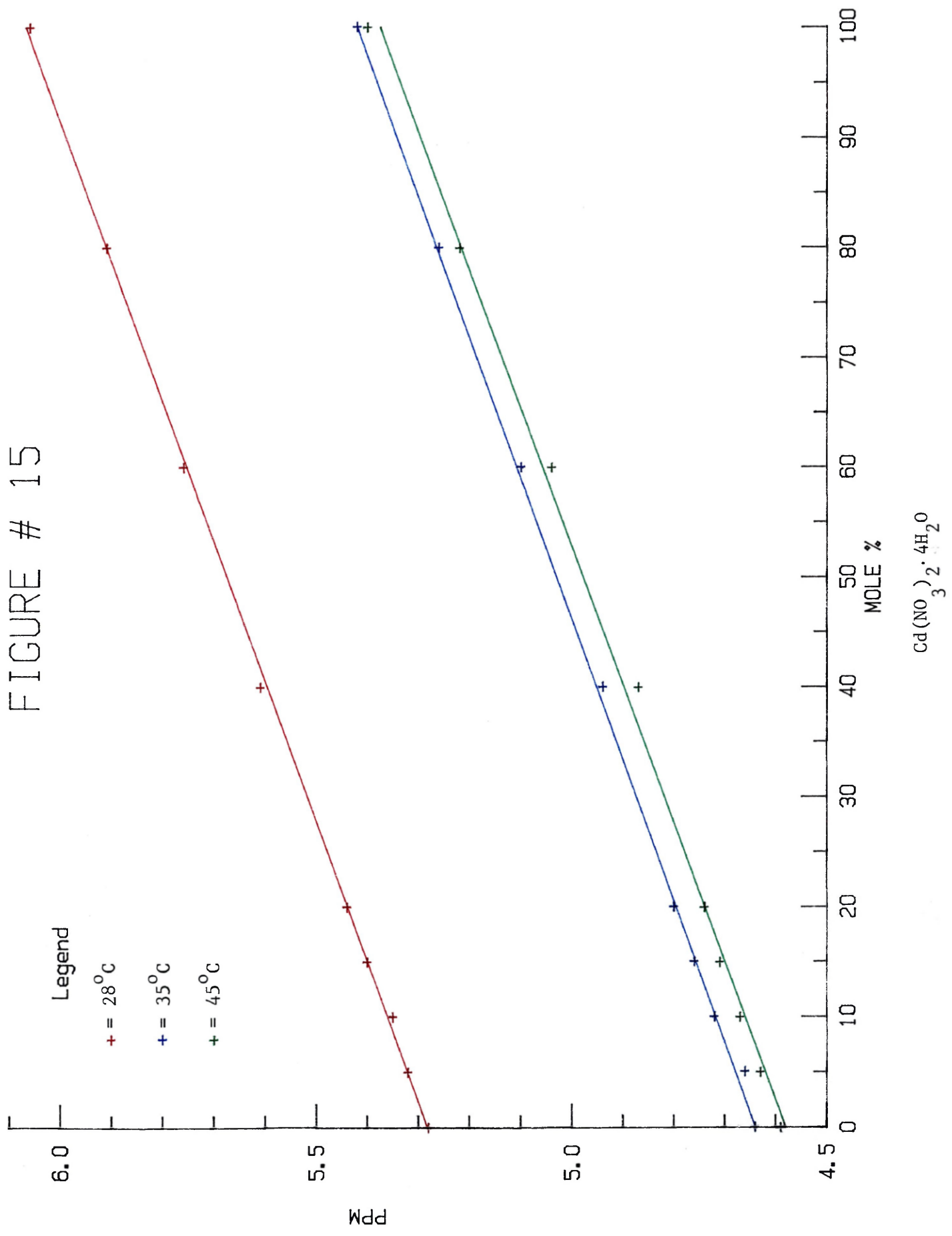


FIGURE # 15

Legend

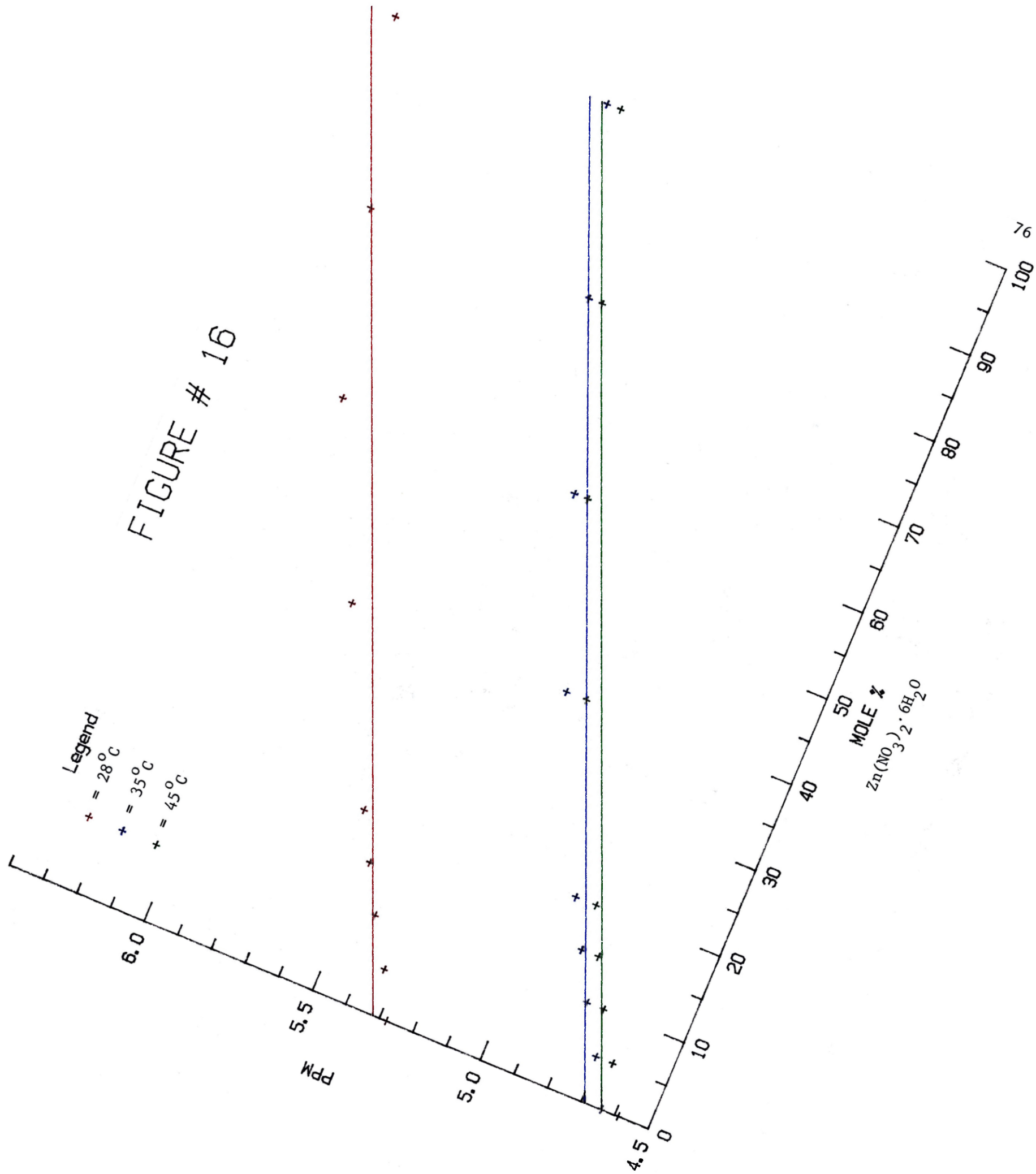
+ = 28°C

+ = 35°C

+ = 45°C

$Cd(NO_3)_2 \cdot 4H_2O$

FIGURE # 16



Using the three classical Hammett base indicators, p-nitroaniline ($pK = 0.99$), o-Nitroaniline ($pK = 0.29$) and 4-chloro-2-nitroaniline ($pK = 1.03$), and spectrophotometric methods (See Appendix II), the Hammett Acidity Function values were obtained for these molten salt hydrate systems (See Tables #7 - 10).

Graphical analysis of these data revealed a linear relationship between the H_0 values and the log of the mole % of the solute (See Figure #17).

From these results a linear extrapolation can be performed in order to predict Hammett Acidity Function Values for higher mole % of the hydrate melt which cannot be measured directly using Hammett base indicators due to decomposition reactions. (See Tables #11 - 14; also Figure #17.)

TABLE #7

Mole % of $\text{Cd}(\text{NO}_3)_2 \cdot 4\text{H}_2\text{O}$	Log Mole % of $\text{Cd}(\text{NO}_3)_2 \cdot 4\text{H}_2\text{O}$	Measured H_2O	Linear Regression Data
10.00	-1.000	0.63	Slope = -1.510 Intcp = -0.820 Corr. = 0.996
5.00	-1.301	1.22	
3.31	-1.480	1.43	
1.99	-1.701	1.75	
1.00	-2.000	2.17	

TABLE #8

Mole % of $\text{Zn}(\text{NO}_3)_2 \cdot 6\text{H}_2\text{O}$	Log Mole % of $\text{Zn}(\text{NO}_3)_2 \cdot 6\text{H}_2\text{O}$	Measured H_2O	Linear Regression Data
14.80	-0.830	0.15	Slope = -1.504 Intcp = -1.137 Corr. = 0.998
10.00	-1.000	0.30	
5.00	-1.301	0.86	
1.99	-1.701	1.40	
1.00	-2.000	1.88	

TABLE #9

Mole % of $\text{AlCl}_3 \cdot 6\text{H}_2\text{O}$	Log Mole % of $\text{AlCl}_3 \cdot 6\text{H}_2\text{O}$	Measured H_2O	Linear Regression Data
1.00	-2.000	-0.55	Slope = -0.813 Intcp = -2.159 Corr. = 0.998
0.50	-2.301	-0.26	
0.20	-2.699	0.02	
0.10	-3.000	0.28	

TABLE #10

Mole % of $\text{HNO}_3 \cdot 1.65 \text{H}_2\text{O}$	Log Mole % of $\text{HNO}_3 \cdot 1.65 \text{H}_2\text{O}$	Measured H_2O	Linear Regression Data
0.230	-2.638	-1.56	Slope = -1.439 Intcp = -5.420 Corr. = 0.994
0.110	-2.959	-1.26	
0.047	-3.328	-0.62	
0.023	-3.638	-0.16	

TABLE #11

Mole % of $\text{Cd}(\text{NO}_3)_2 \cdot 4\text{H}_2\text{O}$	Log Mole % of $\text{Cd}(\text{NO}_3)_2 \cdot 4\text{H}_2\text{O}$	Predicted H_0	Linear Regression Data
5	-1.301	1.145	Slope = -1.510 Intcp = -0.820 Corr. = 0.999
10	-1.000	0.691	
15	-0.824	0.425	
20	-0.699	0.236	
40	-0.398	-0.219	
60	-0.222	-0.484	
80	-0.097	-0.673	
100	0	-0.820	

TABLE #12

Mole % of $\text{Zn}(\text{NO}_3)_2 \cdot 6\text{H}_2\text{O}$	Log Mole % of $\text{Zn}(\text{NO}_3)_2 \cdot 6\text{H}_2\text{O}$	Predicted H_0	Linear Regression Data
5	-1.301	0.820	Slope = -1.504 Intcp = -1.137 Corr. = 0.999
10	-1.000	0.367	
15	-0.824	0.102	
20	-0.699	-0.086	
40	-0.398	-0.538	
60	-0.222	-0.803	
80	-0.097	-0.991	
100	0	-1.137	

TABLE # 13

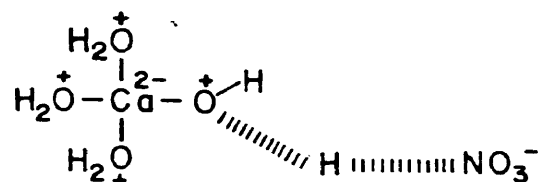
Mole % of $\text{AlCl}_3 \cdot 6\text{H}_2\text{O}$	Log of Mole % $\text{AlCl}_3 \cdot 6\text{H}_2\text{O}$	Predicted H_0	Linear Regression Data
1	-2.000	-0.534	Slope = -0.812 Intcp = -2.159 Corr. = 0.999
5	-1.301	-1.102	
10	-1.000	-1.347	
15	-0.824	-1.490	
20	-0.699	-1.591	
40	-0.398	-1.836	
60	-0.222	-1.979	
80	-0.097	-2.080	
100	0	-2.159	

TABLE # 14

Mole % of $\text{HNO}_3 \cdot 1.65\text{H}_2\text{O}$	Log Mole % of $\text{HNO}_3 \cdot 1.65\text{H}_2\text{O}$	Predicted H_0	Linear Regression Data
1	-2.000	-2.54	Slope = -1.439 Intcp = -5.420 Corr. = 0.999
5	-1.301	-3.55	
10	-1.000	-3.98	
15	-0.824	-4.23	
20	-0.699	-4.41	
40	-0.398	-4.85	
60	-0.222	-5.10	
80	-0.097	-5.28	
100	0	-5.42	

These experimental results clearly show that these molten salt hydrate systems are highly acidic in nature and these enhanced acidic properties are comparable to strong mineral acids such as HNO_3 and H_2SO_4 (See Table #15 and #16).

This enhanced acidity in molten salt hydrate systems comes from a metal cation-water interaction which involves appreciable polarization of the oxygen atom towards the metal center. Additionally, the anion exhibits a strong attraction for the water protons.



These combined effects cause a decrease in electron density around the proton, allowing a metal-aquoion to behave as a Bronsted-Lowry acid.

As the water content of the metal-aquo complex decreases, minimizing outer-sphere hydration, the protonating power of the species increases rapidly. (See Figure #3.)

Since the molten salt hydrates have a water content insufficient to satisfy more than the first coordination sphere of the system, they possess acidic properties similar to those of strong mineral acids. Also this decrease in electron density around the water proton accounts for the deshielding of the proton and for the magnitude of the downfield shift of the pmr spectra.

TABLE # 15

Wt. % of HNO_3	Mole % of HNO_3	H_0	Wt. % of HNO_3	Mole % of HNO_3	H_0
2	0.395	0.33	50	16.259	-2.88
4	0.803	-0.08	55	19.179	-3.13
6	1.224	-0.29	60	22.555	-3.42
8	1.660	-0.46	65	26.502	-3.72
10	2.112	-0.64	70	31.178	-3.99
15	3.313	-0.97	75	36.807	-4.30
20	4.629	-1.28	80	43.713	-4.62
25	6.078	-1.57	85	52.386	-4.96
30	7.682	-1.85	90	63.602	-5.31
35	9.465	-2.10	95	78.673	-5.75
40	11.460	-2.36	100	100	-6.3
45	13.708	-2.62			

(Adapted from reference #70)

TABLE # 16

The Molten Salt Hydrate system of $\text{HNO}_3 \cdot 1.65\text{H}_2\text{O} / \text{Ca}(\text{NO}_3)_2 \cdot 4\text{H}_2\text{O}$

Wt % of $\text{HNO}_3 \cdot 1.65\text{H}_2\text{O}$	Mole % of $\text{HNO}_3 \cdot 1.65\text{H}_2\text{O}$	H_0
0.398	1.00	-2.542
2.018	5.00	-3.548
4.180	10.00	-3.981
6.477	15.00	-4.234
8.946	20.00	-4.414
20.745	40.00	-4.847
37.067	60.00	-5.101
61.097	80.00	-5.281
100.000	100.00	-5.420

Measuring the Hammett Acidity Function of these molten salt hydrate systems by spectrophotometric techniques using base indicators presented quite a few problems.

The viscosity of the medium itself presented a number of experimental difficulties. An especially significant problem was in obtaining a homogeneous mixture of the melt and the indicator. Also the tendency of the melt to recrystallize made it difficult to work with.

Probably the most significant problem was that H_0 could not be measured over a wide range of concentrations, since at higher mole percentages of melt the base indicators often decomposed through apparent oxidation or nitration reactions.

In order to resolve these problems it was our goal to draw an analogy between the Hammett Acidity Function and the 1H NMR chemical shift for a given hydrate melt system, so that we could predict H_0 values by simply measuring the proton magnetic resonance spectra of the system.

Since we had already established a linear relationship between the chemical shift and mole %, and between H_0 and $\log(\text{mole } \%)$, we assumed that there should be some correlation between the Hammett Acidity Function and the proton chemical shift.

From the results of experimental work we have shown that in the relevant areas of concentration that we considered, there is a linear relationship between H_0 and the log the chemical shift of the hydrate melt relative to the solvent $\text{Ca}(\text{NO}_3)_2 \cdot 4\text{H}_2\text{O}$. (See Tables #17 - 20; also Figure #18.)

TABLE #17

Mole % of $\text{Cd}(\text{NO}_3)_2 \cdot 4\text{H}_2\text{O}$	Measured δ (ppm)	Predicted δ (ppm)*	Log $\Delta\delta$ rel. to Solvent(5.28 ppm)	Measured H_0	Predicted H_0 **
1.00		5.29	-2.000	2.17	
1.99		5.30	-1.699	1.75	
3.31		5.31	-1.523	1.43	
5.00	5.32	5.32	-1.398	1.22	1.145
10.00	5.35	5.36	-1.125	0.63	0.691
15.00	5.40		-0.921		0.425
20.00	5.44		-0.796		0.236
40.00	5.61		-0.482		-0.219
60.00	5.76		-0.319		-0.484
80.00	5.91		-0.201		-0.673
100.00	6.06		-0.108		-0.820

Linear Regression Data:

Slope = -1.5835

Intcp = -1.0074

Corr = 0.9990

TABLE #18

Mole % of $\text{Zn}(\text{NO}_3)_2 \cdot 6\text{H}_2\text{O}$	Measured δ (ppm)	Predicted δ (ppm)*	Log $\Delta\delta$ rel. to Solvent(5.28 ppm)	Measured H_0	Predicted H_0 **
1.00		5.29	-2.000	1.88	
1.99		5.30	-1.699	1.40	
5.00	5.34	5.33	-1.260	0.86	0.820
10.00	5.42	5.38	-0.921	0.30	0.367
14.80		5.43	-0.824	0.15	
15.00	5.49		-0.678		0.102
20.00	5.56		-0.553		-0.086
40.00	5.81		-0.276		-0.538
60.00	6.05		-0.114		-0.803
80.00	6.18		-0.046		-0.991
100.00	6.32		-0.017		-1.137

Linear Regression Data:

Slope = -1.4493

Intcp = -1.0005

Corr = 0.9964

* Predicted δ values are derived from a linear extrapolation of the plot of δ vs. mole % salt.

** Predicted H_0 values are derived from a linear extrapolation of the plot of H_0 vs. log mole % salt.

TABLE #19

Mole % of $\text{AlCl}_3 \cdot 6\text{H}_2\text{O}$	Measured δ (ppm)	Predicted δ (ppm)*	$\text{Log} \Delta\delta$ rel to Solvent(5.28 ppm)	Measured H_0	Predicted H_0 **
0.10		5.266	-2.484	0.28	
0.20		5.268	-2.277	0.02	
0.50		5.277	-1.845	-0.26	
1.00	5.29	5.291	-1.549	-0.55	-0.534
5.00	5.38		-1.000		-1.102
10.00	5.54		-0.585		-1.347
15.00	5.70		-0.377		-1.490
20.00		5.83	-0.260		-1.591
40.00		6.40	0.049		-1.836
60.00		6.97	0.228		-1.979
80.00		7.53	0.352		-2.080
100.00		8.10	0.450		-2.159

To obtain $\text{Log} \Delta\delta$ values for initial predicted δ values used the intercept of the plot of δ vs. mole % salt which was 5.263 ppm

Linear Regression Data:

Slope = -0.8168 Intcp. = -1.8074 Corr. = 0.9988

* Predicted δ values are derived from a linear extrapolation of the plot of δ vs. mole % salt

** Predicted H_0 values are derived from a linear extrapolation of the plot of H_0 vs. mole % salt

TABLE # 20

Mole % of HNO ₃ · 1.65H ₂ O	Measured δ (ppm)	Predicted δ (ppm)*	Log Δδ rel. to Solvent(5.28 ppm)	Measured H ₀	Predicted H ₀ **
0.023		5.1998	-3.126	-0.16	
0.047		5.2006	-2.810	-0.62	
0.110		5.2027	-2.438	-1.26	
0.230		5.2067	-2.116	-1.56	
1.00	5.31		-1.523		-2.542
5.00	5.40		-0.921		-3.548
10.00	5.55		-0.569		-3.981
15.00	5.68		-0.398		-4.234
20.00	5.80		-0.284		-4.414
40.00	6.42		0.057		-4.847
60.00	7.08		0.255		-5.101
80.00	7.78		0.398		-5.281
100.00	8.74		0.539		-5.420

To obtain Log Δδ values for predicted δ values used the intercept of the plot of δ vs. mole % salt which was 5.1991 ppm

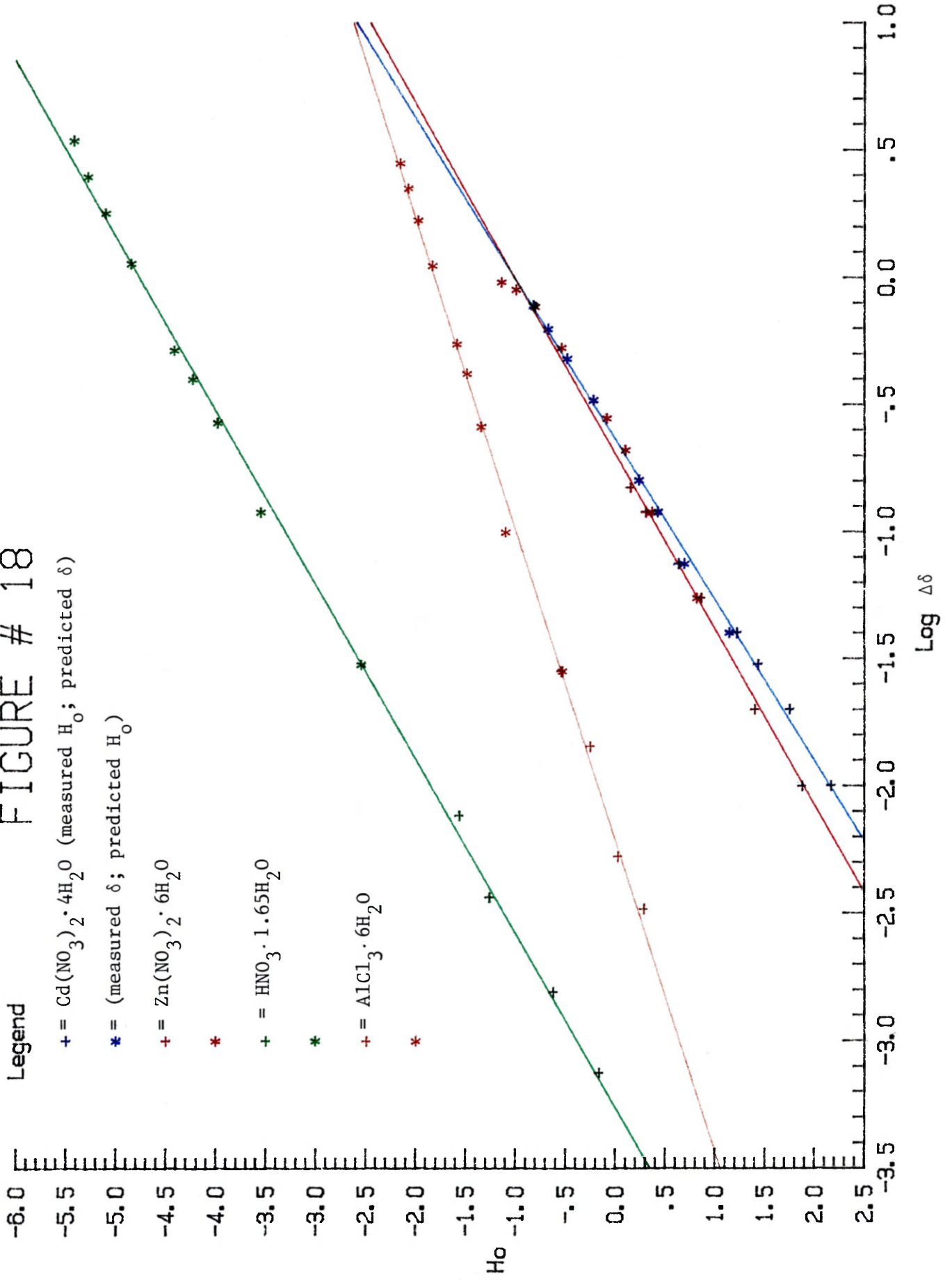
Linear Regression Data:

Slope = -1.4590 Intcp.= -4.7570 Corr.= 0.9992

* Predicted δ values are derived from a linear extrapolation of the plot of δ vs. mole % salt

** Predicted H₀ values are derived from a linear extrapolation of the plot of H₀ vs. log mole % salt

FIGURE # 18



As a result of this linear correlation between H_0 and the $\log \Delta\delta$, values for the Hammett Acidity Function can be determined by an experimentally easier and more straightforward method, as well as being more precise, by simply measuring the 1H NMR chemical shift of the melt.

Beside the experimental convenience of measuring H_0 in this manner, this technique also has some important advantages. One relevant aspect is that NMR spectroscopy is a non-invasive type of measurement; therefore, it cannot affect the chemical nature of the hydrate melt system.

Another very important advantage is that H_0 can be accurately determined over a wide range of concentrations of the hydrate melt, which is not possible using base indicators.

This linear correlation also reinforces the theory that 1H NMR chemical shift and protonation of organic indicators respond very similarly to changes in proton acidity.

Once the relative acidities of these hydrate melts had been established, our next goal was to attempt to study the kinetics of certain acid catalyzed organic reactions in the molten salt hydrate medium, in an effort to obtain a more thorough understanding of the chemical properties and reactivity of these systems.

The primary reaction we wanted to focus on was acid-catalyzed ester hydrolysis reaction. By studying the kinetics of this reaction we expected to:

- (1) Obtain a relative measure of the acidity of the medium as a synthetic agent.
- (2) Get an idea of the amount of "free" water present in the hydrate melt system, since the reaction is driven by water.
- (3) Determine the mechanistic route of the reaction by stereochemical methods (Acyl-Oxygen vs Alkyl-Oxygen Cleavage).

We also felt this medium had the potential for nitrating aromatic compounds since the decomposition of many of the Hammett base indicators was due apparently to oxidation or nitration reactions.

The initial results obtained from using the hydrate melt as a medium for performing the acid-catalyzed ester hydrolysis reaction were very surprising.

Instead of obtaining the appropriate alcohol, we obtained a large number of unknown products. Upon repeating these experiments we found that the results were very reproducible.

Therefore, it was obvious from the number of unknown products obtained, that it would probably be impossible to obtain accurate kinetic data on this reaction. But in order to obtain a qualitative understanding of the chemical nature and reactivity of this medium, we decided to identify the products and determine a likely mechanistic route for these reactions.

The products of the reactions were analyzed by capillary gas chromatography and the identity of the products was confirmed by comparing retention times with standards, by spiking the reaction mixture with authentic samples, and experimental techniques described earlier.

The products are listed for each ester in a specific mole percentage of nitric acid in $\text{Ca}(\text{NO}_3)_2 \cdot 4\text{H}_2\text{O}$ over exact time intervals (See Tables #21 - 35).

TABLE 21
 10% $\text{HNO}_3 \cdot 1.65 \text{H}_2\text{O}$ in $\text{Ca}(\text{NO}_3)_2 \cdot 4 \text{H}_2\text{O}$ + n-Hexyl Acetate

RxN Time (hrs)	% Hexyl Acetate	% Hexanoic Acid	% Pentanoic Acid	% Hexyl Nitrate
2	76	8	7	9
4	47	18	13	22
6	26	20	27	27
8	11	30	44	15
12	-	49	44	7
16	-	47	53	-
24	-	46	54	-

TABLE 22
 7% $\text{HNO}_3 \cdot 1.65 \text{H}_2\text{O}$ in $\text{Ca}(\text{NO}_3)_2 \cdot 4 \text{H}_2\text{O}$ + n-Hexyl Acetate

RxN Time (hrs)	% Hexyl Acetate	% Hexanoic Acid	% Pentanoic Acid	% Hexyl Nitrate	% Hexyl Nitrite
2	82	-	7	7	4
4	60	8	9	20	3
6	47	22	13	16	2
8	31	27	27	15	-
12	9	34	41	16	-
16	-	43	48	9	-
24	-	52	48	-	-
30	-	54	46	-	-

TABLE 23
 5% $\text{HNO}_3 \cdot 1.65 \text{H}_2\text{O}$ in $\text{Ca}(\text{NO}_3)_2 \cdot 4 \text{H}_2\text{O}$ + n-Hexyl Acetate

RxN Time (hrs)	% Hexyl Acetate	% Hexanoic Acid	% Pentanoic Acid	% Hexyl Nitrate	% Hexyl Nitrite
2	75	2	5	11	7
4	68	7	16	9	-
6	57	11	19	13	-
8	47	20	22	11	-
12	25	27	37	11	-
16	9	27	56	8	-
24	-	27	73	-	-

TABLE 24
 2% $\text{HNO}_3 \cdot 1.65 \text{H}_2\text{O}$ in $\text{Ca}(\text{NO}_3)_2$ - n-Hexyl Acetate

RxN Time (hrs)	% Hexyl Acetate	% Hexanoic Acid	% Pentanoic Acid	% Hexyl Nitrate	%Hexyl Nitrite
2	93	-	-	-	7
4	91	-	4	-	5
6	87	-	6	-	7
8	84	3	10	-	3
12	76	8	10	6	-
16	60	11	21	8	-
24	48	26	26	-	-
32	27	35	31	7	-

TABLE 25
 1% $\text{HNO}_3 \cdot 1.65 \text{H}_2\text{O}$ in $\text{Ca}(\text{NO}_3)_2 \cdot 4 \text{H}_2\text{O}$ + n-Hexyl Acetate

RxN Time (hrs)	% Hexyl Acetate	% Hexanoic Acid	% Pentanoic Acid	% Hexyl Nitrate	%Hexyl Nitrite
2	100	-	-	-	-
4	97	-	-	-	3
8	94	-	4	-	2
12	92	-	6	-	2
16	88	4	6	-	2
24	77	7	12	-	4
48	61	18	17	4	-

TABLE 26
 10% $\text{HNO}_3 \cdot 1.65 \text{H}_2\text{O} - \text{Ca}(\text{NO}_3)_2 \cdot 4\text{H}_2\text{O} + \text{n-Octyl Acetate}$

RxN Time (hrs)	%n-Octyl Acetate	% Octanoic Acid	% Heptanoic Acid	% Hexanoic Acid	% Octyl Nitrate	% Octyl Nitrite
2	78	3	6	3	6	4
4	65	6	14	4	11	-
6	51	7	19	6	17	-
8	33	18	27	8	14	-
12	22	22	32	10	14	-
16	15	24	30	10	21	-
24	5	39	33	10	13	-

TABLE 27
 7% $\text{HNO}_3 \cdot 1.65 \text{H}_2\text{O}$ in $\text{Ca}(\text{NO}_3)_2 \cdot 4\text{H}_2\text{O} + \text{n-Octyl Acetate}$

RxN Time (hrs)	%n-Octyl Acetate	% Octanoic Acid	% Heptanoic Acid	% Hexanoic Acid	% Octyl Nitrate	% Octyl Nitrite
2	80	2	2	-	4	12
4	71	5	9	1	10	4
6	60	9	12	3	13	3
8	47	21	14	4	11	3
16	24	24	24	6	22	-
24	12	38	27	9	14	-

TABLE 28
 5% $\text{HNO}_3 \cdot 1.65 \text{H}_2\text{O}$ in $\text{Ca}(\text{NO}_3)_2 \cdot 4\text{H}_2\text{O} + \text{n-Octyl Acetate}$

RxN Time (hrs)	%n-Octyl Acetate	% Octanoic Acid	% Heptanoic Acid	% Hexanoic Acid	% Octyl Nitrate	% Octyl Nitrite
2	89	-	-	-	-	11
4	73	-	5	-	9	13
6	69	4	7	-	12	8
8	55	7	12	2	18	6
12	34	9	14	2	25	16
16	34	22	20	4	17	3
24	22	32	24	6	16	-

TABLE 29
 2% $\text{HNO}_3 \cdot 1.65 \text{H}_2\text{O}$ in $\text{Ca}(\text{NO}_3)_2 \cdot 4\text{H}_2\text{O}$ + n-Octyl Acetate

RxN Time (hrs)	% Octyl Acetate	% Octanol	% Oct. Acid	% Hept. Acid	% Hex. Acid	% Octyl Nitrate	% Octyl Nitrite
2	98	2	-	-	-	-	-
4	91	8	-	-	-	-	1
6	89	-	-	-	-	1	10
8	72	-	2	-	-	3	23
12	68	-	3	4	-	9	16
16	72	-	4	7	2	11	4
48	33	-	23	15	3	20	6

TABLE 30
 1% $\text{HNO}_3 \cdot 1.65 \text{H}_2\text{O}$ in $\text{Ca}(\text{NO}_3)_2 \cdot 4\text{H}_2\text{O}$ + n-Octyl Acetate

RxN Time (hrs)	% Octyl Acetate	% Oct. Acid	% Hept. Acid	% Hex. Acid	% Octyl Nitrate	% Octyl Nitrite
2	100	-	-	-	-	-
4	100	-	-	-	-	-
8	99	-	-	-	-	1
12	91	-	-	-	-	9
16	78	1	1	-	4	16
24	61	3	1	-	7	28

TABLE 31
 10% $\text{HNO}_3 \cdot 1.65 \text{H}_2\text{O}$ in $\text{Ca}(\text{NO}_3)_2 \cdot 4\text{H}_2\text{O}$ + 2-Octyl Acetate

RxN Time (hrs)	% 2-Octyl Acetate	% Hept. Acid	% Hex. Acid	% Pent. Acid	% 2-Octyl Nitrate	% 2-Octyl Nitrite
2	93	1	2	1	1	2
4	90	2	4	1	1	2
6	85	2	8	3	2	-
8	82	3	9	3	3	-
12	63	7	20	6	4	-
16	60	7	22	5	6	-
24	34	15	37	10	4	-

TABLE 32
 7% $\text{HNO}_3 \cdot 1.65 \text{H}_2\text{O}$ in $\text{Ca}(\text{NO}_3)_2 \cdot 4\text{H}_2\text{O}$ + 2-Octyl Acetate

RxN Time (hrs)	% 2-Octyl Acet.	% 2-Octanol	% 2-Octanone	% Hep. Acid	% Hex. Acid	% Pent. Acid	% 2-Octyl Nitrate	% 2-Octyl Nitrite
2	94	5	1	-	-	-	-	-
4	94	-	-	-	4	-	2	-
6	87	-	-	-	7	1	5	-
8	81	-	-	2	11	2	4	-
24	50	-	-	7	21	6	16	-

TABLE 33
 5% $\text{HNO}_3 \cdot 1.65 \text{H}_2\text{O}$ in $\text{Ca}(\text{NO}_3)_2 \cdot 4\text{H}_2\text{O}$ + 2-Octyl Acetate

RxN Time (hrs)	% 2-Octyl Acet.	% 2-Octanol	% 2-Octanone	% Hep. Acid	% Hex. Acid	% Pent. Acid	% 2-Octyl Nitrate	% 2-Octyl Nitrite
1	79	20	-	-	-	-	-	1
2	80	16	2	-	-	-	-	2
4	81	8	10	-	-	-	1	-
6	89	-	1	1	3	1	2	2
8	83	-	2	2	6	2	3	2
12	82	-	2	2	7	1	6	-
16	77	-	-	4	11	2	6	-
24	62	-	-	9	19	5	5	-

TABLE 34
 2% $\text{HNO}_3 \cdot 1.65 \text{H}_2\text{O}$ in $\text{CA} (\text{NO}_3)_2 \cdot 4\text{H}_2\text{O}$ + 2-Octyl Acetate

RxN Time (hrs)	% 2-Octyl Acet.	% 2-Octanol	% 2-Octanone	%Hep. Acid	%Hex. Acid	%Pent. Acid	% 2-Octyl Nitrate	% 2-Octyl Nitrite
2	92	5	3	-	-	-	-	-
4	89	10	1	-	-	-	-	-
6	93	-	2	-	2	-	2	1
8	95	-	-	-	3	-	2	-
12	92	-	-	-	4	-	3	1
16	88	-	2	1	4	-	3	2
24	80	-	2	1	8	2	6	1

TABLE 35

1% $\text{HNO}_3 \cdot 1.65 \text{H}_2\text{O}$ in $\text{Ca}(\text{NO}_3)_2 \cdot 4\text{H}_2\text{O}$ + 2-Octyl Acetate

RxN Time (hrs)	% 2-Octyl Acet.	% 2-Octanol	% 2-Octanone	%Hep. Acid	%Hex. Acid	%Pent. Acid	% 2-Octyl Nitrate	% 2-Octyl Nitrite
2	90	7	3	-	-	-	-	-
4	90	6	4	-	-	-	-	-
6	90	4	3	-	1	-	1	1
8	90	2	5	-	1	-	1	1
12	91	2	1	-	2	-	2	2
16	91	1	2	-	3	-	2	1
24	91	-	2	-	4	-	3	-

The percentages given in these tables represent relative G.C. peak areas. For the various reactions carried out over time, the relative overall peak areas remained nearly constant, allowing us to assume a proper mass balance was to a large extent maintained throughout the reaction. Therefore these values give a reasonably good qualitative understanding of the extent of the reaction as well as the chemical nature of the molten salt hydrate medium.

Inspection of these tables shows, as expected, a steady decrease in the starting ester as the reaction proceeds and that the rate of decrease is dependent on the acidity of the medium.

Further examination shows that the major products detected for the 1⁰ esters, n-hexyl and n-octyl acetate, are a series of carboxylic acids, and the corresponding nitrate and nitrite esters. (Although 1-octanol was detected after two and four hours in 2% HNO₃ with n-octyl acetate.) But, under milder conditions (< 10% HNO₃) and using a 2⁰ ester(2-octyl acetate) the product of ester hydrolysis, 2-octanol, was consistently detected, along with the corresponding ketone, 2-octanone. Also a series of carboxylic acids were detected as well as the nitrate and nitrite esters.

From these results we were able to derive a path for the reaction of the secondary ester.

Initially the expected acid-catalyzed ester hydrolysis takes place to give a 2⁰ alcohol. The alcohol is then oxidized in the acidic medium to a ketone, which is then further oxidized to its appropriate carboxylic acid.

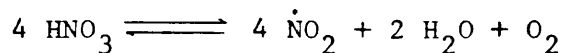
Since it is well known that 1⁰ alcohol oxidizes much more rapidly than 2⁰ alcohol,⁵⁶ then we can assume that the primary ester is being hydrolyzed in the medium to give a 1⁰ alcohol. But because the 1⁰ alcohol is so reactive it is immediately oxidized to its corresponding aldehyde and is not detected.

The aldehyde is also a very reactive species in this acidic medium and will easily oxidize to the appropriate carboxylic acid. The aldehyde is not detected also, since the oxidation reaction occurs so rapidly.

Therefore we have proposed that for both 1⁰ and 2⁰ esters the presumed acid catalyzed hydrolysis takes place giving the appropriate alcohol. But since the 1⁰ alcohol and aldehyde are so easily and rapidly oxidized in this medium they are rarely detected. Whereas the less reactive 2⁰ alcohol and corresponding ketone can be readily observed. A number of controlled reactions performed in this medium reinforce this theory.

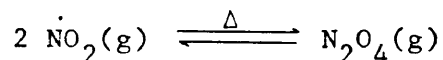
A very curious aspect of this reaction was that early in the reaction, before any of the oxidation products were observed, the presence of the nitrite ester was detected. This lead us to believe that somehow nitrous acid was present in our reaction medium and was responsible for the formation of the nitrite ester via a nucleophilic displacement type reaction with either the ester or the alcohol.

It has been reported⁸⁰ that nitric acid is fairly stable at room temperature. However upon exposure to light or upon heating, especially above 68°C, nitric acid undergoes a reversible decomposition:

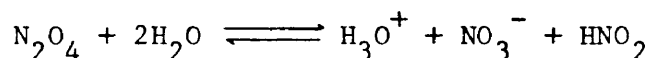


Since we were running our reactions at 76°C it was feasible that this reaction could be taking place. It was also evident that this decomposition was occurring since a brown gas was observed in our sealed reaction vessels, which is a consequence of the unpaired electron of $\dot{\text{N}}\text{O}_2$ gas.

It is well known that NO_2 exists in equilibrium with N_2O_4 which is temperature dependent,



and in the presence of an aqueous medium N_2O_4 reacts in the following manner:



It has also been stated⁸⁰ that, even though nitric acid is a stronger oxidizing agent than nitrous acid from a thermodynamic stand point by comparing standard potentials, it seems from a kinetic stand point nitrous acid reacts faster. Therefore, it seems very plausible to assume HNO_2 does exist in our hydrate melt reaction medium and is responsible for the formation of the nitrite ester.

Some of the more significant and decisive conclusions regarding identification of products, determination of mechanistic routes, and about the chemical nature of the molten salt hydrate medium itself came about as a result of a large number of controlled reactions which were performed.

In these controlled reactions previously identified products of the ester hydrolysis reaction were introduced into various mole % of the hydrate melt reaction medium ($\text{HNO}_3 \cdot 1.65 \cdot \text{H}_2\text{O} / \text{Ca}(\text{NO}_3)_2 \cdot 4\text{H}_2\text{O}$), allowed to react over a range of times, and their products analyzed and identified (See Table #36).

When 1⁰ alcohols were introduced into the medium and allowed to react, the products obtained were a series of carboxylic acids, and the nitrate and nitrite esters. When a 2⁰ alcohol was used it gave, in addition to these products, the appropriate ketone.

The 1⁰ nitrite esters, n-hexyl and n-octyl nitrite gave only a series of carboxylic acids. Whereas the 2⁰ nitrite ester, 2-octyl nitrite, also gave the corresponding ketone, 2-octanone, in addition to a number of carboxylic acids.

When the appropriate aldehyde or ketone was introduced into the medium and allowed to react, the same corresponding series of carboxylic acids were once again obtained.

TABLE #36

1 ⁰ Alcohol	—————→	Carboxylic Acids, Nitrate Ester, Nitrite Ester
2 ⁰ Alcohol	—————→	Ketone, Carboxylic Acids, Nitrate Ester, Nitrite Ester
1 ⁰ Nitrite Ester	—————→	Carboxylic Acids
2 ⁰ Nitrite Ester	—————→	Ketone, Carboxylic Acids
Aldehyde	—————→	Carboxylic Acids
Ketone	—————→	Carboxylic Acids
1 ⁰ Nitrate Ester	—————→	Stable
2 ⁰ Nitrate Ester	—————→	Stable
Carboxylic Acids	—————→	Stable

When either the 1° or 2° nitrate esters were placed in the hydrate melt no reaction occurred. Even in the highly acidic melts, 10% HNO_3 , over long periods of time, 48 hours, at 76°C the nitrate ester remained stable (the relative peak areas on the G.C. remained constant over time).

Finally the specific groups of carboxylic acids, which were obtained as products, were introduced individually and as a series into the reaction medium. But they all remained stable and no reaction occurred, even at high acidities and after long reaction times.

As a result of these controlled reactions we were able to predict the path of the reaction, and using both permanganate and chromic acid⁸¹ as model systems in order to obtain probable mechanisms for oxidation reactions, we were able to propose the following mechanistic routes which explain the occurrence of all the products of the ester hydrolysis reaction for both 1° and 2° esters (See Schemes #1-9).

Scheme #1 shows a typical acid catalyzed hydrolysis of a 1° ester (n-octyl acetate). In the acidic medium the carbonyl oxygen is protonated to give the two resonance contributing structures. This allows water to act as a nucleophile and add to the carbocation. An internal hydrogen abstraction then takes place to give an intermediate species which falls apart to the appropriate alcohol (1-octanol) and acetic acid.

The 1⁰ alcohol is then oxidized to its aldehyde via the formation of a nitrite ester (Scheme #2). As already mentioned, HNO₃ undergoes a disproportionation reaction to give HNO₂, which is a thermodynamically weaker oxidizing agent, but from a kinetic stand point it reacts faster.

Initially the 1⁰ alcohol is protonated and then the nitrite anion acts as a nucleophile to displace water and form the nitrite ester. The nitrite ester then undergoes an internal hydrogen abstraction and falls apart to the corresponding aldehyde (octanal).

The aldehyde can be protonated to give the two resonance contributing structures. This cation is then most likely attacked by the more powerful oxidizing agent, the nitrate anion, which undergoes an internal hydrogen abstraction to give the appropriate carboxylic acid (octanoic acid).

The other possibility is that the aldehyde could enolize and add the nitrate anion across the double bond in a 1,3-Dipolar Cycloaddition type reaction by the allowed $\pi 4s + \pi 2s$ transition, similar to an ozonolysis reaction (Scheme #3).

This cyclic intermediate can then fall apart via the reverse cycloaddition reaction to give a one carbon shorter aldehyde (in this case heptanal). This aldehyde can then be oxidized to its appropriate carboxylic acid (heptanoic acid) or it can enolize and undergo a 1,3-Dipolar cycloaddition of NO₃⁻ to give the next shorter chain aldehyde (hexanal). This cycle can continue, finally giving a complete series of carboxylic acids.

The 1⁰ nitrate ester can form from either of two possible routes (Scheme #4). It could be formed when the protonated ester is attacked by the nitrate anion which undergoes an internal rearrangement and falls apart to give the nitrate ester.

A more likely possibility is simply protonation of the 1⁰ alcohol (formed via hydrolysis of the ester), and then the nucleophilic displacement of water by NO_3^- to give the 1⁰ nitrate ester directly.

Scheme #5 shows a typical acid-catalyzed hydrolysis of a 2⁰ ester (2-octyl acetate). In the acidic medium the carbonyl oxygen is protonated to give the two resonance contributing structures. Once again, this allows water to act as a nucleophile and add to the cation. An internal hydrogen abstraction takes place, to give an intermediate species which falls apart to the appropriate alcohol (2-octanol).

In Scheme #6 the 2⁰ alcohol is oxidized by the nitrite anion to give the 2⁰ nitrite ester (2-octyl nitrite). The nitrite ester undergoes an internal hydrogen abstraction to give the appropriate ketone (2-octanone).

The ketone can then enolize in two different ways. The more stable, highly substituted enol undergoes oxidative degradation via the 1,3-Dipolar cycloaddition reaction to give a two carbon shorter aldehyde (hexanal).

This aldehyde can then be oxidized to its corresponding carboxylic acid (hexanoic acid) or it can enolize and undergo

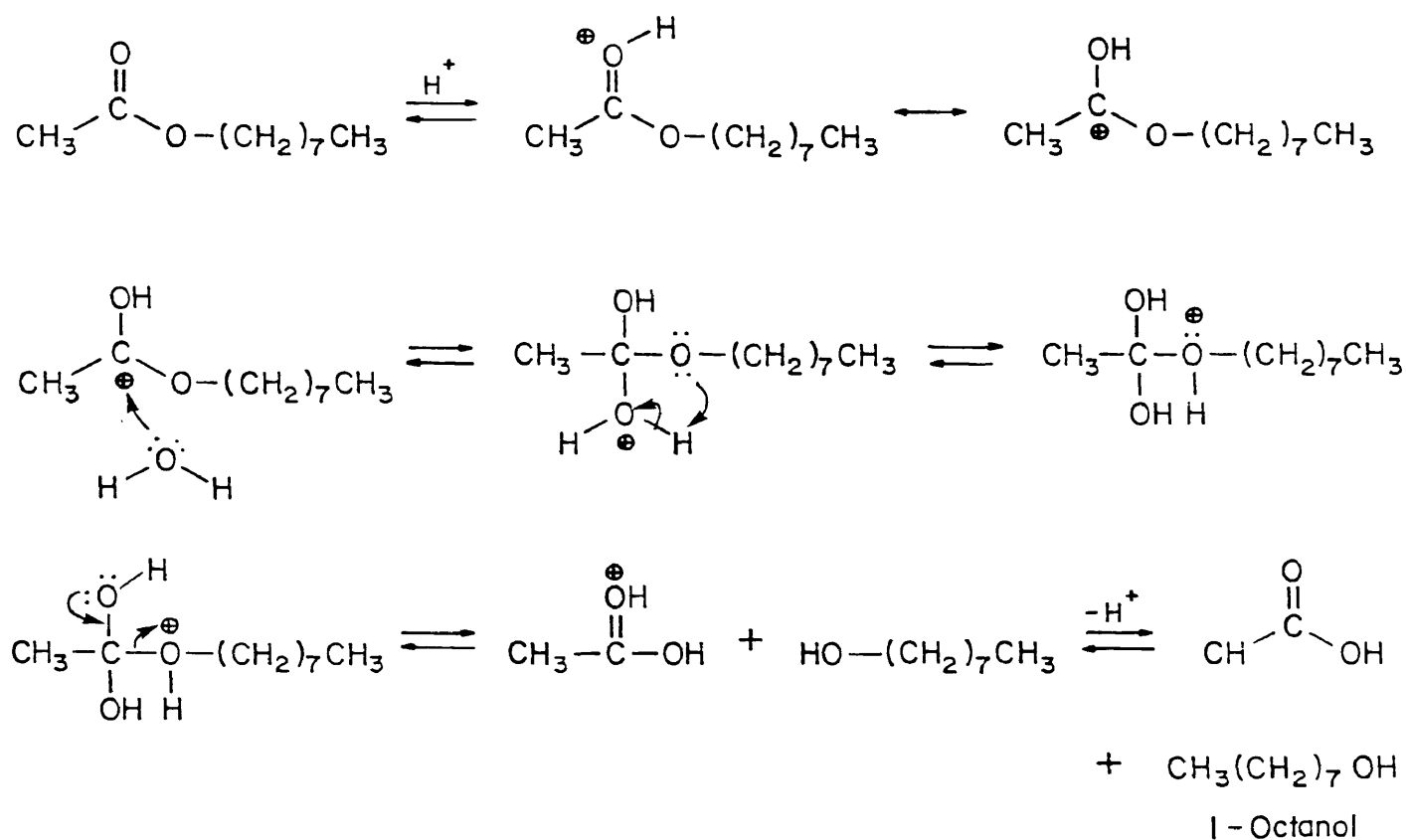
oxidative degradation to the next shorter chain aldehyde (pentanal), and the two-fold process can continue (Scheme #7).

Scheme #8 shows the less substituted enol also undergoes oxidative degradation via the 1,3-Dipolar cycloaddition reaction to give a one carbon shorter carboxylic acid (heptanoic acid).

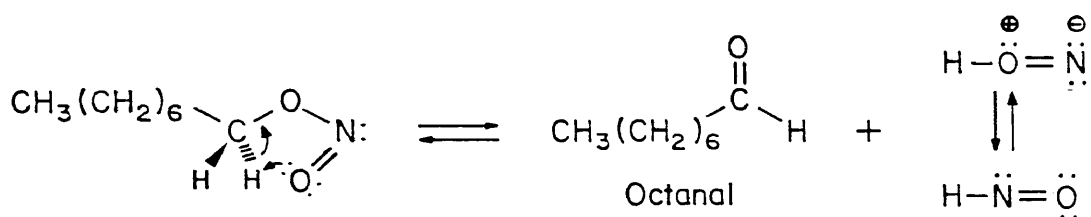
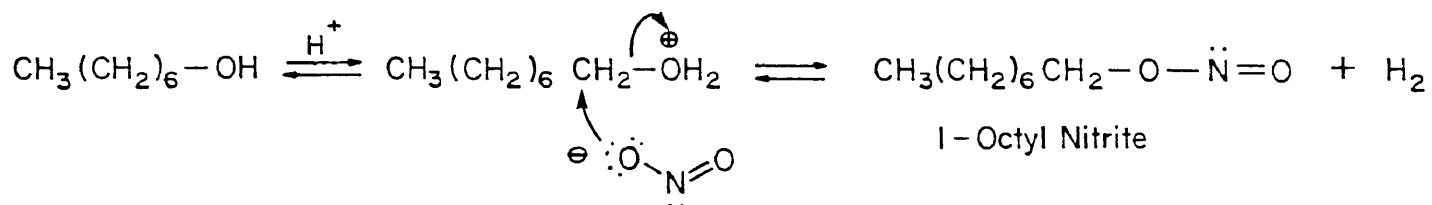
The 2⁰ nitrate ester can be formed from either the 2⁰ ester or the 2⁰ alcohol (Scheme #9). The ester can be protonated in the acidic medium to give the two resonance contributing structures. The nucleophilic nitrate anion attacks the cationic species to give an intermediate which rearranges and falls apart to the 2⁰ nitrate ester (2-octyl nitrate).

The other possibility is protonation of the 2⁰ alcohol and then nucleophilic displacement of water by NO_3^- to give the 2⁰ nitrate ester.

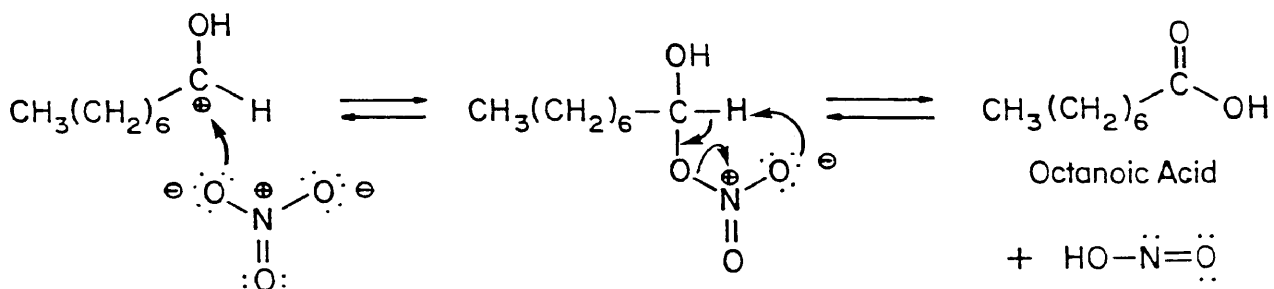
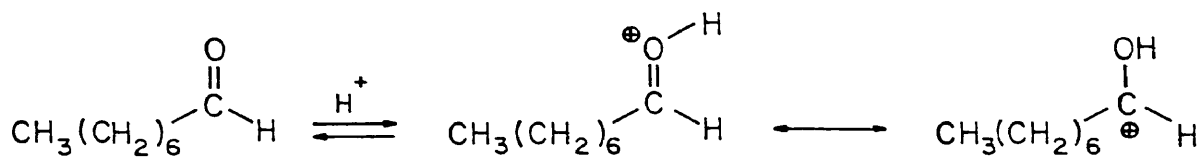
SCHEME # 1

Acid-Catalyzed Ester Hydrolysis of *n*-Octyl Acetate

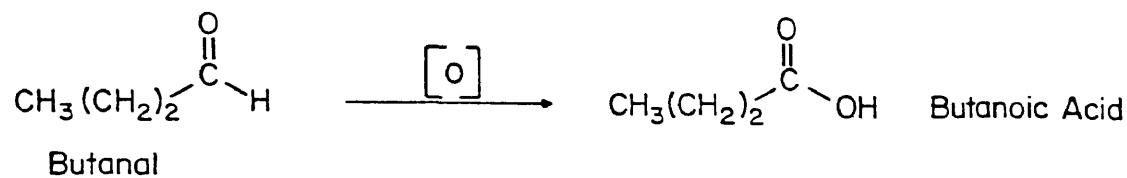
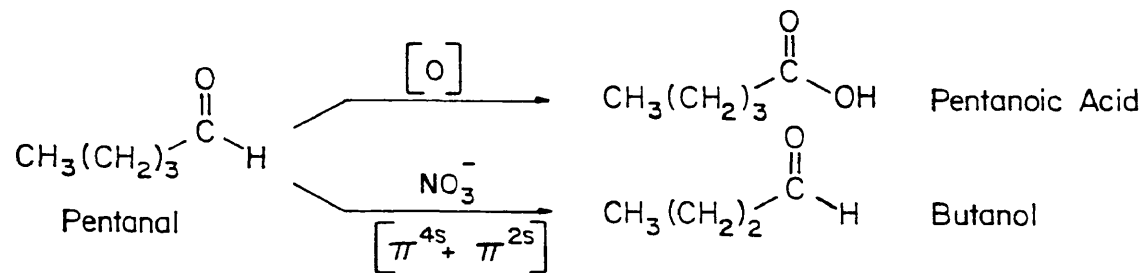
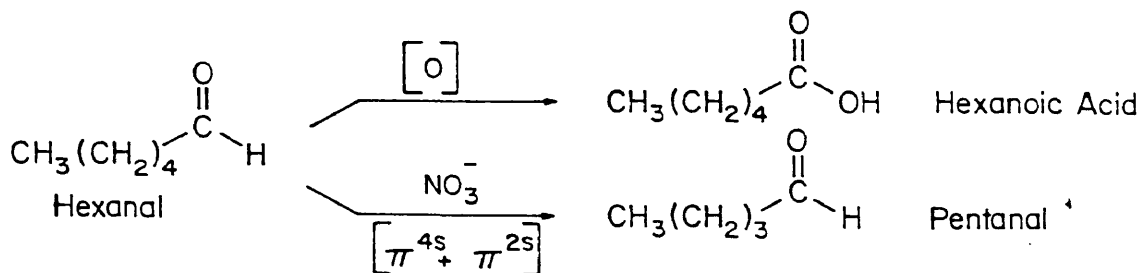
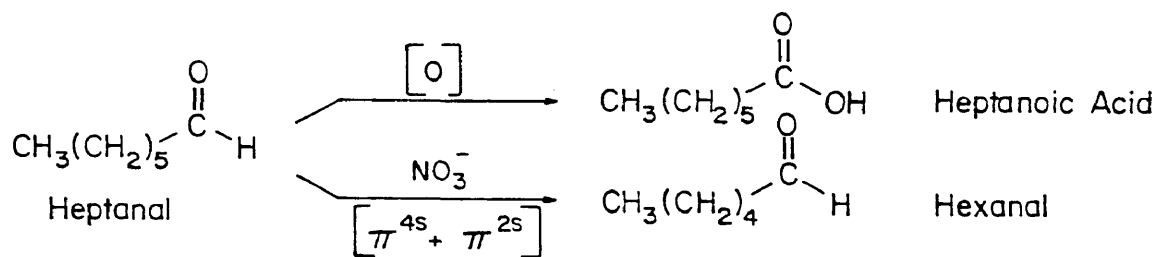
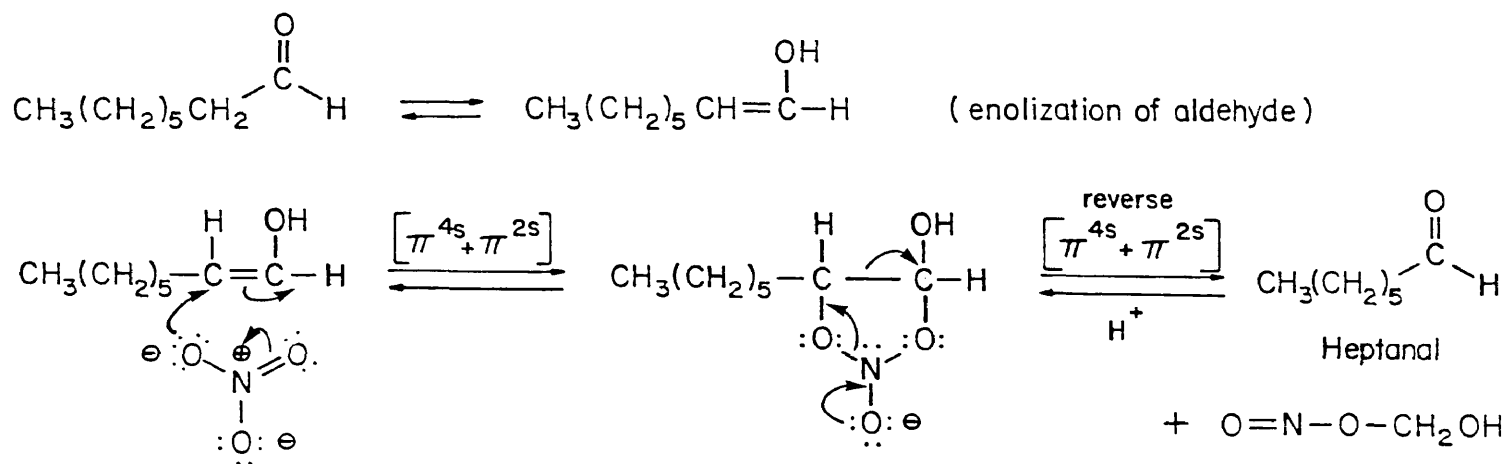
Oxidation of 1-Octanol to Octanal



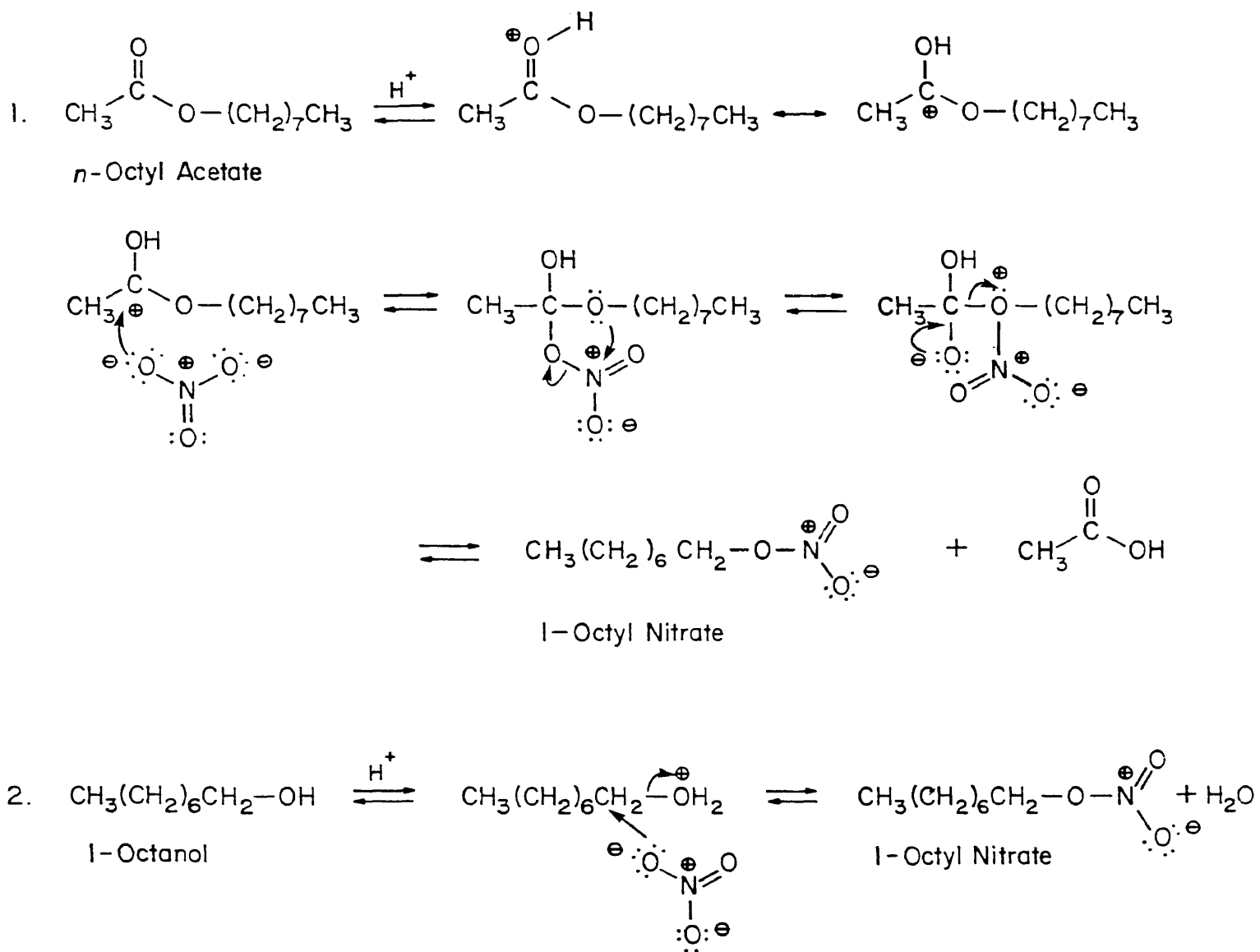
Oxidation of 1-Octanal to Octanoic Acid



SCHEME # 3

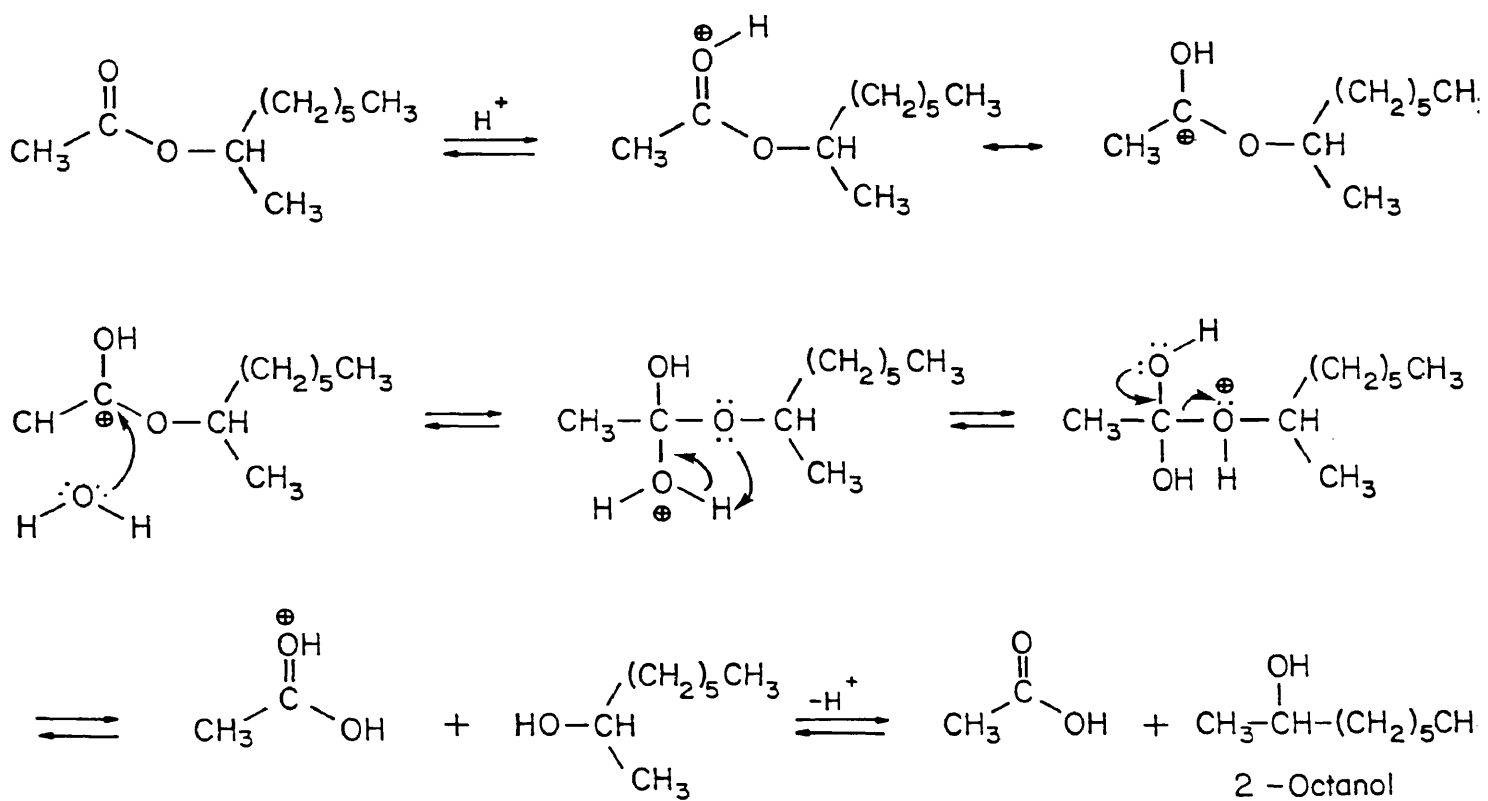
1,3 Dipolar Cycloaddition of NO_3^- to Octanal

Formation of 1-Octyl Nitrate Ester



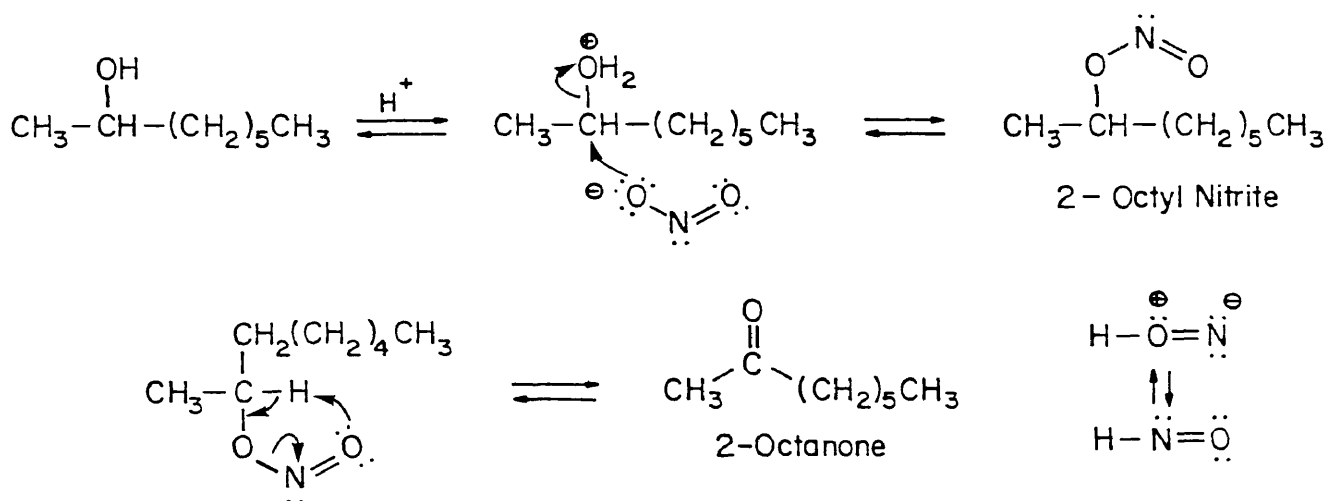
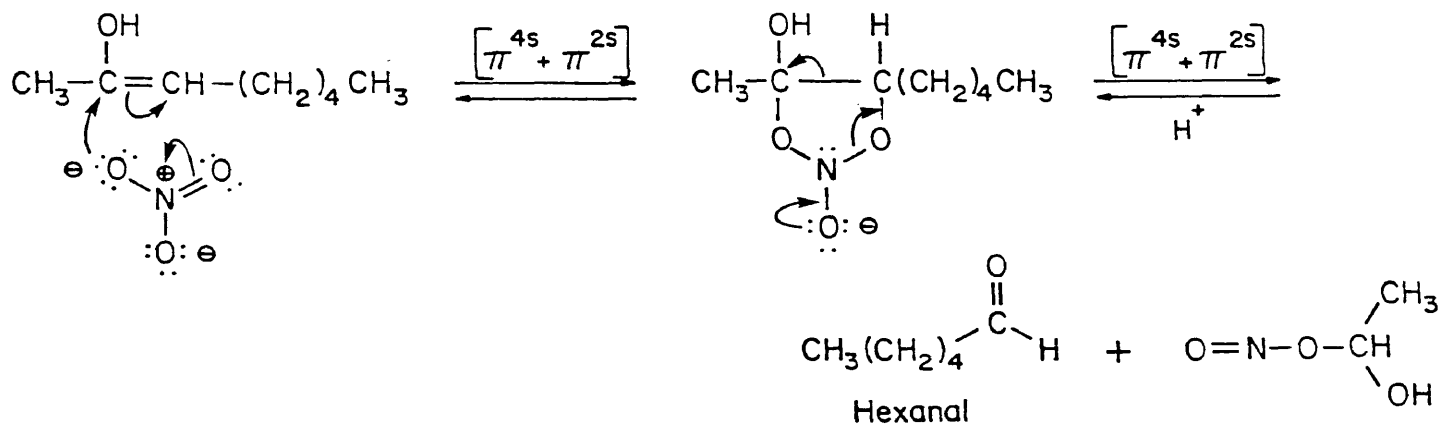
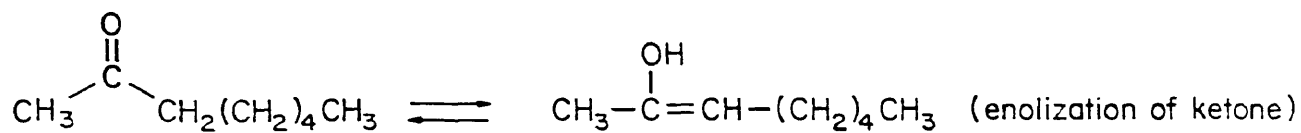
SCHEME # 5

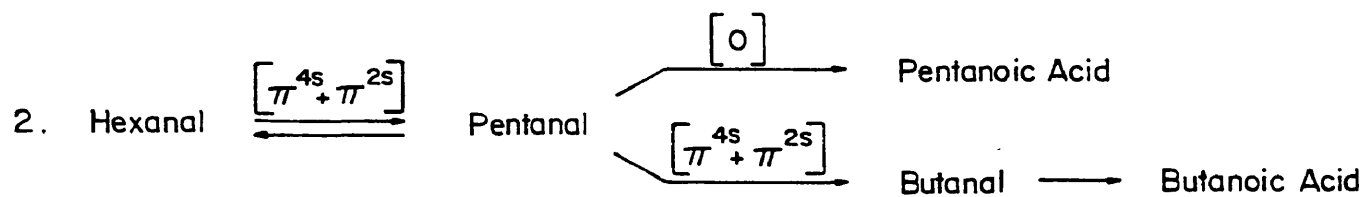
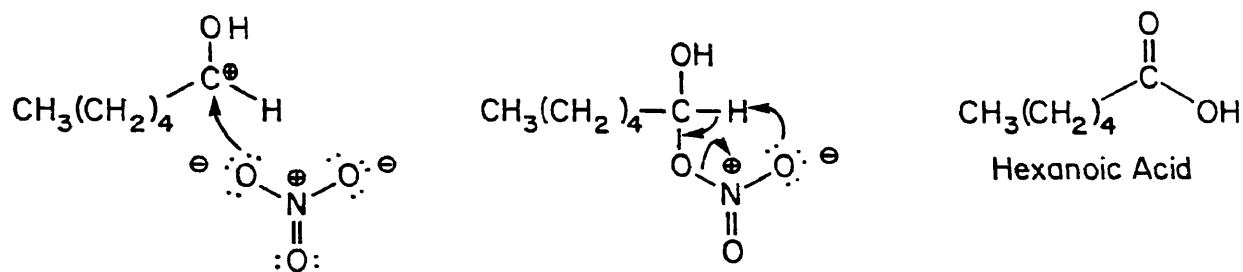
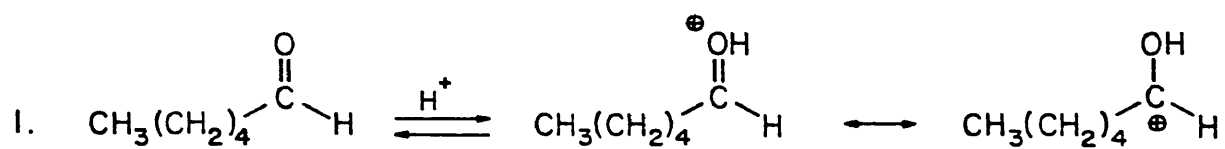
Acid-Catalyzed Ester Hydrolysis of 2-Octyl Acetate



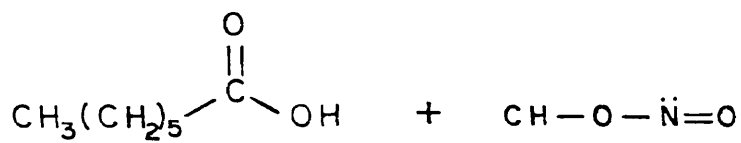
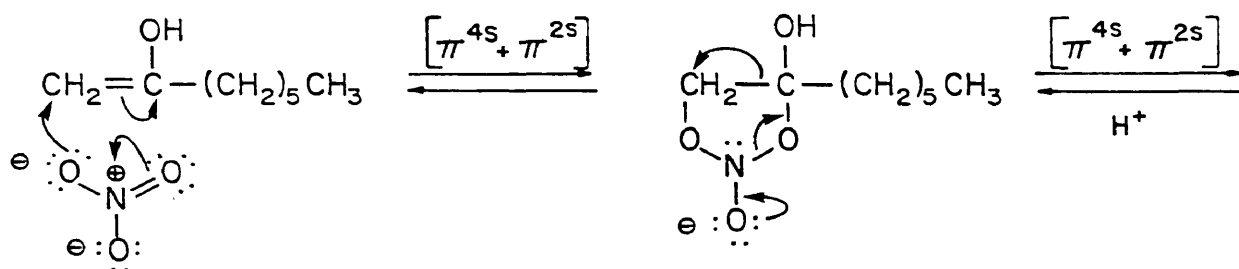
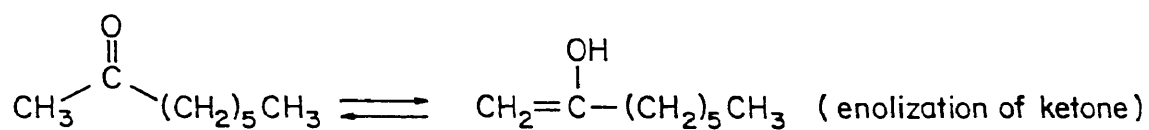
SCHEME # 6

Oxidation of 2-Octanol

Oxidation of 2-Octanone to give Hexanoic Acid via
1,3 Dipolar Cycloaddition

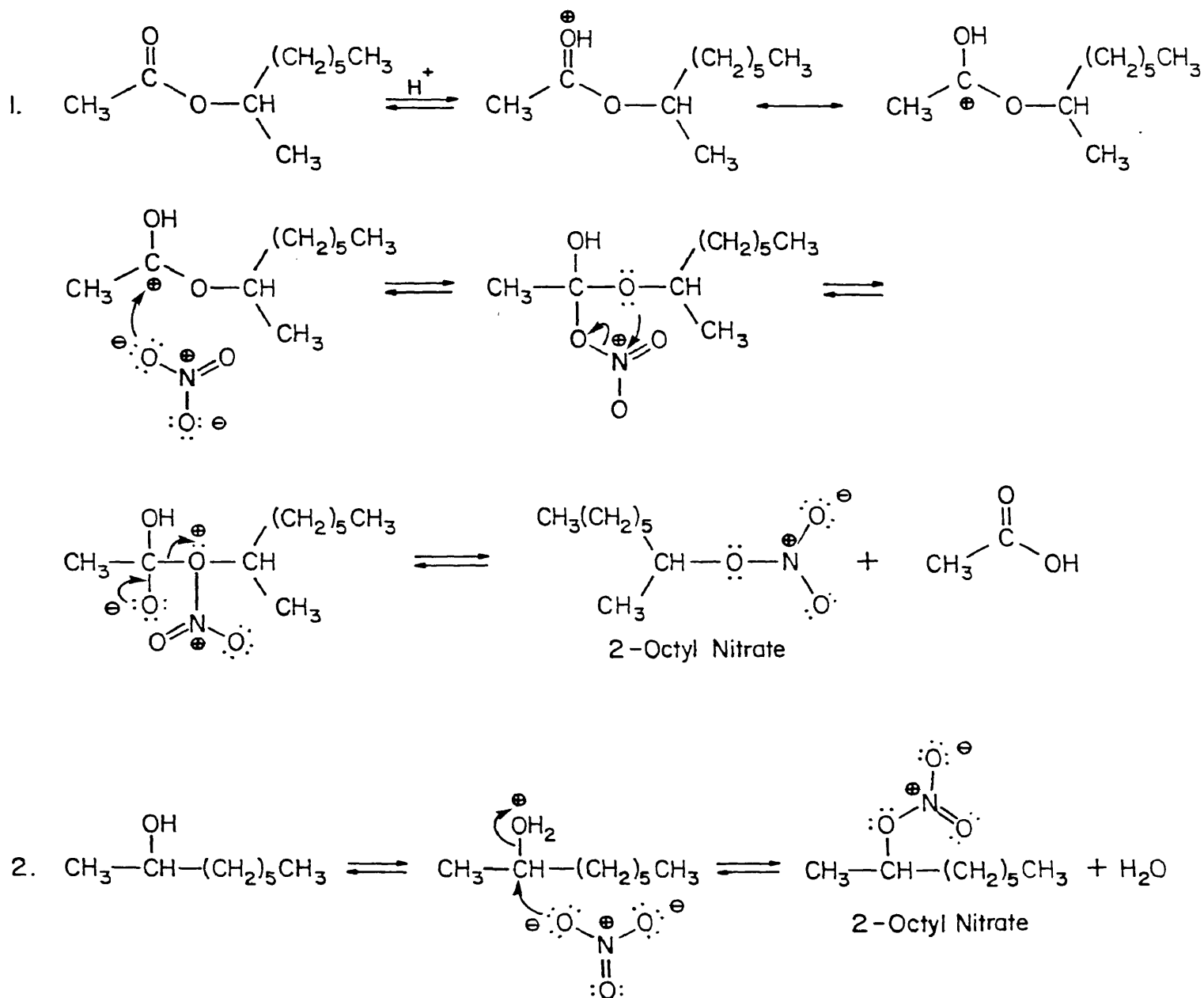


Oxidation of 2-Octanone to give Heptanoic Acid
via a 1,3-Dipolar Cycloaddition



Heptanoic Acid

Formation of 2-Octyl Nitrate Ester



Some introductory experimental work was performed in order to assess the potential usefulness of molten salt hydrates as a medium for nitrating aromatics.

The preliminary results demonstrated that aromatic compounds are rapidly nitrated in these hydrate melts without any complicating side reactions. Although much more experimental work needs to be done before conclusive results can be obtained, it seems that these molten salt hydrate systems could serve as a potentially useful synthetic medium for nitrating aromatic compounds.

C O N C L U S I O N S

We have shown that the molten salt hydrate melts of $\text{Cd}(\text{NO}_3)_2 \cdot 4\text{H}_2\text{O}$, $\text{Zn}(\text{NO}_3)_2 \cdot 6\text{H}_2\text{O}$, $\text{AlCl}_3 \cdot 6\text{H}_2\text{O}$ and $\text{HNO}_3 \cdot 1.65\text{H}_2\text{O}$ in the solvent $\text{Ca}(\text{NO}_3)_2 \cdot 4\text{H}_2\text{O}$ are highly acidic. This enhanced acidity is attributed to the polarization of the oxygen atom towards the metal center and the attraction of the anion for the water protons, resulting in a decrease in electron density around the proton, thereby causing an increase in the proton's acidity.

The standard approach of expressing this acidity is the Hammett Acidity Function and the traditional way of measuring H_0 is through spectrophotometric techniques, but a number of problems and experimental obstacles were encountered in using this method.

The viscosity of the medium itself presented a number of problems. Samples were hard to work with, it was difficult to obtain a homogeneous mixture with the indicator, it was equally hard to deal with the melts volumetrically and on this scale gravimetric measurements introduced larger errors, and the melts had a tendency to recrystallize .

Probably the most significant problem was that the Hammett Acidity Function could not be measured over a wide range of concentrations, since at higher mole percentages of melt (higher acidities) the base indicators often decomposed.

Therefore we have proposed a rather novel approach to measuring

the acidities of these molten salt hydrates by correlating the Hammett Acidity Function with the Proton Magnetic Resonance shift of these hydrate melts.

As a result of this linear correlation we can accurately predict the H_0 values for any of these hydrate melt systems by simply measuring its ^1H NMR chemical shift.

This method eliminates the experimental difficulties encountered in measuring H_0 by traditional spectrophotometric techniques, and it offers a number of advantages over this previous procedure.

In addition to the fact that it is an easier method for determining H_0 values, it is a more accurate technique when one considers the dilutions and correction factors associated with the spectrophotometric technique. It is also a non-invasive measurement; nothing is introduced into the hydrate melt which could alter its chemical nature. But most importantly, the Hammett Acidity Function can be measured over a wide range of concentrations.

These results have also reinforced the theory that ^1H NMR chemical shifts and protonation of organic indicators respond very similarly to changes in proton acidity.^{18,19,22}

The results of the experimental studies using the molten salt hydrate systems as a synthetic medium, have shown that these highly acidic melts can be used to perform certain acid catalyzed organic reactions. Although at this point a method needs to be established to control these reactions and make them more selective.

From experimental research we have uncovered some rather unique and potentially useful properties of these molten salt hydrates which could make them a valuable synthetic organic medium in the future

One of the more distinct properties that these systems have in common is that the acidity of the molten salt hydrate medium can be changed without altering the water content of the system, unlike most mineral acids.

Another interesting aspect is that for a medium as acidic as these molten salt hydrates, the rate of acid-catalyzed ester hydrolysis appears to be exceedingly slow in comparison to typical rates for reactions performed in aqueous mineral acids of similar H_0 values (See Tables # 37 and 38). For example, n-octyl acetate in 10% $\text{HNO}_3 \cdot 1.65\text{H}_2\text{O}/\text{Ca}(\text{NO}_3)_2 \cdot 4\text{H}_2\text{O}$ melt ($H_0 = -3.98$) has a half life ($T_{1/2}$) of 360 minutes in comparison with n-propyl acetate in 55% (wt %) H_2SO_4 ($H_0 = -3.91$) has a $T_{1/2} = 6$ minutes. An example of a 2^o ester is 2-octyl acetate in 7% $\text{HNO}_3 \cdot 1.65 \text{H}_2\text{O}/\text{Ca}(\text{NO}_3)_2 \cdot 4\text{H}_2\text{O}$ ($H_0 = -3.75$) has a $T_{1/2} = 1440$ minutes whereas sec-butyl acetate in 55% H_2SO_4 ($H_0 = -3.91$) has a $T_{1/2} = 14$ minutes.

Assuming the order of the reaction is the same, the decrease in the rate can be attributed to two main factors. One is the heterogenous nature of the medium and the other is the limited amount of free water available in the hydrate melt.

Finally these molten salt hydrate systems exhibited properties of being both a strong oxidizing agent and a powerful nitrating agent.

Typical Ester Hydrolysis rates in Sulfuric Acid at 25°C

Pseudo-first-order rate constants in min^{-1}

$\%$ H_2SO_4	$10^2 k_1^a$	$\%$ H_2SO_4	$10^2 k_1$	$\%$ H_2SO_4	$10^2 k_1$
Methyl acetate		<i>n</i> -Propyl acetate		Isopropyl acetate	
14.1	1.50	14.1	1.47	14.1	0.890
20.7	2.61	20.7	2.52	25.3	1.99
28.3	4.22	30.2	5.23	34.8	3.30
34.8	6.41	34.8	6.78	40.4	4.21
40.4	8.14	40.4	8.47	45.4	4.96
45.4	10.4	45.4	9.76	50.2	5.38
50.2	11.4	50.2	11.4	55.2	5.48
55.2	13.3	55.2	11.5	60.4	4.54
60.4	13.8	60.4	10.4	65.2	3.60
65.2	11.9	65.2	8.23	70.4	1.80
70.4	7.25	70.4	4.48	74.1	1.14
74.1	3.83	74.1	2.20	80.0	1.48
80.0	0.931	89.7	0.205	81.7	2.30
		95.0	0.323	84.7	4.69
		98.6	0.450	88.2	11.2
				89.7	13.5
				90.8	17.0
<i>sec</i> -Butyl acetate		Benzyl acetate		Phenyl acetate	
14.1	0.964	10.1	0.740	15.1	1.08
45.4	4.72	25.3	2.52	20.1	1.62
50.2	5.00	30.2	4.04	25.3	2.38
55.2	5.02	34.8	4.61	30.2	3.30
60.4	3.96	40.4	6.08	34.8	4.34
65.2	2.99	45.4	7.13	40.4	6.20
70.4	1.71	50.2	9.81	45.4	8.36
74.1	2.03	52.8	9.30	50.2	10.9
77.7	3.90	55.2	9.91	55.2	14.5
80.0	7.00	60.4	8.52	60.4	19.2
81.7	11.00	62.5	9.24	65.2	22.6
84.7	23.6	65.2	10.1	70.4	27.2
88.2	63.2	66.8	13.7	74.1	29.3
		67.3	15.7		
		69.0	22.3		

(adapted from reference # 65)

TABLE # 38

The Hammett Acidity Function for aqueous Sulfuric Acid @ 25°C

wt % H ₂ SO ₄	-H ₀	wt % H ₂ SO ₄	-H ₀	wt % H ₂ SO ₄	-H ₀
1	-0.84	42	2.69	87	8.60
2	-0.31	45	2.95	90	9.03
5	0.02	47	3.13	92	9.33
8	0.28	50	3.41	94	9.59
10	0.43	52	3.60	96	9.88
12	0.58	55	3.91	98	10.27
14	0.73	57	4.15	99	10.57
16	0.85	60	4.51	99.1	10.62
18	0.97	62	4.83	99.2	10.66
20	1.10	65	5.18	99.3	10.71
22	1.25	67	5.48	99.4	10.77
25	1.47	70	5.92	99.5	10.83
27	1.61	72	6.23	99.6	10.92
30	1.82	75	6.71	99.7	11.02
32	1.96	77	7.05	99.8	11.18
35	2.19	80	7.52	99.85	11.28
37	2.34	82	7.84	99.90	11.42
40	2.54	85	8.29	99.95	11.64
				100.00	11.94

(adapted from reference # 81)

A P P E N D I X I

Independence of H_0 with regards to the nature of the Base Indicators

The logarithm of the conjugate acid dissociation constant for an indicator base in an acidic medium is defined as:

$$(1) \text{pK}_{\text{BH}^+} = -\log(a_{\text{H}^+} f_{\text{B}} [\text{B}] / f_{\text{BH}^+} [\text{BH}^+])$$

If two different base indicators, X and Y, have fairly similar pK_A values, are dissolved into two solutions of a particular acid with the same concentration so that both solutions have the same value for a_{H^+} , and the concentrations of the indicators are low enough so as not to effect the nature of the medium, then $\Delta \text{pK}_{\text{BH}^+}$ is defined as:

$$(2) \Delta \text{pK}_{\text{BH}^+} = \log(f_{\text{XH}^+} / f_{\text{X}}) - \log(f_{\text{YH}^+} / f_{\text{Y}}) + \log I_{\text{Y}} - \log I_{\text{X}}$$

$$\text{where } I = [\text{B}] / [\text{BH}^+]$$

$$(3) \Delta \log I = \Delta \text{pK}_{\text{BH}^+} - [\log(f_{\text{XH}^+} / f_{\text{X}}) - \log(f_{\text{YH}^+} / f_{\text{Y}})]$$

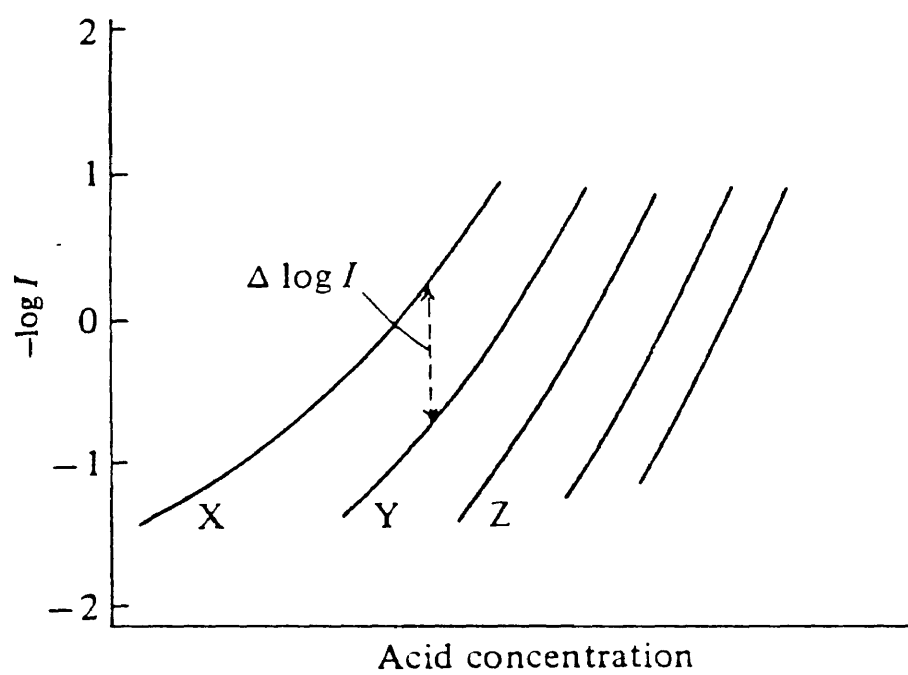
Using weakly basic anilines as indicators, Hammett found that plots of $\log I_{\text{X}}$ and $\log I_{\text{Y}}$ against acid concentration were virtually parallel over the whole range of concentrations (See Figure #19). In other words $\log \Delta I$ remains constant for the two different indicators over a full range of acid concentrations. Therefore $\Delta \log I$ is independent of a_{H^+} ($= f_{\text{H}^+} [\text{H}^+]$). Since ΔpK is in no way dependent on the acidity of the medium, then according to equation #3 the term: $\log(f_{\text{XH}^+} / f_{\text{X}}) - \log(f_{\text{YH}^+} / f_{\text{Y}})$ must also be independent of a_{H^+} .

In dilute acidic solutions $f \longrightarrow 1$ and the $\log f \longrightarrow 0$.

If the term $\log (f_{XH^+}/f_X) - \log (f_{YH^+}/f_Y)$ is zero in dilute acid solution, it must be zero at any concentration of acid since the term is independent of a_{H^+} .

Therefore the ratio f_{BH^+}/f_B depends only on the acidity of the medium and not on the nature of the indicator, since, $h_0 = a_{H^+} f_B / f_{BH^+}$ and $H_0 = -\log h_0$ then H_0 is independent of the indicator used.

FIGURE # 19



(adapted from reference # 82)

A P P E N D I X II

Using the equation $H_0 = pK_{BH^+} - \log ([BH^+]/[B])$, one can obtain a quantitative measure of the acidity of a solution by measuring the degree to which a base is protonated in this solution. In this case the base functions as an indicator.

Spectrophotometric methods provide a reliable means of measuring the ionization ratios of weak bases and the dissociation constants of their conjugate acids. Therefore, when the weak base (B) is protonated to the conjugate acid (BH^+) a color change takes place which means the weak base and conjugate acid have a measurably different electronic absorption spectrum.

Initially the molar extinction coefficient of the Hammett indicators was determined by making a solution of known concentration in 95% ethanol and measuring its absorbance spectrophotometrically. Then using a Beer's Law relationship, $A = \epsilon bc$, the molar extinction coefficient can be calculated.

Next a stock solution of the indicators in 95% ethanol were made up at specific concentrations such that a given number of microliters of stock indicator solution added to a specific volume of water gave a known absorbance for that solution. Then the same number of microliters of stock indicator was added to the same volume of $Ca(NO_3)_2 \cdot 4H_2O$, and the absorbance measured.

It was shown that the two absorbances, $A_B^{H_2O}$ and A_B^{MELT} , with the melt giving a slightly lower absorbance. An important fact

though was that the magnitude of the difference in the two absorbances remained the same no matter what indicator was used; therefore, we know that the indicator base is not being protonated by $\text{Ca}(\text{NO}_3)_2 \cdot 4\text{H}_2\text{O}$. Also the λ_{MAX} for these two systems are different. All of these facts can probably be attributed to solvent effects on the absorbance spectra (solvent shift). Therefore, the absorbance of the melt must be corrected for these solvent effects in the following manner:

$$A_{\text{MELT},B} = \text{measured } A_{\text{MELT},B} (A_B^{\text{H}_2\text{O}}/A_B^{\text{MELT}})$$

H_0 can be measured directly by absorbance spectroscopy since there is a linear relationship between absorbance and concentration, using the following relation:

$$\text{H}_0 = \text{pK}_{\text{BH}^+} + \log ([\text{B}]/[\text{BH}^+]) = \text{pK}_{\text{BH}^+} + \log (A_{\text{MELT},B}/A_{\text{BH}^+})$$

Where $A_{\text{MELT},B}$ = absorbance of the weak base in the melt and A_{BH^+} = difference in the experimental absorbance of the diluted solution (which is total base) and $A_{\text{MELT},B}$. This is rationalized by the following argument:

$$\% \text{ base} = A_{\text{MELT}}/A_{\text{BASE}}$$

$$\% \text{ acid} = (A_{\text{BASE}} - A_{\text{MELT}})/A_{\text{BASE}}$$

Therefore the ratio of base to acid =

$$(A_{\text{MELT}}/A_{\text{BASE}})/[(A_{\text{BASE}} - A_{\text{MELT}})/A_{\text{BASE}}] = A_{\text{MELT}}/(A_{\text{BASE}} - A_{\text{MELT}})$$

Therefore $A_{\text{BH}^+} = A_{\text{DIL},B} - A_{\text{MELT},B}$, but the measured absorbance of the diluted melt (total base form) must be corrected for the fact that the concentration of the indicator has decreased:

$$A_{\text{DIL,B}} = (\text{measured } A_{\text{DIL,B}}) \times \frac{\text{Total Vol. Soln. (mL)} \times \text{Density melt (g/mL)}}{\text{Weight melt (g)}}$$

BIBLIOGRAPHY

1. Sundermeyer, W., Angew. Chem. Internat. Edn 1965, 4, 222
2. Moynihan, C.T., Smalley, C.R., Angell, C.A., Sare, E.J., J. Phys. Chem. 1969, 73, 2287
3. Hammett, L., J. Phys. Chem. 1928, 50, 2666
4. Hantzsch, Z. Elektrochem 1923, 29, 221
5. Bronsted, J. Phys. Chem. 1926, 30, 777
6. Hammett, L. and Deyrup, J., J. Am. Chem. Soc 1932, 54, 2721
7. Skoog and West, "Fundamentals of Analytical Chemistry" 3rd ed., Sander College, Philadelphia, 1976
8. Paul, M.A. and Long, F.A., Chem. Rev. 1957, 56, 1
9. Gelbstein, A.I., Shcheglova, G.G., Temkin, M.I., Zhur. Neorg. Kim. 1956, 1, 282, 506
10. Harbottle, G., J. Am. Chem Soc. 1951, 73, 4024
11. Paul, M.A., J. Am. Chem. Soc. 1954, 76, 3236
12. Moiseev, I. and Flid, R., Zhur. Priklad. Kim. 1954, 27, 1110
13. Bascombe, K. and Bell, R., Discuss. Faraday Soc. 1957, 24, 158
14. Wyatt, P.A.H., Discuss. Faraday Soc. 1957, 24, 162
15. Dawber, J.G. and Wyatt, P.A.H. J. Chem. Soc. 1960, 3859
16. Young, Maranville and Smith, "The Structure of Electrolyte Solutions," ed., Hamer, New York, 1959, Chap 4
17. Critchfield, F and Johnson, J., Anal. Chem. 1959, 31, 570
18. Duffy, J.A. and Ingram, M.D., Inorg. Chem. 1978, 17, 2798
19. Duffy, J.A. and Ingram, M.D., Inorg. Chem. 1977, 16, 2988
20. Sare, E.J., Moynihan, C.T. and Angell, C.A., J. Phys. Chem. 1973, 77, 1869
21. Duffy, J.A. and Ingram, M.D., J. Inorg. Nucl. Chem. 1976, 38, 1831
22. Duffy, J.A. and Ingram, M.D., "Ionic Liquids," Inman & Loverling, ed., Plenum Press, New York, N.Y., 1980

23. Duffy, J.A. and Ingram, M.D., J. Am. Chem. Soc. 1971, 93, 6448
24. Moynihan, C.T. and Fratiello, A., J. Am. Chem. Soc., 1967, 89, 5546
25. Angell, C.A., J. Electrochem. 1965, 112, 1224
26. Angell, C.A., J. Phys. Chem., 1965, 69, 2137
27. Angell, C.A., J. Phys. Chem. 1966, 70, 3988
28. Braunstein, J., Orr, L. and MacDonald W., J. Chem. Eng. Data 1967, 12, 415
29. Braunstein, J., Alvarez-Funes, A. and Braunstein, H., J. Phys. Chem. 1966, 70, 2734
30. Angell, C.A. and Gruen, D.M., J. Am. Chem. Soc. 1966, 88, 5192
31. Moynihan, C.T., J. Phys. Chem 1966, 70, 3399
32. Schiavelli, M.D. and Ingram, M.D., J. Phys. Chem. 1980, 84, 2338
33. Sare, E.J., Moynihan, C.T. and Angell, C.A., J. Phys. Chem. 1973, 77, 1869
34. Meyer, L.H and Gutowsky, H.S., J. Phys. Chem. 1953, 57, 481
35. Ramsey, N.F., Phys. Rev. 1950, 78, 699
36. Ramsey, N.F., Phys. Rev. 1952, 86, 243
37. Gutowsky, H.S. and Saika A., J. Chem. Phys. 1953, 21, 1688
38. Hood, G.C., Redlich, O. and Reilly, C.A., J. Chem. Phys. 1954, 22, 2069
39. Hindman, J.C., J. Chem. Phys. 1962, 36, 1000
40. Bergquist, M.S. and Forslind, E., Acta. Chem. Scand. 1962, 16, 2069
41. Hertz, H.G. and Spalthoff, W., Z. Electrochem 1959, 63, 1096
42. Hartman, K.A., J. Phys. Chem. 1966, 70, 270
43. Glick, R.E., Stewart, W.E. and Tewari, K.C., J. Chem. Phys. 1966, 45, 4049
44. Malinowski, E.R., Knapp, P.S. and Feur, B., J. Chem. Phys. 1966, 45, 4274
45. Hester, R.E. and Ellis, V.S., J. Chem. Soc (A) 1969, 607
46. Schneider, W.G., Bernstein, H.J. and Pople, J.A., J. Chem. Phys. 1958, 28, 601

47. Ruterjams, H.H. and Sheraga, H.A., J. Chem. Phys. 1966, 45, 3296
48. Hester, R.E. and Plane, R.A., Inorg. Chem. 1966, 45, 3296
49. Hester, R.E. and Plane, R.A., J. Chem. Phys. 1966, 45, 4588
50. Trip, T.B. and Braunstein J., Chem. Comm. 1968, 111
51. Creekmore, R.W. and Reilley, C.N., J. Phys. Chem. 1969, 73, 1563
52. Pople, J.A., Schneider, W.G. and Bernstein, H.G., "High-Resolution Nuclear Magnetic Resonance," McGraw-Hill, New York, N.Y., 1959
53. Malionowski, E.R. and Knapp, P.S., J. Chem. Phys. 1968, 48, 4989
54. Gurney, R.W., "Ionic Process in Solution," Dover Publications, New York, N.Y., 1953
55. Zarakhani, N.G. and Vinnik, M.I., Russ. J. Phys. Chem. 1962, 36, 483
56. Streitwieser and Heathcock, "Introduction to Organic Chemistry," Macmillan Publishing Corp., copyright 1976
57. Lowery and Richardson, "Mechanisms and Theory in Organic Chemistry," Harper and Row Publishers, copyright 1981, Chapter 8, pp 648-657
58. Samuel D. and Silver, B.L., Adv. Phys. Org. Chem. 1965, 3, 123
59. Ingold, E.H. and Ingold, C.K., J. Chem. Soc. 1932, 756
60. Ingold, C.K., "Structure and Mechanism in Organic Chemistry," 2nd ed., Cornell University Press, Ithica, N.Y., 1969
61. March, J., "Advanced Organic Chemistry, Reactions, Mechanisms, and Structures," McGraw-Hill Publishers, copyright 1977
62. Bunnett, J.F., J. Am. Chem. Soc. 1961, 83, 4978
63. Yates, K., Accts. Chem. Res. 1971, 4, 136
64. Yates, K. and Stevens, J.B., Can. J. Chem. 1965, 43, 529
65. Yates, K. and McClelland, R.A., J. Am. Chem. Soc. 1967, 89, 2686
66. Bender, M.L., J. Am. Chem. Soc. 1951, 73, 1626
67. Bunton, C.A. and Wood, J.L., J. Chem. Soc. 1955, 1522
68. Yates, K. and Modro, T.A., Accts. Chem. Res. 1978, 11, 190
69. McClellan, R.A., Modro, T.A., Goldman, M.F. and Yates, K., J. Am. Chem Soc. 1975, 97 5223

70. Rochester, C.H., "Acidity Functions," A series of monographs in Organic Chemistry, ed. A.T. Blomquist, Volume 17, Academic Press, New York and London, copyright 1970
71. Temple, R.B., Fay, C., and Williamson, J., J. Chem. Soc., Chem. Commun. 1966, 148
72. Duke, F.R. and Yamamoto, S., J. Am. Chem. Soc. 1959, 81, 6378
73. Temple, R.B. and Thickett, G.W., Aust. J. Chem. 1973, 26, 667
74. Tople, L.E., Osteryoung, R.A. and Christie, J.H., J. Phys. Chem. 1966, 70, 2857
75. Crivello, J.V., J. Org. Chem. 1981, 46, 3056
76. Carey and Suggs, Tetrahedron Letters 1975, 2647
77. Pattison, F.L.M. and Brown, G.M., Can. J. Chem. 1956, 34, 879
78. Noyes, W.A., "Organic Synthesis," Coll. Vol. II, page 108
79. Boston, C.R., James, D.W. and Smith, G.P., J. Phy. Chem. 1968, 72, 293
80. Sneed, M.C. and Brasted, R.C., "Comprehensive Inorganic Chemistry," Volume V, D. Van Nostrand Comp. Inc., copyright 1956, pp 90-94
81. Wiberg, K.B., "Oxidation in Organic Chemistry," A series of monographs in Organic Chemistry, Volume 5A, Academic Press, New York and London, copyright 1965
82. Jones, R.A.Y., "Physical and Mechanistic Organic Chemistry," 2nd Edition, Cambridge University Press, Cambridge, copyright 1979